Calibration of RapidScat Instrument Drift

F. Dayton Minor

A thesis submitted to the faculty of
Brigham Young University
in partial fulfillment of the requirements for the degree of

Master of Science

David G. Long, Chair
Neal Bangerter
Wood Chiang

Department of Electrical and Computer Engineering

Brigham Young University

August 2016

ABSTRACT

Calibration of RapidScat Instrument Drift

F. Dayton Minor

Department of Electrical and Computer Engineering

Master of Science

RapidScat is a Ku-band radar that measures the normalized backscatter coefficient σ^o of the Earth's surface. Launched in 2015, it currently operates on the International Space Station. Nearly one year into its mission, RapidScat measurements began exhibiting strange behavior that is believed to be caused by a change in receiver gain. Changes in gain are compensated for during post-processing, but the measurements have a lower signal-to-noise ratio (SNR). Calibration and validation of σ^o measurements from this low SNR state are performed using extended land targets with various signal strengths. Study areas include the Amazon rainforest, Congo rainforest, Argentina pampas, two regions in the Sahara desert, and a desert region in Australia. The effects of seasonal, azimuthal, incidence angle and local-time-of-day variations on σ^o are studied using data from two Ku-band sensors, QuikSCAT and RapidScat, for each study area. Calibration is preformed comparing RapidScat data from all SNR states to QuikSCAT data as well as comparing RapidScat low SNR state data to the nominal (high SNR) state data. Results from both calibrations are consistent with each other. Results suggest that σ^o is unbiased by noise for the ranges of σ^o covered in this study (-7 dB to -27 dB). However, the second low SNR state vertically polarized σ^0 appears to be biased lower than would be expected from year-to-year seasonal variation. The third low SNR state σ^o appears unbiased compared to the nominal RapidScat SNR σ^o.

Keywords: scatterometry, calibration, validation, land

Table of Contents

List of Tables

List of Figures

Chapter 1

Introduction

Wind scatterometers, which are microwave radars designed to measure the normalized backscatter coefficient (σ^o), see extensive use in weather modeling and prediction, and numerous other applications. When operating on a spaceborne platform, these sensors have the ability to make global observations with short revisits. Wind data gathered by these scatterometers over the ocean are used as inputs to the weather model to track and predict weather phenomenon from rain to hurricanes and even see use in monitoring shipping lanes. While the primary function of wind scatterometers is to gather wind data from over the ocean, data over land and ice also has many applications: Deforestation in the Amazon over time is measured using data from multiple scatterometers gathered over the years. Soil moisture over land is estimated. Ice bergs are tracked as they leave Antarctica, and the data is used to create safe shipping lanes. The ice melt cycle for large glaciers is observed, including annual changes in the cycle. The spatial coverage of ice in the Arctic region is measured and multiyear ice is distinguished from first year ice. In short, numerous fields depend on scatterometer data.

RapidScat is the fourth Ku-band wind scatterometer launched by NASA since 1996. It was preceded by NSCAT in 1996 and SeaWinds in 1999 and 2002. Another Ku-band scatterometer, OSCAT was launched by India in 2009. Since August 2014, the sensor has operated on the International Space Station (ISS). It is nearly identical to the hardware of SeaWinds on QuikSCAT (1999), except for modifications necessary to operate on the ISS instead of a weather satellite. RapidScat is unique among wind scatterometers; because of the orbit of the ISS, RapidScat can observe the diurnal cycle of σ^o over land. Like other wind scatterometers, the primary mission of RapidScat is to measure wind over the ocean and performed that function since its launch.

In August 2015, RapidScat began to exhibit strange behavior in its measurements that is believed to be caused by a change in receiver gain. Because of the this change in receiver gain, the measurements have a lower signal-to-noise ratio (SNR). For this reason, the new state is called a "Low SNR" state; in contrast, the nominal state is called "High SNR." This change is compensated for by adjusting the gain during post processing so that measurements are similar to what they were like before. By March 2016, three distinct low SNR states have been observed whose measurements require different adjustments in gain to be comparable to the measurements from the High SNR state.

The numerous applications of RapidScat data depend on the consistency of the measurements, so calibration and validation of the low SNR states is desirable. Adjusting the gain during post processing is a linear operation on the data, but it is unknown if the change in the RapidScat system is linear. There is a possibility that for low-valued σ^o measurements the gain adjustment is inappropriate. Furthermore, calibration and validation of the gain adjustment can establish that the RapidScat dataset is self consistent.

1.1 Approach

In this thesis, the range of RapidScat σ^o values is sampled by using land calibration targets that have different responses so that the linearity of the system may be observed. If the low signal study areas have similar behavior to the high signal study areas then the system is linear. The study areas are chosen to be homogeneous in measurement value and are analyzed for year-to-year seasonal variation, and measurement variation with respect to azimuth angle, incidence angle and the diurnal cycle. These study areas are used as land calibration targets for calibration throughout this thesis.

Two methods of calibration are used in this thesis. The first, and most established, is to calibrate RapidScat data from each RapidScat SNR state against QuikSCAT data. Observations are made about the differences between all of the RapidScat SNR states. Instrument drift over time is observed. Second, RapidScat Low SNR states (2 and 3 only, for reasons explained later) are calibrated against the High SNR state. This allows for more detailed observations of the differences between the RapidScat SNR states. Hypothesis testing is used

to detect if the SNR states are biased. Between the two calibration methods, a thorough analysis of the gain adjustment or calibration of each RapidScat SNR state is possible.

1.2 Results Summary

In this thesis, five land targets are developed for use in calibration. It is shown that from -7 dB to -27 dB, RapidScat Low SNR state measurements are unbiased by noise. Instrument drift over time is correlated with the Low SNR states. The adjustment gain for the RapidScat Low SNR 2 state could use some fine tuning. The RapidScat Low SNR 1 and 3 states are appear consistent with the RapidScat High SNR state. The system is linear and simple gain adjustments are appropriate to make Low SNR state measurements consistent with RapidScat High SNR state measurements.

1.3 Outline

The thesis proceeds as follows: Chapter 2 introduces topics of scatterometry, radar calibration, RapidScat, the RapidScat SNR states and datasets used in this thesis. Chapter 3 outlines a method for choosing and analysing land calibration targets by going into detail of the creation and analysis of the Amazon rainforest study area and summarizes the important details about the additional study areas used for calibration in this thesis. In Chapter 4, calibration of RapidScat against QuikSCAT is performed to observe differences in calibration between RapidScat SNR states and observe RapidScat instrument drift over time. In Chapter 5, RapidScat low SNR states 2 and 3 are calibrated against the nominal RapidScat high SNR state and hypothesis testing is used to detect if the SNR states are biased. A conclusion is given in Chapter 6. Appendix A uses the method from Chapter 3 and provides analysis of the additional calibration targets.

Chapter 2

Background

This section includes background material helpful to understanding the rest of the thesis. An introduction to spaceborne scatterometry and the many applications of scatterometer data is made. Elements of radar operation and calibration that relate to the accuracy of scatterometer measurements are discussed. The RapidScat scatterometer and its predecessor QuikSCAT are introduced and differences between the two sensors are highlighted. An explanation of the RapidScat SNR states is given. Datasets used in this study are introduced.

2.1 An Introduction to Spaceborne Scatterometry

A scatterometer is a microwave radar designed to measure the normalized radar-cross section, or backscatter coefficient (σ^o). In 1974, experiments were performed using the S-193 scatterometer aboard the Skylab space station and it was discovered that scatterometers are well suited for observation of ocean winds on a global scale. The continuous and global wind observations by these sensors provide valuable inputs to the global weather model. Since 1978, many wind scatterometer missions have followed, including these Ku-band sensors: SASS (1978), NSCAT (1996-1997), SeaWinds (1999-2009 and 2002), OSCAT (2009-2014) and RapidScat (2014-Present) [1, 2, 3].

When there are steady winds over the ocean, friction between the wind and the ocean surface causes waves to form. These waves result in a surface roughness that, when observed by microwave radar, results in backscatter that is related to the wind speed and direction relative to the radar look direction. Generally, increased wind speed means increased surface roughness and thus increased backscatter. When is backscatter measured at multiple look directions, both wind speed and direction can be estimated. The model for estimating

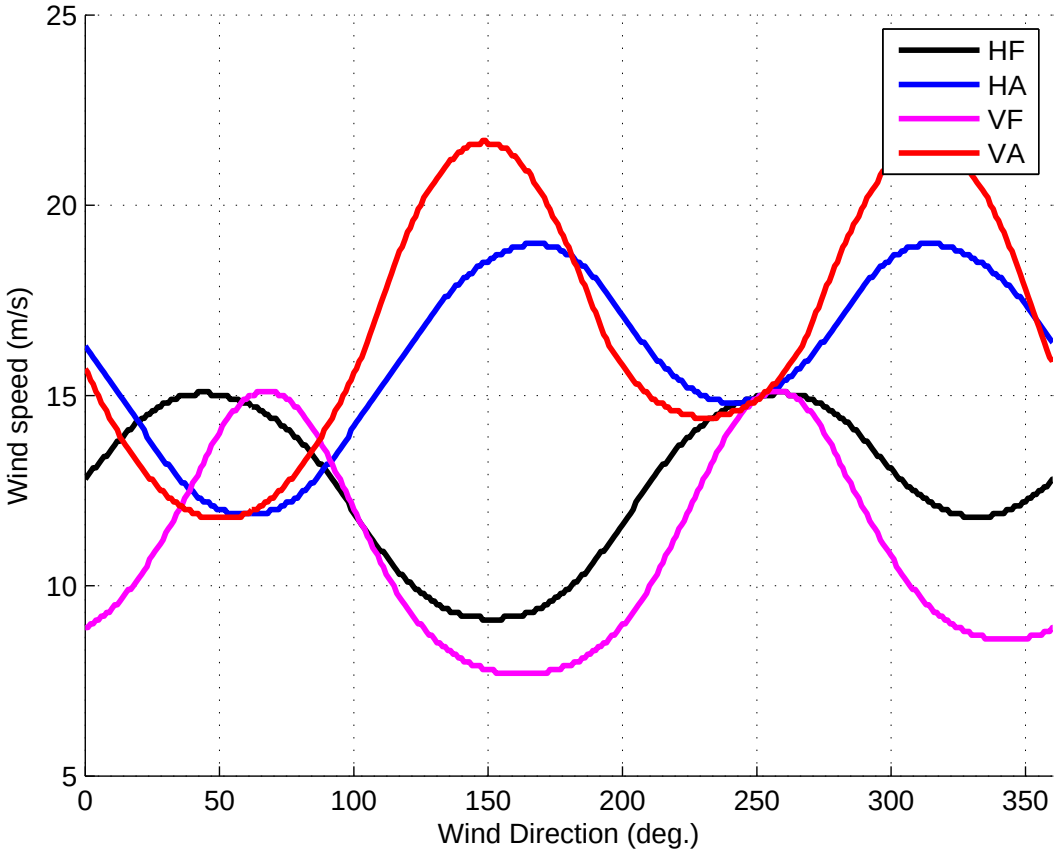

Figure 2.1: Possible OVW solutions corresponding to each observation flavor of a vector of noise-free QuikSCAT observations for a true wind speed of 15 m/s and direction of 250°.

wind speed and directions from scatterometer measurements is called the Geophysical Model Function (GMF). The GMF of σ^o does not provide one unique solution (see Figure 2.1). Wind retrieval requires three or more σ^o measurements to estimate Ocean Vector Winds (OVWs) and the retrieval is sensitive to noise in the σ^o measurements [1].

In addition to OVW contributions, scatterometer data has been used over land and ice to observe deforestation of the Amazon, track ice berg, ice melt, and multiyear ice, and other applications [1, 4, 5, 6, 7, 8].

2.2 Radar calibration

Radar calibration is an important part of ensuring a sensor's measurements are accurate and consistent enough for scientific use. Three strategies are employed together to

obtain the best σ^o measurements possible. First, internal calibration is done to allow us to measure the ratio P^r/P^t. Second, noise subtraction is performed to help remove receiver noise. Third, external calibration supplements the first two strategies by measuring the backscatter of a target with a known radar cross section and comparing the error [1].

Internal calibration is performed using the ratio method described in [1]. A calibration pulse is made by passing a transmitted signal through a known impedance and directly into the receiver. The power received during calibration, P_0^c, is measured. P_0^c is then a function of the transmit power, P^t, and the losses associated with the known impedance (which are modeled as a constant). The received power during target reception, P_0^r, can then be used in conjunction with P_0^c to measure the ratio

$$\frac{P^r}{P^t} = K_s \frac{P_0^r}{P_0^c}, \tag{2.1}$$

where P^r is the received power and K_s is an overall calibration constant that accounts for the internal losses of the system as modeled. Of course, the accuracy of internal calibration is dependent on the model for the system. The measured ratio P^r/P^t may then be used in the radar equation to calculate σ^o [1].

Noise subtraction is a technique to mitigate the noise in a received signal. The radar transmits a signal of known duration, and radar measurements are made while receiving the transmitted signal. Between radar measurements the receiver noise alone is measured. The noise-only measurement is scaled (to account for differences in bandwidth, integration time, etc.) and subtracted from the radar measurement to obtain an estimate of the signal alone. This greatly improves the accuracy of the radar measurements [1].

External calibration is desirable because the accuracy of internal calibration depends our model for the system, which is not perfect. Internal calibration provides a relative calibration, between measurements from the same sensor, while external calibration is more absolute, making measurements comparable with other sensors. External calibration can be preformed with a large homogeneous target with a known σ^o. The target's σ^o should have a smooth and slowly varying function of incidence angle (θ) and be independent of azimuth angle (ϕ). The Amazon rainforest is a well known, large, and homogeneous target that

Parameter	Seawinds	RapidScat
Frequency	13.6 GHz	13.6 GHz
Antenna Azimuths	All	All
Polarizations	v-outer/h-inner	v-outer/h-inner
Incidence Angles	46° and 54.4°	49° and 56° (nominal)
Daily Coverage	92%	65% between 58° N and 58° S
Mission and	QuikSCAT: 6/1999-11/2009	International Space Station
Dates	ADEOS II: 1/2002-1-/2002	10/2014-
Orbit Type	Sun-synchronous	Non sun-synchronous

Table 2.1: Seawinds and RapidScat system parameters.

can be used for external calibration. The Amazon has seen use in calibrating radiometers, scatterometers, and has been used to calibrate RapidScat against QuikSCAT [1, 9, 10, 11, 12, 13].

2.3 RapidScat

RapidScat is a Ku-band pencil beam scatterometer that was launched in August 2014 and is currently operating on the International Space Station. RapidScat is the fifth Ku-band wind scatterometer mission by NASA. The sensor replaces the Seawinds scatterometer on NASA's QuikSCAT satellite which operated from 1999 to 2009. For the rest of this thesis, Seawinds on QuikSCAT is referred to as QuikSCAT, to distinguish it from the other Seawinds mission. The RapidScat sensor is nearly identical to QuikSCAT, except that adjustments have been made so that it can operate on the ISS. Selected system parameters for both sensors are shown in Table 2.1.

2.3.1 Local time of day

While the adjustments to RapidScat make it operate similar to QuikSCAT in theory, in practice the irregular orbit of the ISS turns RapidScat into a unique sensor. First, large pitch has been shown to cause issues with the backscatter measurements [13]. Second, RapidScat has the ability to observe the diurnal cycle over land. Polar orbiting sun-synchronous sensors like QuikSCAT always pass over a given location at the same local time of day (LTOD). Because the orbit of the ISS is not sun-synchronous, the LTOD of measurements

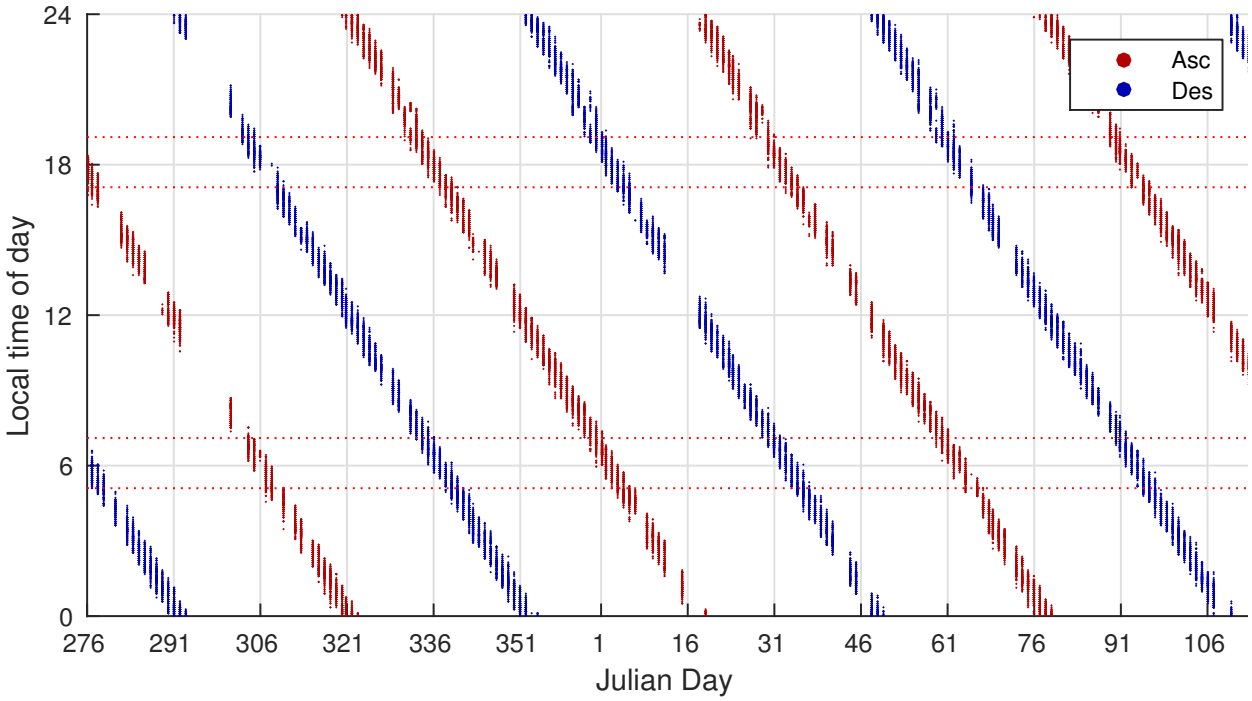

Figure 2.2: Local time of day of RapidScat observations over the Amazon rainforest for ascending and descending passes. For reference, QuikSCAT ascending and descending passes are always around 6h and 18h. Intervals denoted by the small red dotted lines represent local times of day show when RapidScat observations are within 1 hour of QuikSCAT observations.

at a given location on the earth's surface drift over time like is shown for observations over the Amazon rainforest in Figure 2.2. It has been shown that there is diurnal variability of Ku-band backscatter [13, 14].

2.3.2 SNR states

Nearly one year into the RapidScat mission, the sensor's measurements began to exhibit strange behavior that is believed to be caused by a change in the receiver gain. Due to the change in gain, resulting measurements have a lower signal-to-noise ratio (SNR). For this reason the altered state is considered low SNR. To allow continued use of the sensor, a linear correction is applied to σ^o to compensate for the change. The linear correction to σ^o is basically adjusting the gain after internal calibration and noise subtraction. The change in SNR is not stable. So far there are four known SNR states: the nominal (High SNR) state and Low SNR states 1, 2, and 3. Figure 2.3 shows how the RapidScat SNR states have

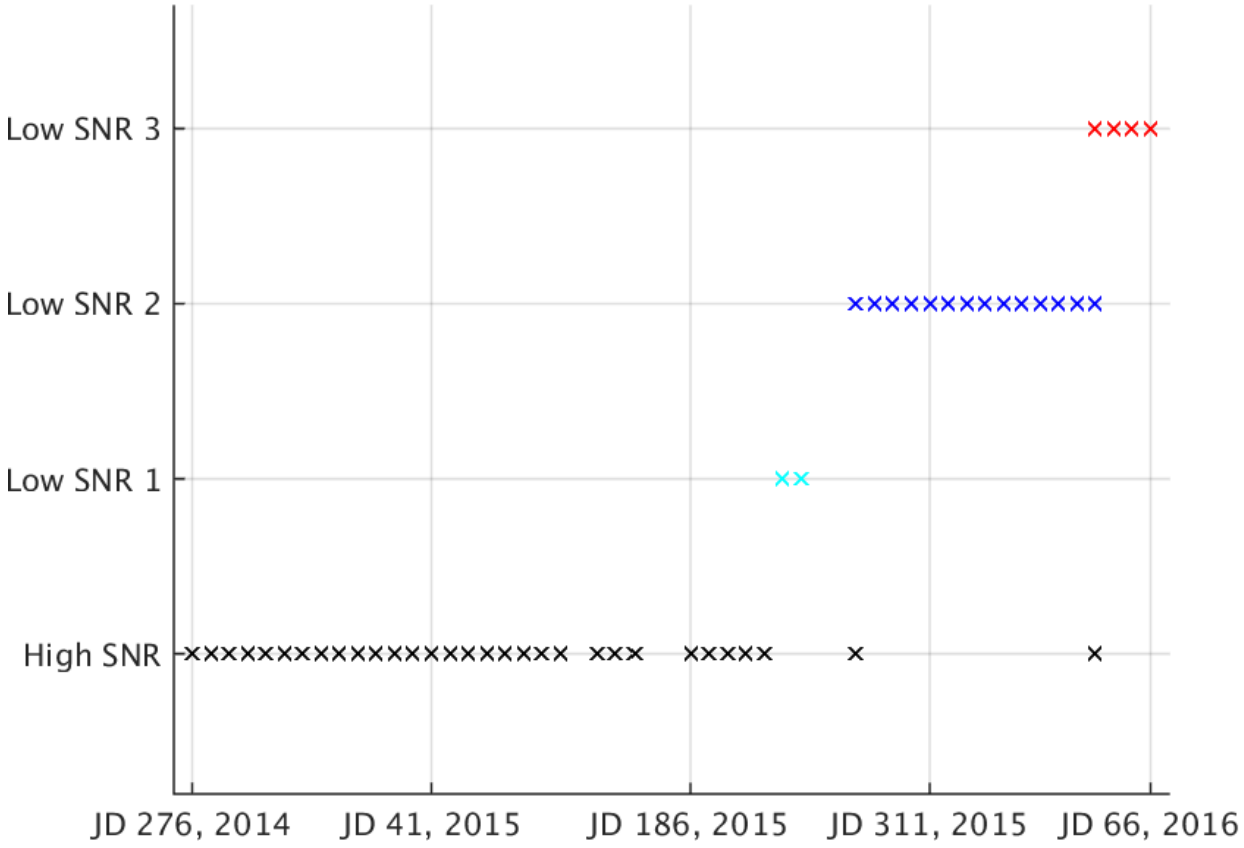

Figure 2.3: RapidScat SNR states over time.

progressed over time. The degraded state of RapidScat data was first noticed in data from August 2015, but some revolutions since then have the nominal (High SNR) state. Low SNR states 1, 2 and 3 each require different corrections to be comparable to the High SNR state and are considered separately in this thesis.

2.4 Datasets

Two QuikSCAT products are used in this study. The first is the QuikSCAT Enhanced Resolution Slice Image Product [15] which consists of enhanced resolution over-land σ^o measurements (for ascending/descending passes and h/v polarizations) on a 2.225 km/pixel grid for various land targets. The product is in the Scatterometer Image Reconstruction (SIR) file format, and the data is referred to SIR data. This product covers the entire QuikSCAT wind mission (1999-2009). SIR data used in this study comes from the Amazon, North Africa, South Africa, and South America regions. The second QuikSCAT dataset used in

this study is the QuikSCAT L1B product. L1B data contains σ^o, θ, and ϕ measurements, their time and locations (latitude and longitude information) [16].

RapidScat data used in this study, RapidScat L1B and ancillary data, is published and publicly accessible [17]. The L1B products for RapidScat and QuikSCAT are comparable. The ancillary data includes a "revtime.csv" file that includes the 5-digit orbital rev number, start date/time, stop date/time and a quality indicator. The quality indicator summarizes if the data is "GOOD", "BAD", or "MARGINAL", specifies the RapidScat SNR state and if there is large pitch. Examples of SNR states include: "High SNR", "Low SNR 1","Low SNR 2","Low SNR 3", or "Mixed SNR state". For this study, RapidScat L1B data flagged as "GOOD", one of the SNR states (not "Mixed"), and not "Large Pitch" is used [17].

Chapter 3

Calibration Targets

3.1 Introduction

In this section, the methodology for identifying land targets for external calibration is outlined. Land calibration targets are analyzed for consistency, and so that it is understood under what circumstances observations of the study areas are accurate. The method is shown in detail for the Amazon rainforest study area, while details for the other study areas are discussed in Appendix A. The results for all study areas are summarized at the end of this section.

3.2 Methodology

Extended land targets are selected using QuikSCAT data and analyzed using both QuikSCAT and RapidScat data. For this report, the closest thing to truth data is the QuikSCAT data set. The sensor was in operation for ten years, allowing for sufficient averaging to be very confident in its data. First, the average QuikSCAT σ^o for the entire mission is used to identify the spatial extent of homogeneous land targets. Then, seasonal and azimuthal analysis are done. Further analysis is done using RapidScat data to measure the σ^o dB/deg incidence angle relationship and examine the effects of local time of day (LTOD) on σ^o. This method is explained step by step for the Amazon rainforest study area.

Enhanced resolution land σ^o images [15], created using Scatterometer Image Reconstruction (SIR), are used to identify the homogeneous land target. The QuikSCAT SIR dataset containing data over the Amazon region from 1999 to 2008 is averaged for each flavor (where a "flavor" is a combination of ascending or descending orbit, and horizontal or vertical polarization). The average ascending horizontal polarization QuikSCAT σ^o SIR image is shown in Figure 3.1. A histogram of the pixel valuesis given in Figure 3.2, showing

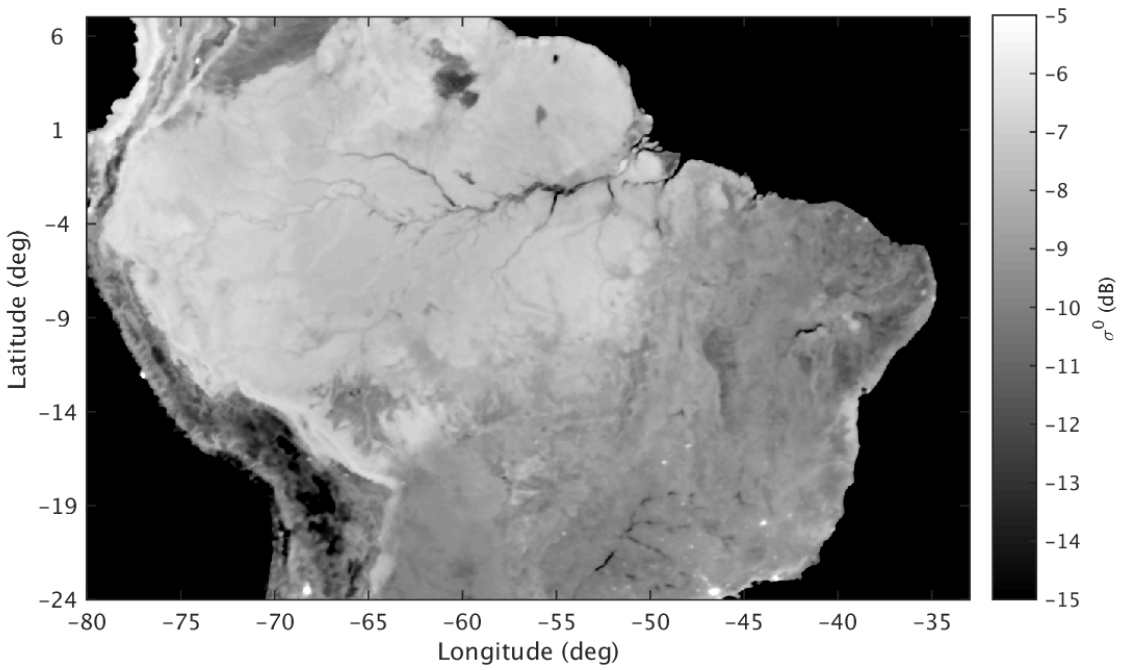

Figure 3.1: This SIR image shows the average ascending H-pol σ^o for the QuikSCAT SIR dataset for the Amazon region for the years 1999 to 2008. The extent of the Amazon rainforest is already visible to the eye.

three distinct modes which generally correspond to ocean measurements (around -25 dB), rainforest (around -7 dB) and non-rainforest (around -10 dB) pixels. An iterative moving average approach is used to select the largest number of pixels in a 1 dB range of σ^o, effectively selecting the pixels to corresponding to the rainforest mode observed in Figure 3.2 (a histogram of σ^o included in the final mask is shown in Figure 3.4). All locations that are included in all four flavors are included in a mask by latitude and longitude, which is shown in Figure 3.3 for the same area shown in the SIR image (Figure 3.1) [13].

The initial mask (Figure 3.3) has a lot of spatial outliers that the author subjectively chooses to remove. While these outliers match the σ^o of our study area and may very well be rainforest, it is desirable that the mask be robust to pointing and positioning errors that may

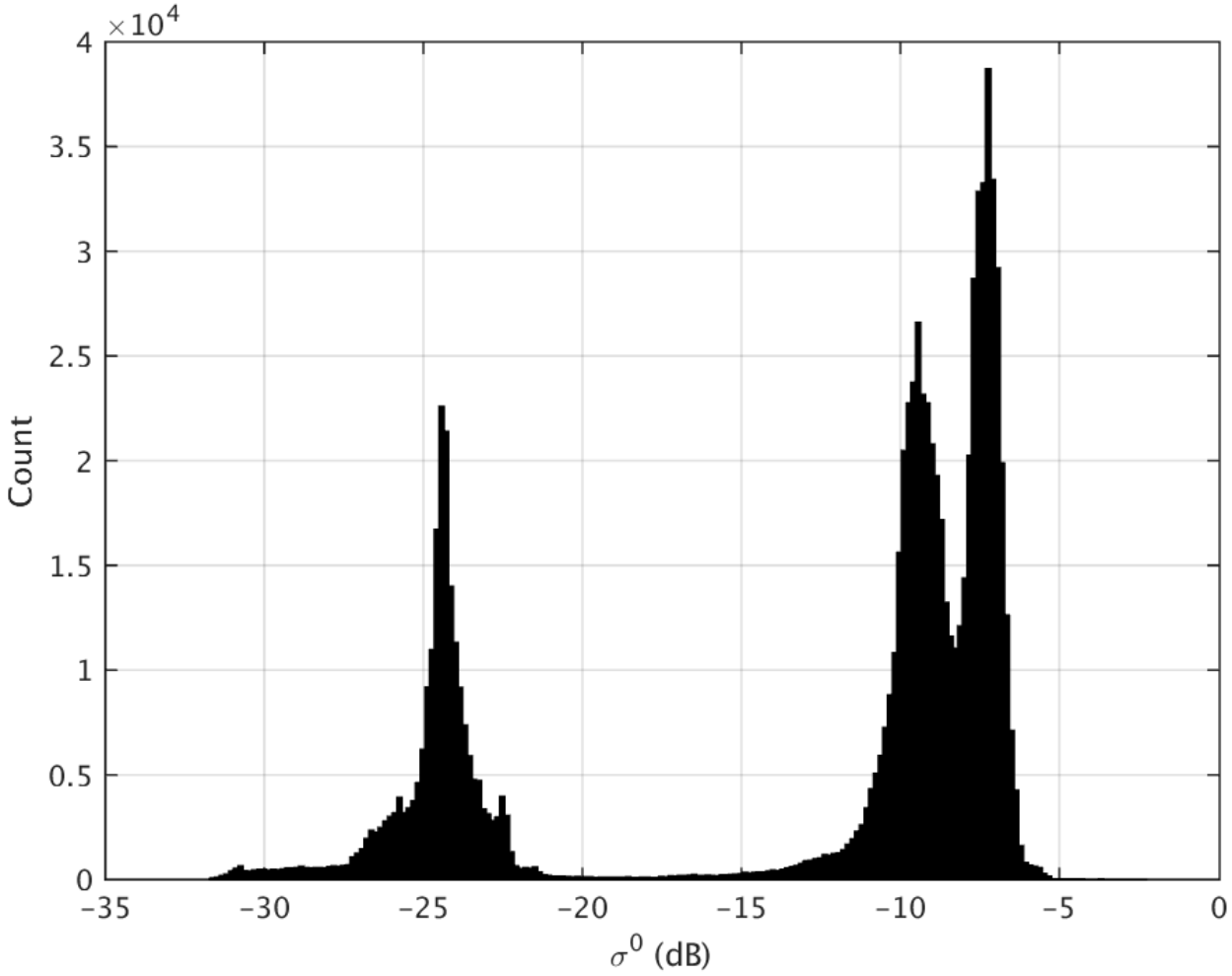

Figure 3.2: A histogram of QuikSCAT ascending H-pol σ^o for the Amazon region, created from the mission dataset. Three modes are evident in the histogram that generally correspond to ocean/water (-25 dB), rainforest land (-7dB) and non-rainforest land (-10 dB).

occur. Spatial outliers are subjectively removed, especially where the mask is thin. Areas inside the mask that are not initially included are filled in if they are smaller than a certain size. A histogram of σ^o included in this edited mask is shown in Figure 3.4, and shows that this mask generally includes pixels in a 1 dB range, as designed. This mask, created from SIR data and then manually edited, becomes the Amazon rainforest calibration target for this study. The mask is shown in Figure 3.5.

A study of year-to-year seasonal variation of the Amazon rainforest study area is done using 9 years of QuikSCAT L1B data [16]. Data is extracted for the entire QuikSCAT mission (1999-2008) using the Amazon rainforest mask (Figure 3.5). The masked data is used to

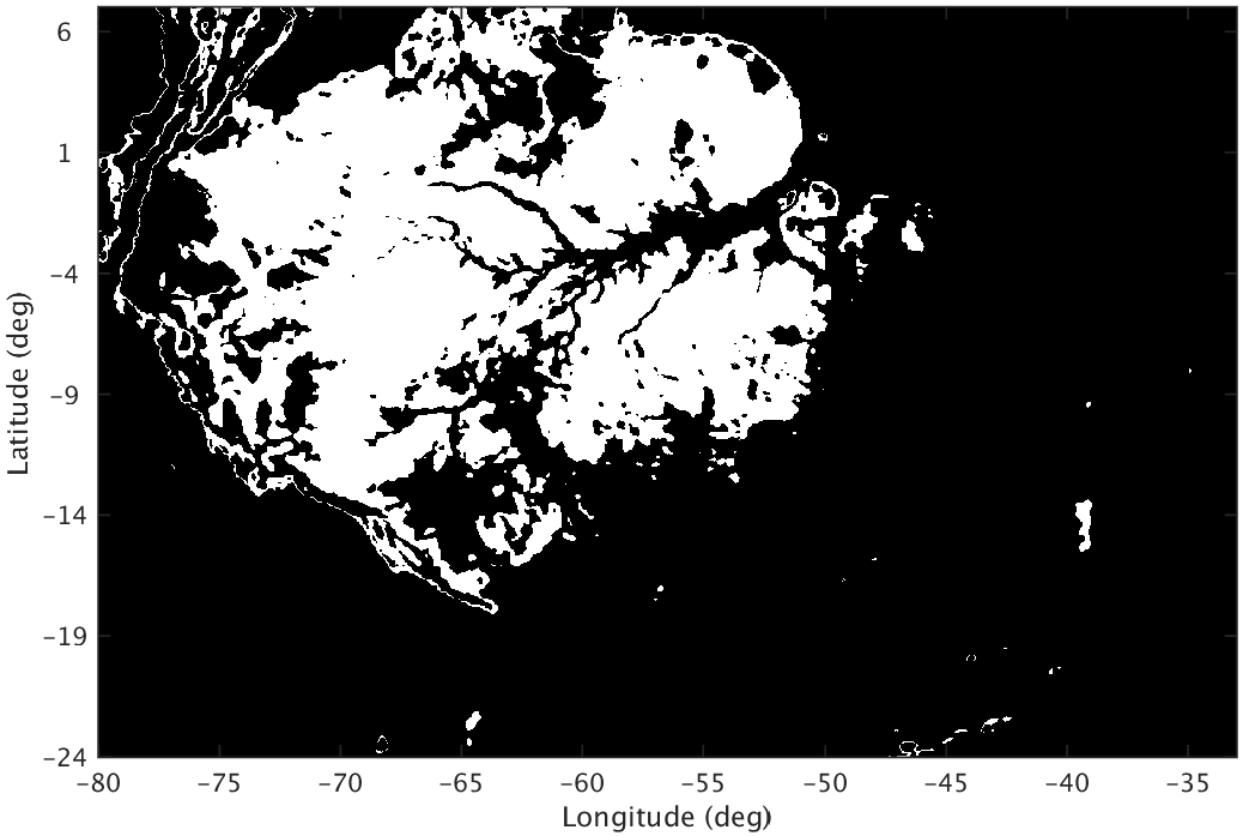

Figure 3.3: Latitude/longitude mask showing the pixels area of the largest number of σ^o values in a 1 dB range for the QuikSCAT SIR data. Notice that there are a lot of spatial outliers and small holes in the rainforest.

create ten-day averages of σ^o for the calibration target from 1999 to 2008. In Figure 3.6, the yearly averages are subtracted from the ten-day averages to obtain the deviation from mean σ^o that shows the seasonal variation that the Amazon rainforest experiences. The confidence interval with respect to year-to-year variation is the standard deviation of the deviation from mean σ^o, with $\gamma = 0.995$. The difference between ascending and descending passes is best explained by the diurnal cycle shown in (Figure 3.9) and is considered later The seasonal variation for the Amazon rainforest (Fig. 3.6) is very small, less than 0.4 dB overall, and is very homogeneous–ideal for a land calibration target. The most accurate calibration comes from measurements of the same season [13].

The azimuth study is done using the masked QuikSCAT L1B data where σ^o measurements are binned by azimuth angle (10 degree bins) for each year. The Amazon rainforest

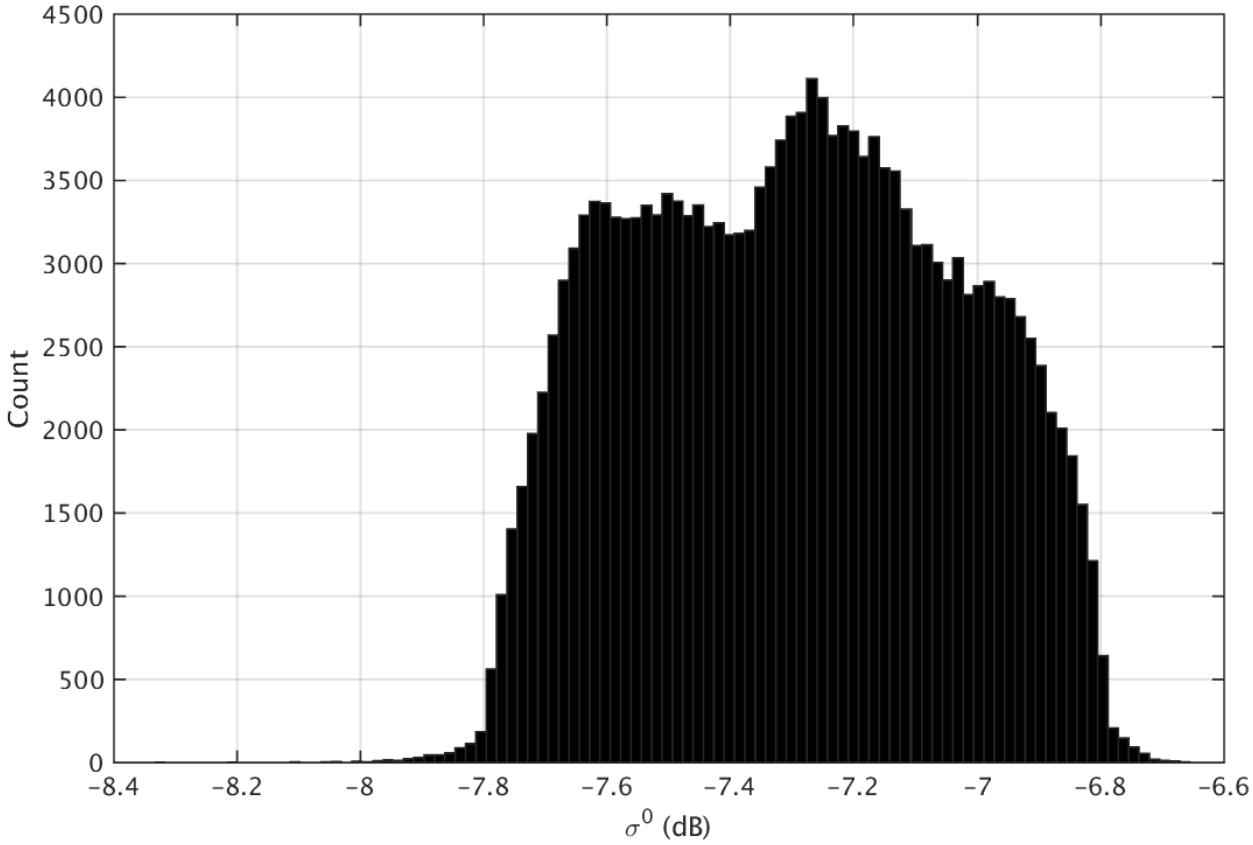

Figure 3.4: Histogram of ascending H-pol QuikSCAT σ^o within edited mask for the study area (Figure 3.5). This shows that the edited mask generally includes pixels with σ^o values within $\pm$ 0.5 dB of the mean, -7.3 dB.

(See Fig. 3.7) has very little azimuth modulation, less than 0.1 dB across all azimuth angles [13]. Because both QuikSCAT and RapidScat measure σ^o at all azimuth angles, and the distribution of azimuth angle is uniform any influence from azimuthal variation over these targets averages out and is ignored during calibration. Even if there was irregular sampling that resulted in a bias, the bias due to azimuth angle would be less than 0.1 dB.

RapidScat makes measurements over a range of θ, between 46° and 52° for the inner beam (h-pol) and 52° and 58° for the outer beam (v-pol), while QuikSCAT θ is fixed, 46.25° for inner beam and 54° for the outer beam. In order to enable accurate calibration, σ^o measurements are normalized in θ. To measure the σ^o dB/ deg relationship, RapidScat L1B data [17] is masked with mask created from QuikSCAT data (Figure 3.5). Binned σ^o data by θ (0.25° bins) is used to see the range of θ (Fig. 3.8). A first-order polynomial fit of the masked σ^o to θ is used to measure the σ^o dB/deg relationship for the Amazon rainforest

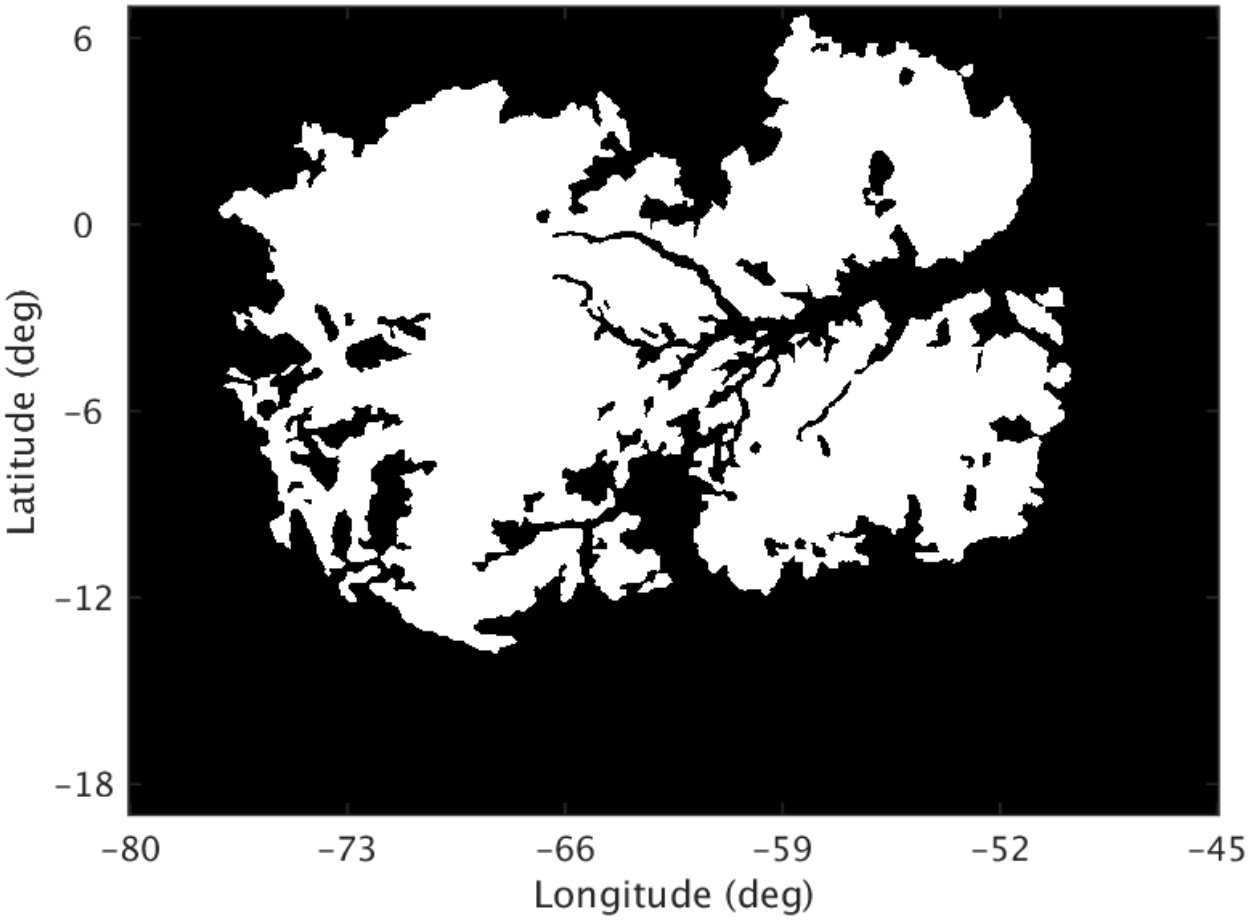

Figure 3.5: Final latitude/longitude Amazon rainforest mask mask representing the Amazon rainforest study area. Spatial outliers have been subjectively removed and holes of a certain pixel size or smaller have been included.

(Fig. 3.8) [13]. The σ^o dB/deg slope (Table 3.2) is used to normalize the σ^o measurements to QuikSCAT incidence angles for calibration.

Unlike other sensors (e.g., the sun synchronous polar-orbiting QuikSCAT) whose ascending and descending orbits happen at approximately the same LTOD each pass, RapidScat observes the Earth's surface in a non-sun-synchronous orbit and thus at different LTOD as the orbits progress. A comparison of σ^o by LTOD (Figure 3.9) shows the general trend of σ^o during the diurnal cycle. The Amazon study area experiences a sharp increase in σ^o around sunrise, which is likely due to the dew cycle [13]. However, between 10 and 16h LTOD, the trend is very consistent. In order for calibration to be independent of the effects of LTOD on σ^o, measurements should come from the same LTOD or from a LTOD range

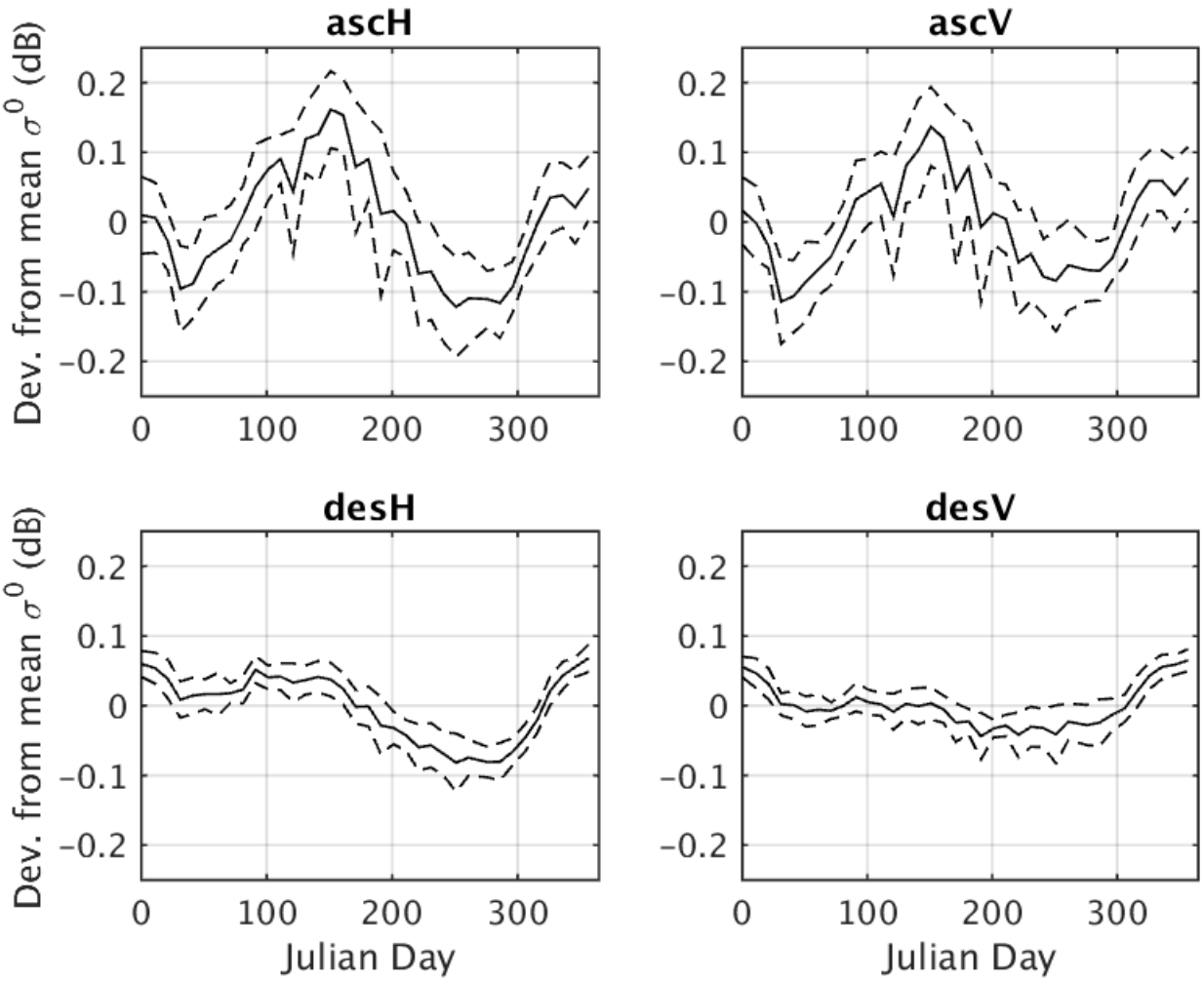

Figure 3.6: Seasonal variation of σ^o for the Amazon rainforest calibration target shown as the deviation from mean σ^o for each flavor of QuikSCAT (with a confidence interval that is the standard deviation of the deviation from mean σ^o). See text for details of how this plot is generated.

where there is little change in σ^o. For this study, measurements are considered the same LTOD when within 45 minutes of each other. Thus, calibration measurements are most accurate for this study area when within 45 minutes LTOD or from 10 to 16h LTOD.

Variance in the diurnal cycle of the Amazon study area as observed by RapidScat is observed by performing the LTOD analysis for different seasons. Three seasons have been defined for the Amazon study area. The wet seasons are: JD 335 to JD 30 and JD 31 to JD 141. The dry season is defined as JD 151 to JD 243. The dry season falls during a time when there is not two entire months of High SNR data (See Figure 2.3) so there are some LTODs

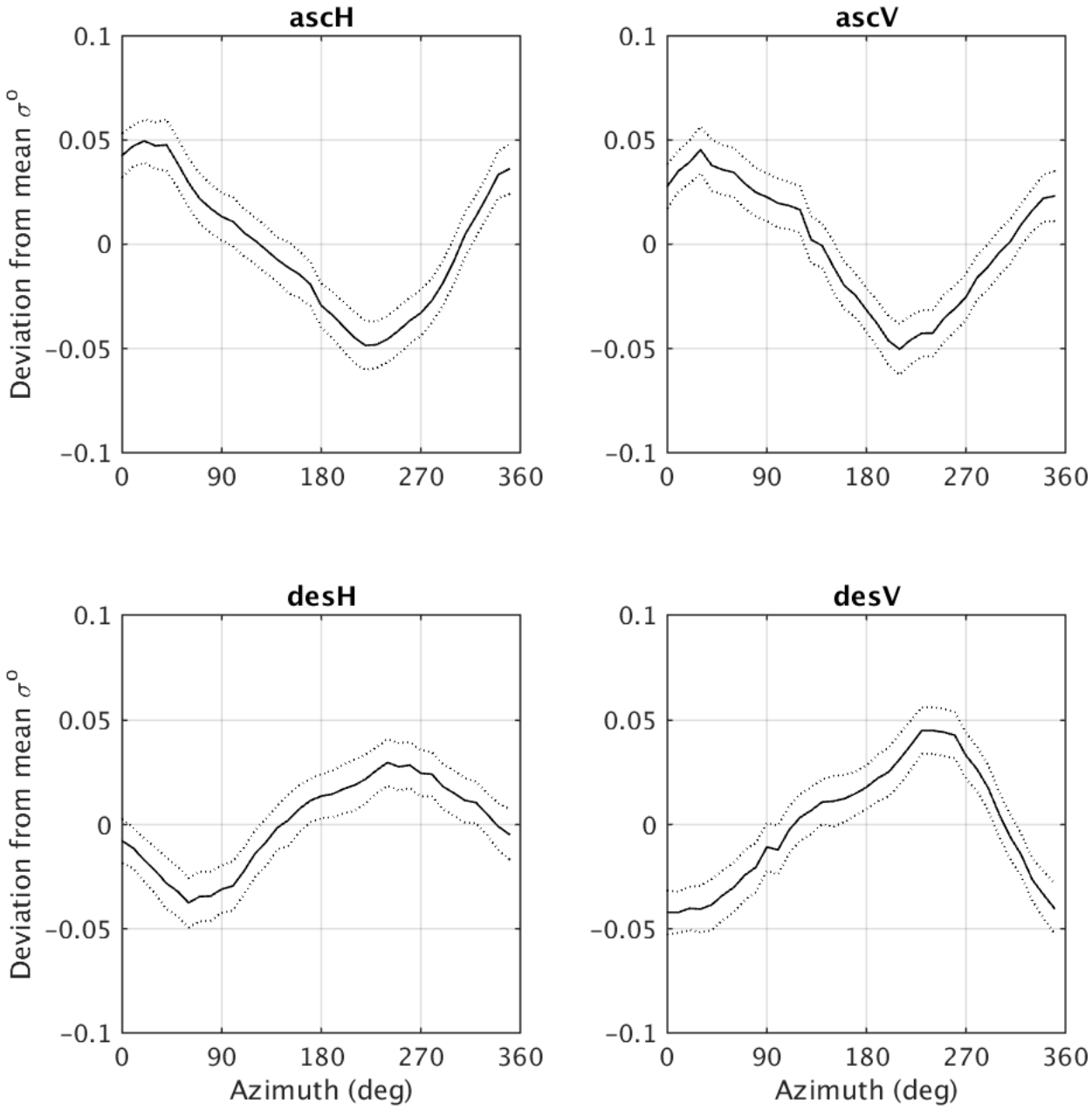

Figure 3.7: Azimuth modulation of the Amazon rainforest relative to the mean σ^o with the confidence interval is the standard deviation of σ^o.

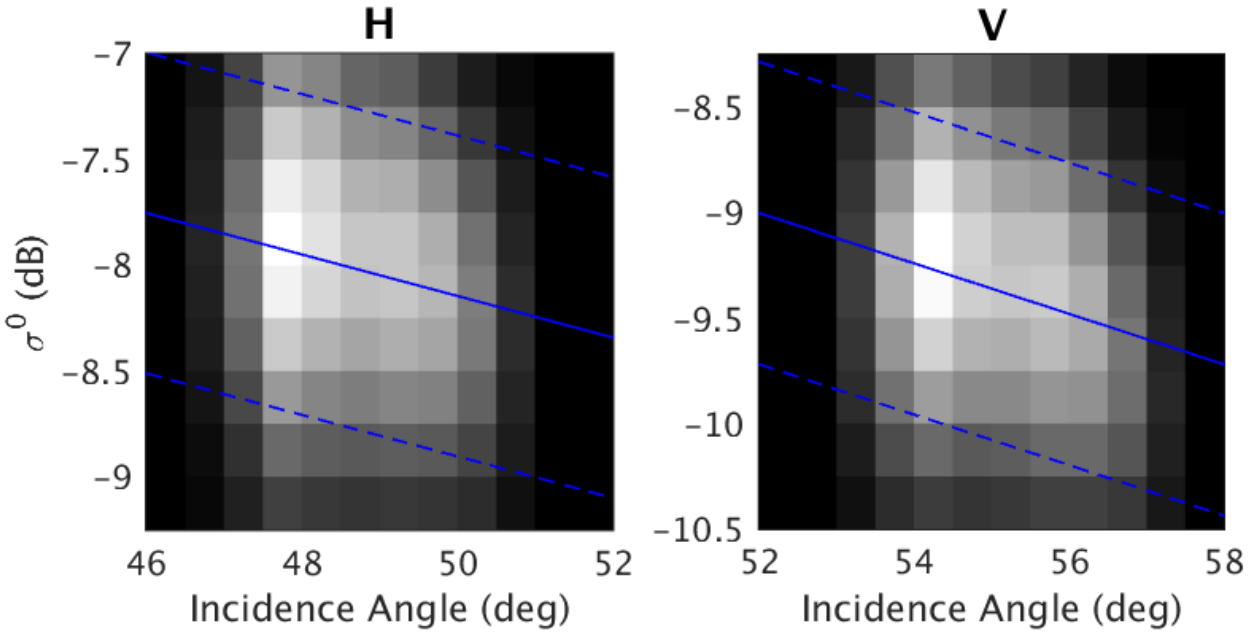

Figure 3.8: Two dimensional PDF of the distribution of σ^o measured by RapidScat at each incidence angle (0.25^o bins) for the Amazon rainforest. The blue line is the first order polynomial fit to the data and the slope of the line represents the σ^o dB/ deg incidence angle relationship. The dashed line is the $\pm$ one standard deviation for the estimate.

that are not observed. The LTOD curves for the three seasons are shown in Figure 3.10. There is an expected shift in mean σ^o, as seasonal variation is observed in Figure 3.6, and some variation in shape. Generally, the curves are very similar to the overall LTOD curve in Figure 3.9, which suggests that the observations calibration measurements are accurate for this region within 45 minutes or from 10h to 16h LTOD no matter the season.

In summary, we confirm that the Amazon rainforest study area is a good calibration target. It is large, homogeneous, azimuth variation is small enough to be ignored, and σ^o is a simple function of θ. For the most accurate calibration of σ^o, measurements should come from the same season and within 45 minutes LTOD or in the 10-16h LTOD range. This

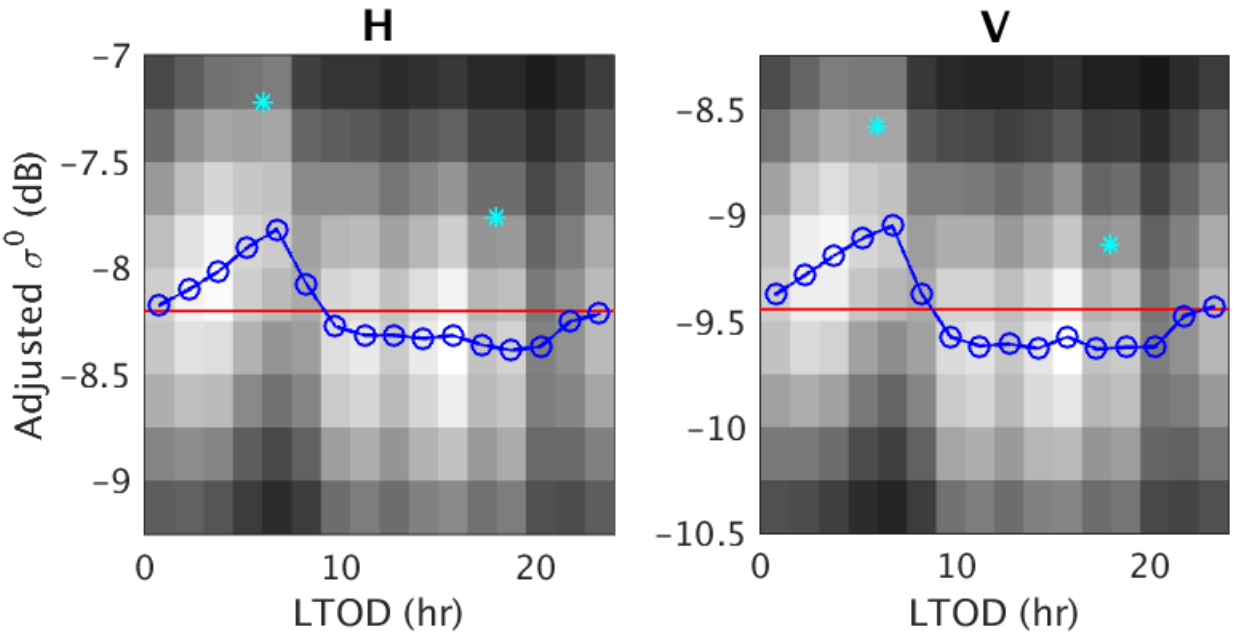

Figure 3.9: Two-dimensional PDF of RapidScat σ^o from the Amazon rainforest calibration target for 90 minute LTOD bins. In blue, the mean σ^o (o) for each LTOD bin is show with a confidence interval that is $\pm$ the standard deviation for that bin. Notice the large increase around sunrise.

calibration target has the potential to measure biases between RapidScat High SNR σ^o and Low SNR σ^o larger than the confidence intervals for the estimates.

3.3 Other targets

The focus of this study is the bias of σ^o measured by RapidScat in it's "High" and "Low" SNR states and whether or not the bias is different in lower signal targets. This analysis requires calibration targets beyond the typically used Amazon rainforest. A 1989 study of over-land σ^o using Ku-band scatterometers [18] demonstrates that there are land regions with various mean σ^o. Some of these land regions were used in the procurement of extended land targets with different mean σ^o, and those used in report are shown Table 3.1.

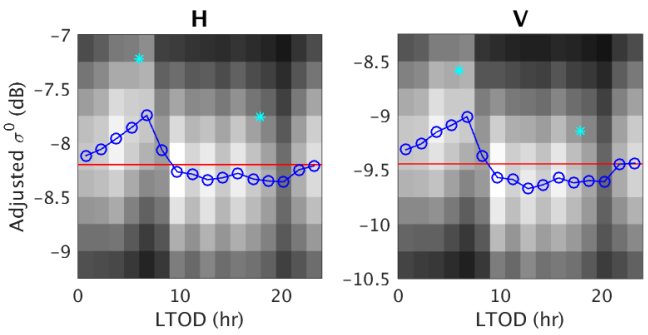

(a) Wet Subseason 1: JD 335 to JD 30

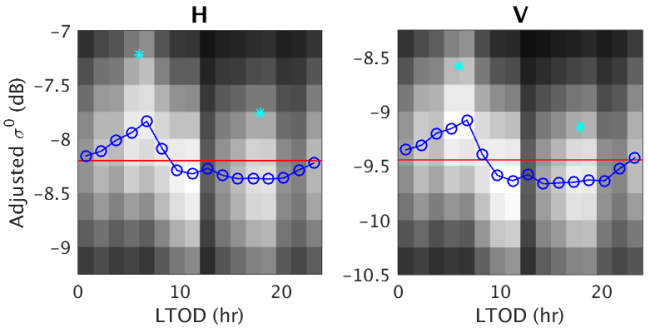

(b) Wet Subseason 2: JD 31 to JD 140

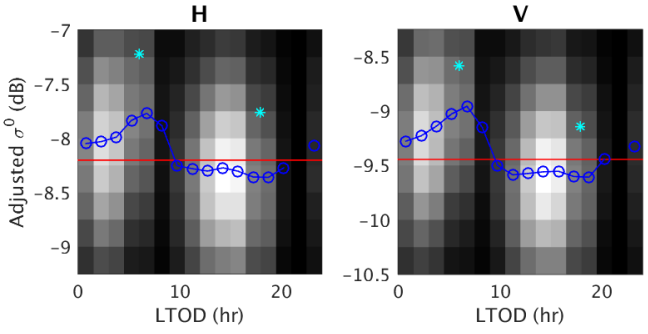

(c) Dry Season: JD 152 to JD 243

Figure 3.10: Two-dimensional PDF of RapidScat σ^o from the Amazon rainforest study area for 90 minute LTOD bins for 3 different seasons. In blue, the mean σ^o (o) for each LTOD bin is shown. The red line is the mean σ^o calculated using all of the RapidScat High SNR data.

Study Area	Size ($\times 10^3$ px)	QuikSCAT Mean σ^o h-pol/v-pol (-dB)	RapidScat Mean σ^o h-pol/v-pol (-dB)
Amazon Rainforest	176.8	7.2/8.5	8.2/9.4
Congo Rainforest	72.6	6.9/8.2	7.9/9
Argentina Pampas	4.8	11.5/13.3	12/13.6
West Sahara	3.8	17.2/17.3	18.3/18.2
Australia Desert	12.4	16.9/18	16.9/18.3
Sahara Erg Sea	12.5	26/27	26.7/27.5

Table 3.1: Study areas for land calibration with different mean σ^o. The size of the study area is measured in pixels included in the mask for the region shown in Figure 3.11. Each pixel is 1/24 deg latitude $\times$ 1/24 deg longitude. The mean σ^o for QuikScat and the nominal RapidScat state (High SNR) are calculated using masked L1B data.

Non-rainforest calibration targets have greater variation of σ^o, the backscatter is a different function of θ which may or may not be as smooth and may not be as independent of azimuth; that is, they may not be as accurate (or deterministic) as the standard rainforest calibration targets. Despite the imperfections non-rainforest calibration targets exhibit, they can provide valuable information rainforest calibration targets cannot and as long as the conditions are right the information can be accurate.

The same method used to identify and analyze the Amazon study area is applied to each study area used in this thesis. Appendix A goes detail about the additional land calibration targets used as study areas in this thesis.

(a) Amazon Rainforest

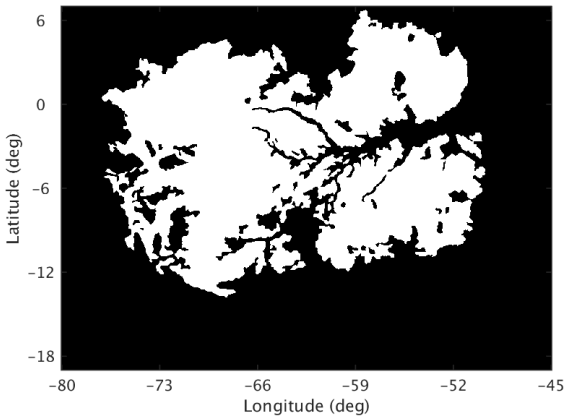

(b) Congo Rainforest

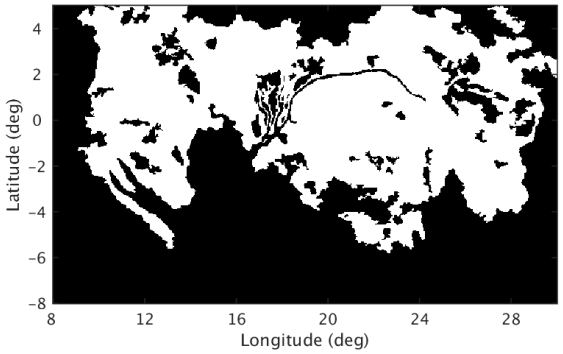

(c) Argentina Pampas

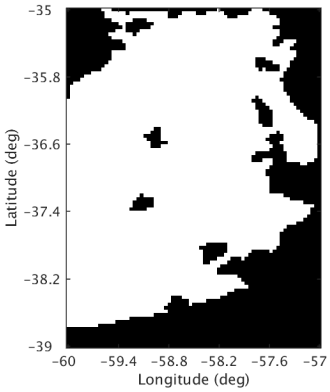

(d) West Sahara

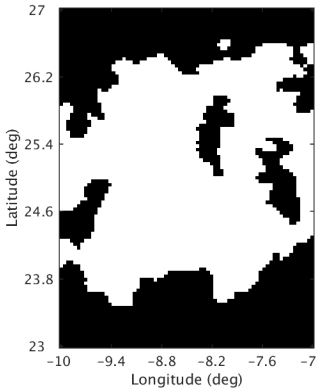

(e) Austrialian Desert

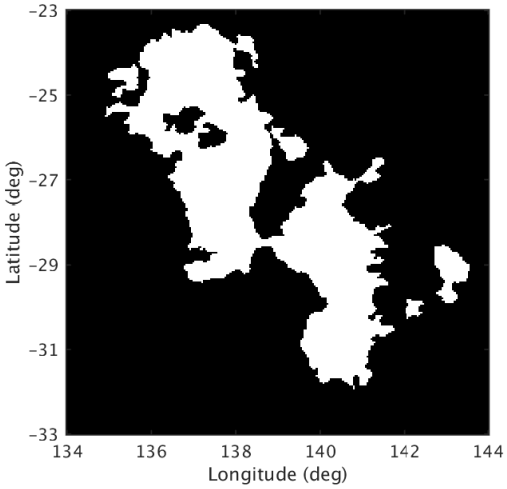

(f) Sahara Desert

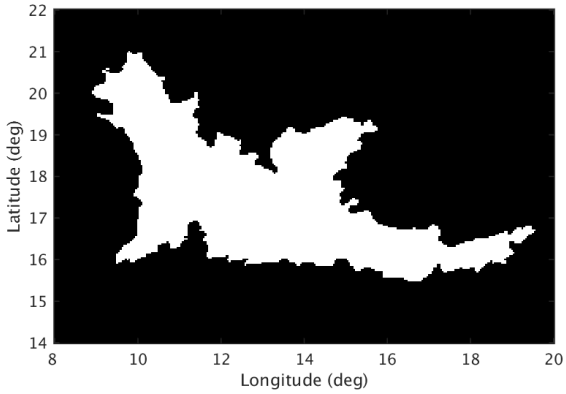

Figure 3.11: Spatial masks for the 6 calibration targets

Study Area	σ^o dB/deg θ		LTOD	
	H-pol	V-pol	Threshold	Range
Amazon	-0.098	-0.120	45 min	10-16h
Congo	-0.096	-0.106	45 min	10-16h
Pampas	-0.094	-0.187	45 min	N/A
W. Sahara	-0.246	-0.181	45 min	6-12h
Aus. Desert	-0.077	-0.029	45 min	N/A
Sahara Erg Sea	-0.015	-0.025	45 min	N/A

Table 3.2: Incidence Angle Dependence (dB/deg) as measured by RapidScat over different land targets.

3.4 Results

Six different study areas are used as calibration targets in this thesis. They were chosen to span a large range in σ^o. The size and mean σ^o as measured by QuikSCAT and RapidScat are shown in Table 3.1. The incidence angle adjustments used to normalize RapidScat σ^o to QuikSCAT incidence angles through out the rest of this thesis are shown in Table 3.2. The LTOD criteria for direct comparisons between RapidScat High SNR and Low SNR σ^o is also shown in Table 3.2.

The largest and most homogeneous are the Amazon and Congo rainforests, which are well suited to measure the small differences between RapidScat High SNR σ^o and Low SNR σ^o during calibration. They both cover a similar range of σ^o, and so comparing the calibrations of the two study areas to each other may decrease the influence of year-to-year seasonal variation on the observations.

The lower signal study areas enable us to validate the linearity and calibration of RapidScat Low SNR σ^o for lower values of σ^o and make observations about whether or not the Low SNR σ^o is biased.

Chapter 4

Calibration using QuikSCAT

4.1 Introduction

This chapter seeks to cross-calibrate RapidScat σ^o to QuikSCAT σ^o. The success of calibration using extended land targets depends on the how stable and consistent the target σ^o is. While it is impossible to know the true σ^o of an extended land target, ten years of QuikSCAT σ^o allow an estimate of σ^o of the land target with a narrow confidence interval.

Different methods have been suggested for calibrating RapidScat against QuikSCAT in [13]. Because of the short duration of some of the RapidScat SNR states, in this thesis the RapidScat data is split by time of year and then compared those averages with QuikSCAT data taken from the same time of year. The QuikSCAT dataset is well suited for this calibration method because data has been collected for all of the study areas discussed in Chapter 3 for all times of the year. This method of comparison also allows for observations of the instrument drift that are not with RapidScat data alone.

This chapter explains the methodology for comparing RapidScat data to QuikSCAT data. Instrument drift over time is analyzed using the comparison of RapidScat data to QuikSCAT data. Overall mean bias estimates of the bias between RapidScat and QuikSCAT σ^o for all of the RapidScat SNR states is reported and discussed.

4.2 Method

Data from the QuikSCAT L1B dataset is extracted for the entire QuikSCAT mission (1999-2008) using the Amazon rainforest mask (Fig. 3.5). Ten-day, yearly, and mission averages of σ^o are calculated using the masked data. Seasonal variation is then measured as deviation from mean σ^o, as shown in Figure 4.1. This is calculated by subtracting the year mean from each ten-day average and then finding the mean and the standard deviation, $s_{\triangle}$, of

the difference. The mission mean σ^o plus the seasonal variation is the QuikSCAT estimate that is compared with the RapidScat data. The confidence interval for this QuikSCAT estimate is

$$\sigma^o \pm \left(z_u \frac{s_\square}{\sqrt{M}} + t_u(10) \frac{s_\triangle}{\sqrt{N}} \right), \tag{4.1}$$

where z_u is the standard normal density function, $t_u(n)$ is the student distribution function, u is the percentile, $s_\square$ is the standard deviation of $M(> 150{,}000)$ measurements and $s_\triangle$ is the standard deviation of the "deviation from mean σ^o" over $N(= 10)$ years. This confidence interval is dominated by the year-to-year variation measured by $s_\triangle$ because M is so large; since $t_{0.995}(10) \approx \sqrt{10}$, the standard deviation of the "deviation from mean σ^o" as shown in Figure 4.1 (for the Amazon rainforest calibration target) is representative of the confidence interval of the QuikSCAT estimate.

RapidScat data is masked using the spatial mask created from the QuikSCAT data (Figure 3.11). The masked data whose LTOD is within 1 hour of QuikSCAT ascending/descending times is averaged into the same ten-(Julian)-day bins as the QuikSCAT data. The confidence estimate for the RapidScat estimate is larger than for QuikSCAT because there are fewer years of data (for most cases, only one "year" is available for comparison purposes in each ten-day bin because of the change in SNR state). In the following comparisons, a 80% confidence interval is used, calculated using $N = 1$ and $u = 0.9$ in (4.1).

Where RapidScat ten-day σ^o estimates exist for a particular SNR state, they are compared to the corresponding ten-day QuikSCAT σ^o estimate as shown in Figure 4.2 for the Amazon rainforest calibration target. Outliers in these figures are generally due to fewer RapidScat measurements falling into the respective ten-day bin; this shows up clearly in the larger than average RapidScat σ^o confidence intervals in Figure 4.2. The bias, shown in Figure 4.3 appears to be generally consistent, with notable outliers near the time when the low SNR state was first diagnosed (JD 213-242). Possible explanations for the outliers include noisier estimates due to fewer measurements, mistaken RapidScat SNR state diagnosis (the wrong σ^o correction used), or that the actual σ^o is outside the 80% confidence interval.

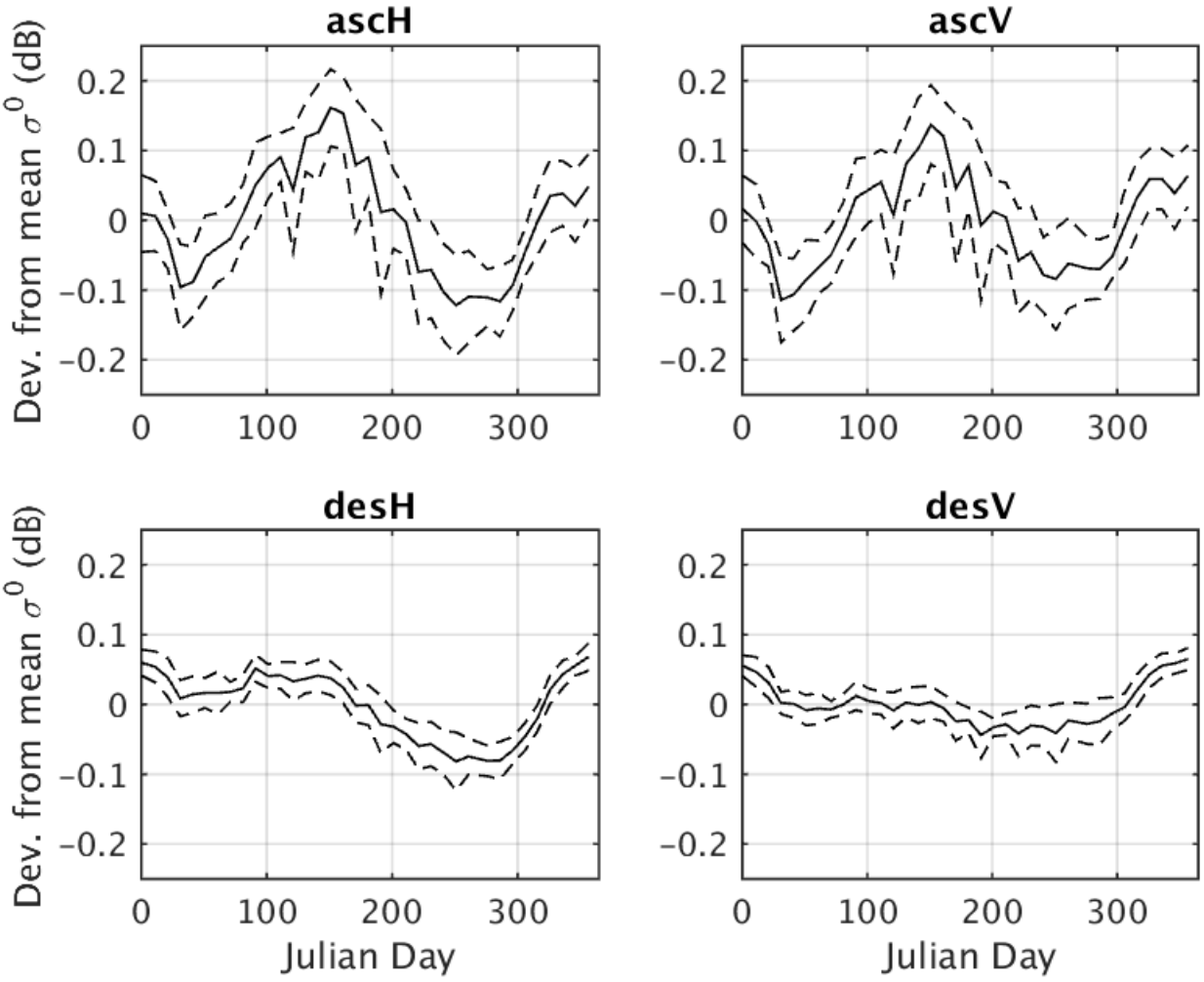

Figure 4.1: Seasonal variation of σ^o for the Amazon rainforest calibration target shown as the deviation from mean σ^o for each flavor of QuikSCAT (the confidence interval shown is the standard deviation of the deviation from mean σ^o).

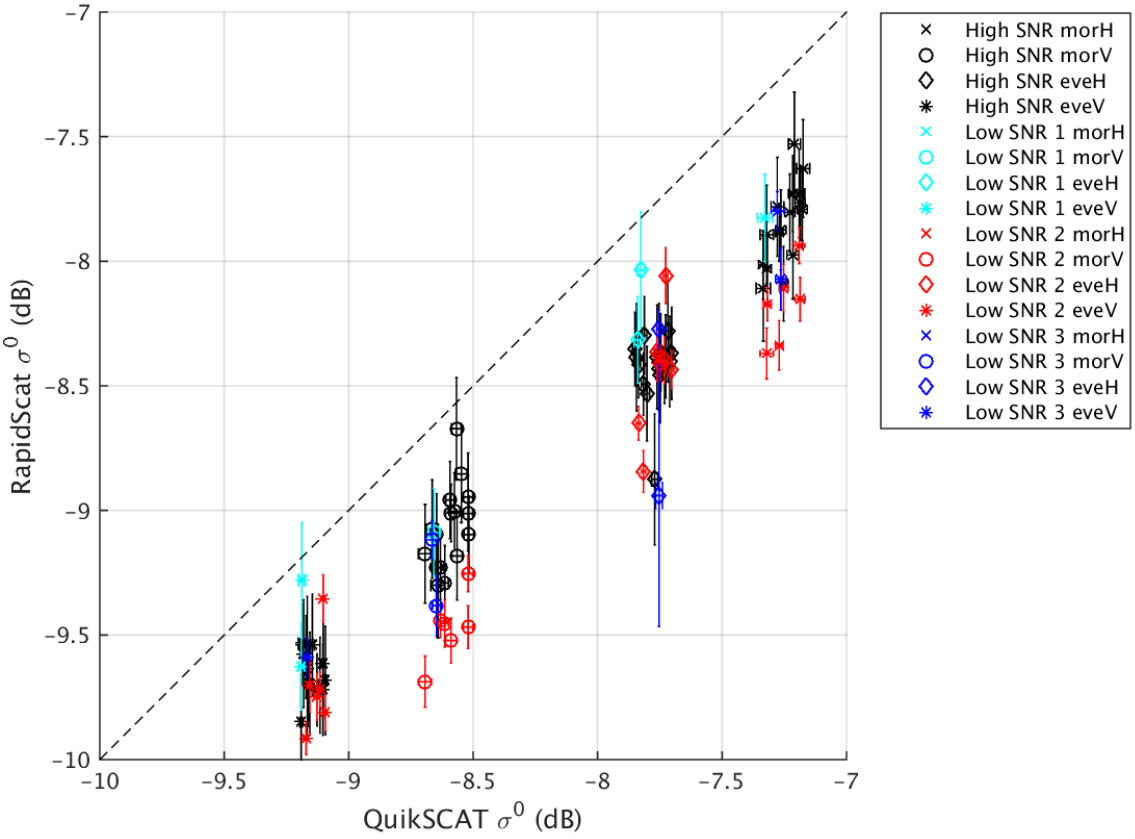

Figure 4.2: RapidScat High and Low SNR 1/2/3 σ^o is compared to QuikSCAT σ for the Amazon study area. Measurements are within 1 hour of QuikSCAT LTOD. QuikSCAT σ^o confidence intervals are small because there are 10 years of data. Larger than average RapidScat σ^o confidence intervals generally correspond to a small number of measurements. RapidScat σ^o is biased low compared to QuikSCAT σ^o. For this study area, the comparisons are grouped by QuikSCAT flavor (Morning or Evening and H-pol or V-pol).

4.3 Instrument Drift Over Time

Analysis of the time series of comparisons between RapidScat σ^o and QuikSCAT σ^o for the Amazon and Congo study areas allows us to make observations about the instrument drift over time. The Amazon and Congo study areas are used because they have bias estimates with the smallest confidence intervals among the study areas. The Low SNR states can be considered a known factor in the instrument drift over time, but may not be the only explanation. Figure 4.3 shows that ten-day bias estimates are much noisier, even for High SNR data, after JD 7/2015 (for reference, the RapidScat was diagnosed with the Low SNR problem August 2015). The High SNR ten-day bias estimates after 6/2015 have larger-than-average confidence intervals, which are likely caused by having fewer than normal measurements in their averages.

The monthly bias estimates have less noise in the estimates because of averaging. Months that average fewer than a threshold of measurements do not report a monthly average bias estimate. Figures 4.4 through 4.7 show the monthly average biases of RapidScat σ^o compared to QuikSCAT σ^o first with all comparisons on the same plot and then separated by QuikSCAT flavor. The trends are similar across polarizations for mornings and evenings. The mornings have greater variation, which is because measurements in the morning have more variation (look at the peak of the LTOD curve around 6h in Figure 3.9). The Amazon and Congo have the similar patterns for Morning Low SNR 2 H and V-pol. Even though morning estimates are noisier (see the LTOD curve in Figure 3.9), the High SNR appears self consistent prior to August 2015 for the mornings. The morning H-pol and V-pol monthly average estimates for the Amazon September 2015 appear low, but the confidence intervals include acceptable mean difference values so nothing conclusive can be drawn from these estimates alone. For the Amazon study area there appears to be a step function in the monthly mean biases when the Low SNR 2 state first appears, but Low SNR 3 mean biases are comparable to the High SNR biases. The Congo study area does not show such a large difference in bias, but the biases for Low SNR 2 in the mornings are noticeably lower than the High SNR biases.

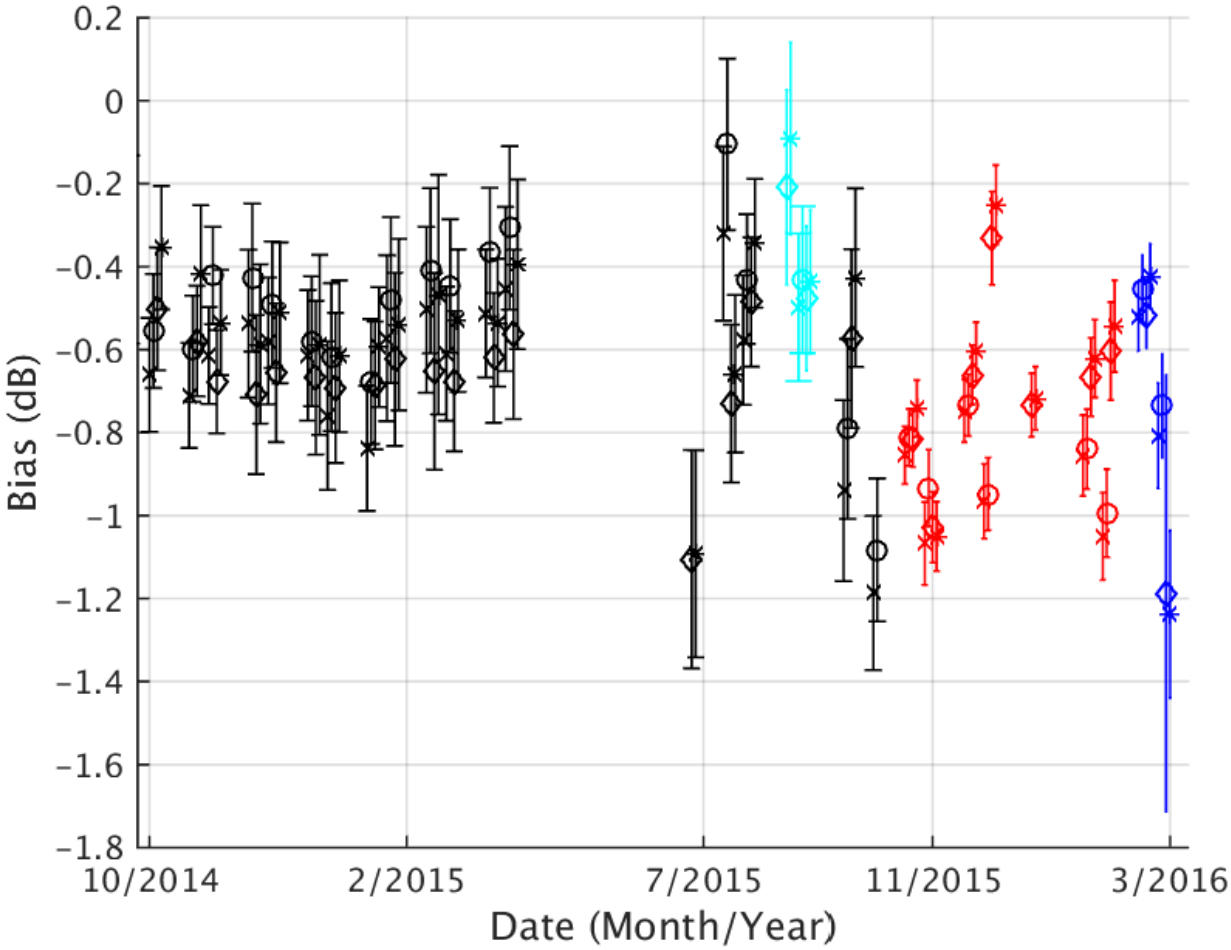

Figure 4.3: The ten-day average bias of RapidScat σ^o compared to QuikSCAT by date of RapidScat measurements for the Amazon study area. Color is used to indicate the RapidScat SNR state and the symbols indicate the flavor of the ten-day average consistent with the legend in Figure 4.2. There are gaps in RapidScat data because data flagged as bad, marginal or large pitch is excluded from this analysis.

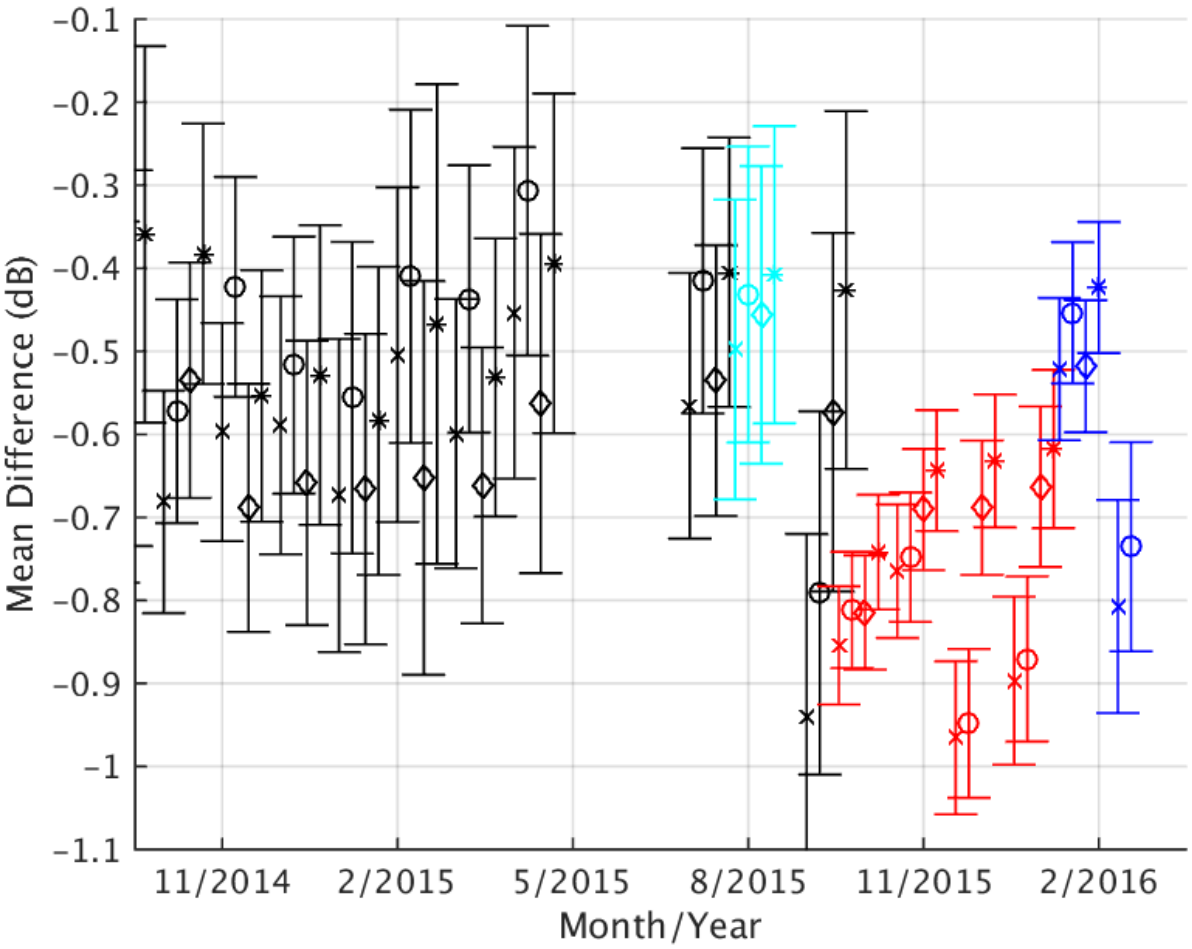

Figure 4.4: The monthly average bias of RapidScat σ^o compared to QuikSCAT σ^o by date of RapidScat measurements for the Amazon study area. Monthly bias estimates with a number of measurements below a threshold are excluded from this figure. Color is used to indicate the RapidScat SNR state and the symbols indicate the flavor of the ten-day average consistent with the legend in Figure 4.2.

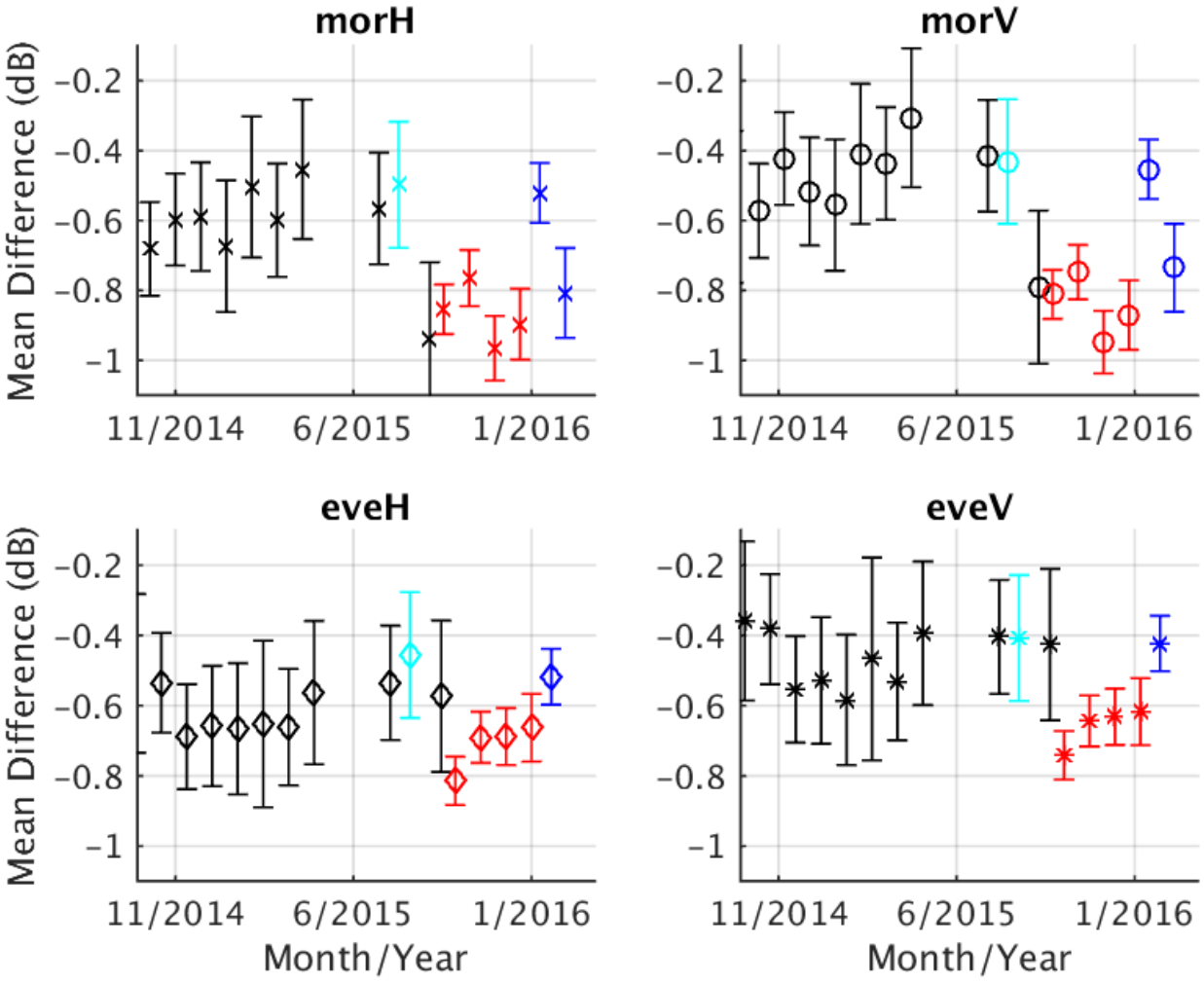

Figure 4.5: The monthly average bias of RapidScat σ^o compared to QuikSCAT σ^o by date of RapidScat measurements for the Amazon study area. Separated by QuikSCAT flavor. Monthly bias estimates with a number of measurements below a threshold are excluded from this figure. Color is used to indicate the RapidScat SNR state and the symbols indicate the flavor of the ten-day average consistent with the legend in Figure 4.2.

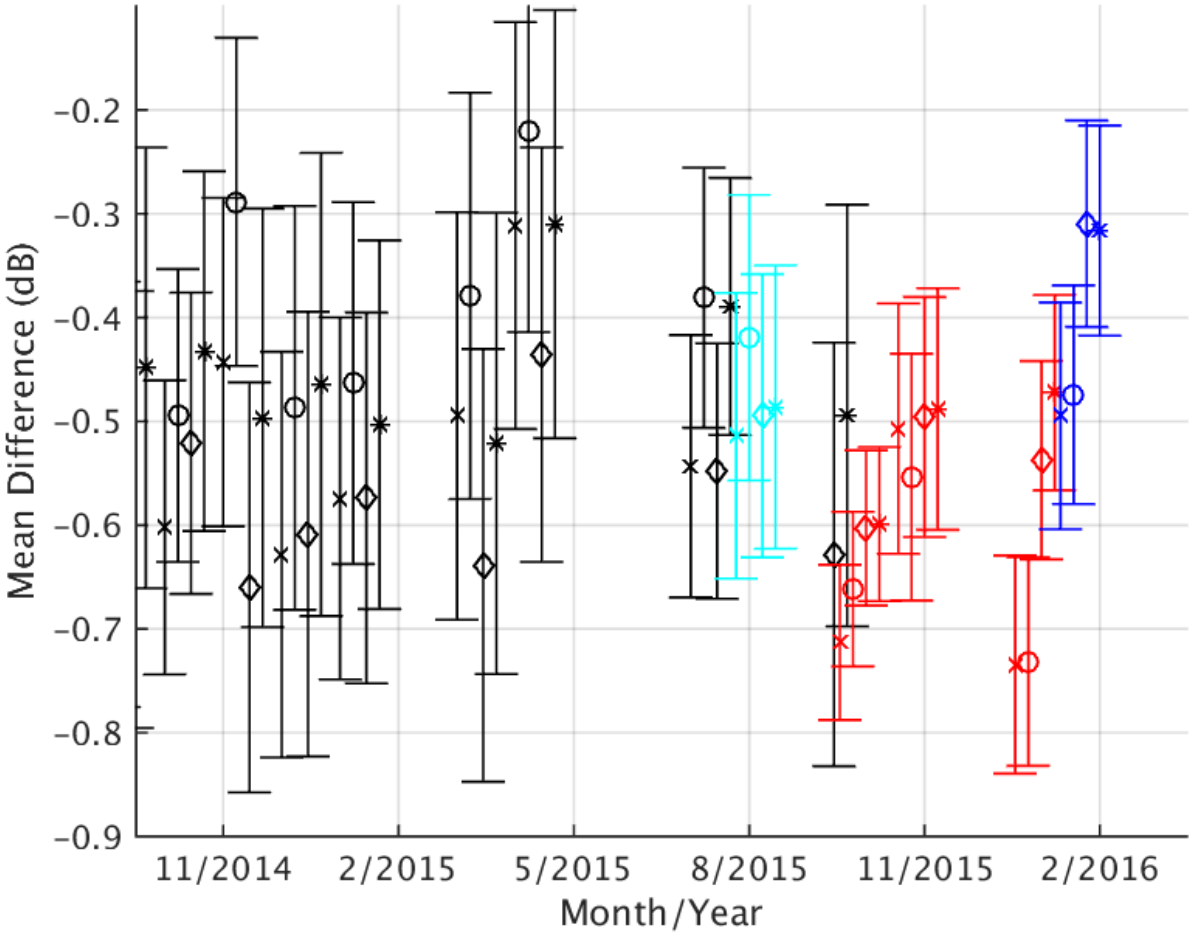

Figure 4.6: The monthly average bias of RapidScat σ^o compared to QuikSCAT σ^o by date of RapidScat measurements for the Congo study area. Monthly bias estimates with a number of measurements below a threshold are excluded from this figure. Color is used to indicate the RapidScat SNR state and the symbols indicate the flavor of the ten-day average consistent with the legend in Figure 4.2.

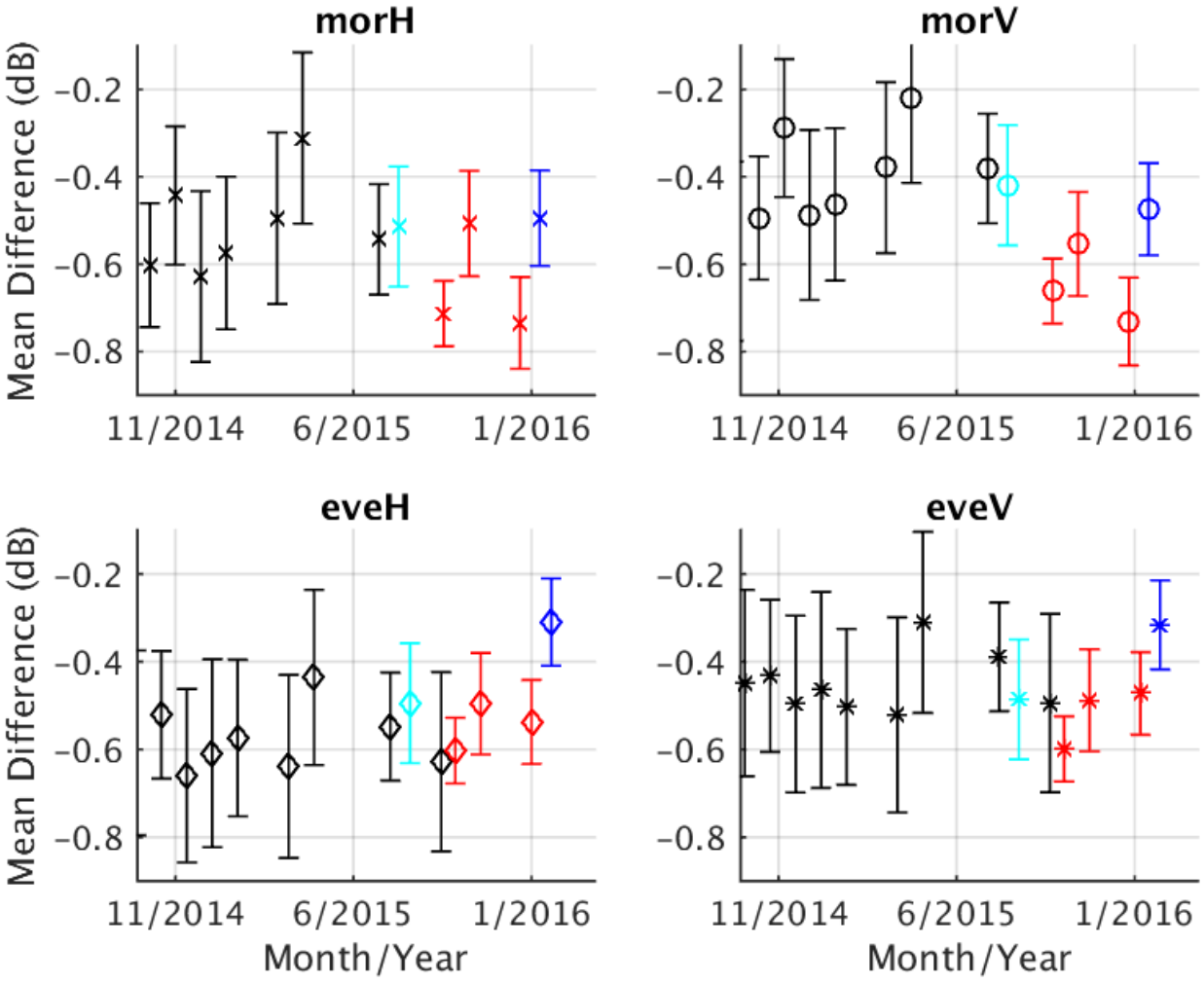

Figure 4.7: The monthly average bias of RapidScat σ^o compared to QuikSCAT σ^o by date of RapidScat measurements for the Congo study area. Separated by QuikSCAT flavor. Monthly bias estimates with a number of measurements below a threshold are excluded from this figure. Color is used to indicate the RapidScat SNR state and the symbols indicate the flavor of the ten-day average consistent with the legend in Figure 4.2.

4.4 Mean-bias estimates

Consistent with other literature [13], a mean calibration bias of RapidScat relative to QuikSCAT is calculated. To find the mean bias, the weighted average (based on the number of RapidScat measurements) is calculated using all of the comparisons for each RapidScat SNR state (High or Low 1/2/3) and flavor (morning or evening and H or V-pol). The confidence interval is the weighted average of the confidence intervals for bias estimates. The mean bias for the Amazon is shown in Figure 4.8a. A lack of Low SNR 1 data is evident in the larger-than-average confidence intervals for the evening comparisons, making it difficult to draw any conclusions from the Low SNR 1 bias alone. However, based on the confidence intervals the Low SNR 1 bias does not contradict the estimates for the High SNR or Low SNR 2/3 biases, so it is possible that the actual Low SNR 1 bias is similar to the other biases.

Mean bias estimates for all of the calibration targets in Table 3.1 are shown in Figure 4.8 and 4.9. The most accurate (smaller confidence intervals) mean bias estimates are found in the Amazon and Congo rainforests, with bias estimates generally between -0.3 and -0.7 and are reported (without confidence intervals) in Table 4.1. There is overlap between the confidence intervals of the Low SNR mean bias estimates and the High SNR mean bias estimates, so conclusions cannot be drawn from these comparisons alone. However, the differences in mean-bias estimates reported in Table 4.1 are consistent with more detailed findings in Chapter 5. Mean bias estimates for the Pampas and Sahara calibration targets are within that range, which suggests that the bias between the RapidScat High SNR and Low SNR states is linear. The confidence intervals for the West Sahara and Australian desert are such that their mean bias estimates do not contradict those found using the Amazon rainforest. Generally, differences in RapidScat σ^o between SNR states for the lower signal targets (Pampas, Australia, W. Sahara and Sahara study areas) are within the bounds of year-to-year seasonal variations in σ^o, suggesting that the linear corrections to σ^o that have been applied previous to this analysis are appropriate.

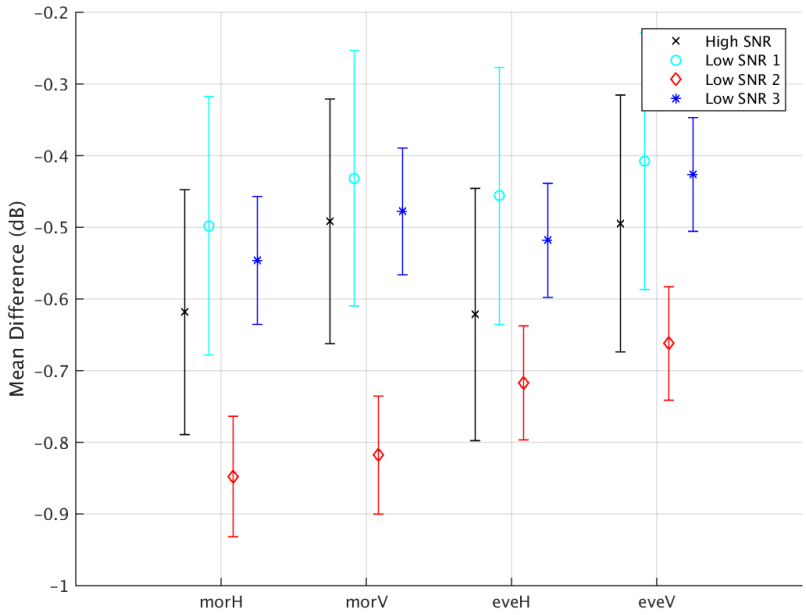

(a) Amazon

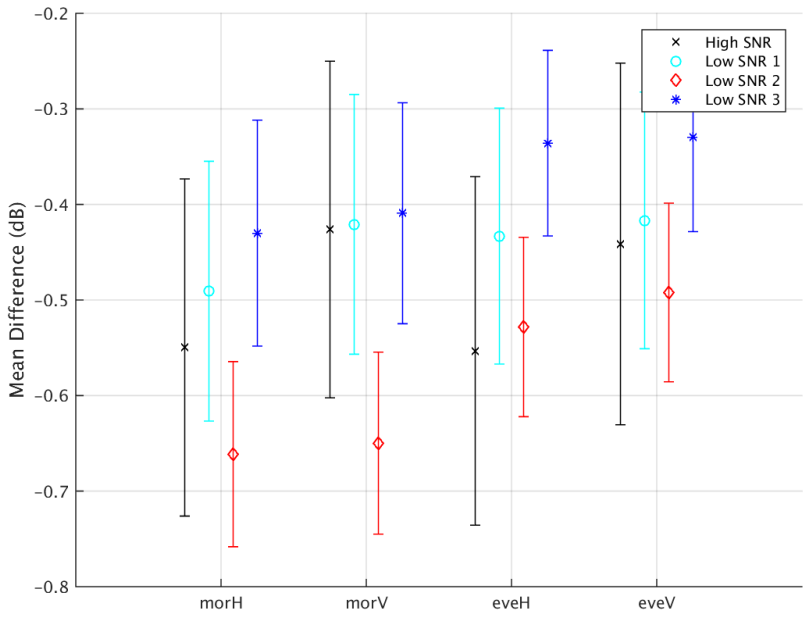

(b) Congo

Figure 4.8: Mean bias estimates of the bias between RapidScat σ^o and QuikSCAT σ^o by QuikSCAT flavor and RapidScat SNR state.

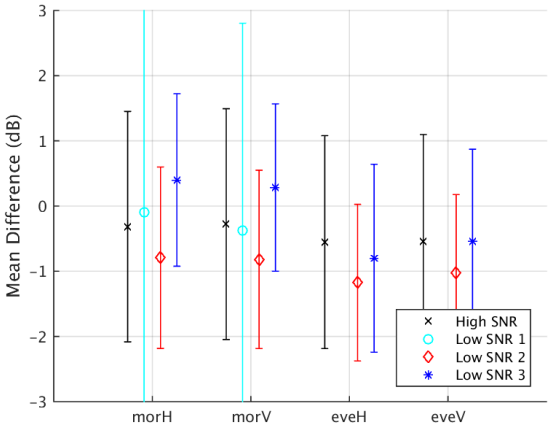

(a) Pampas

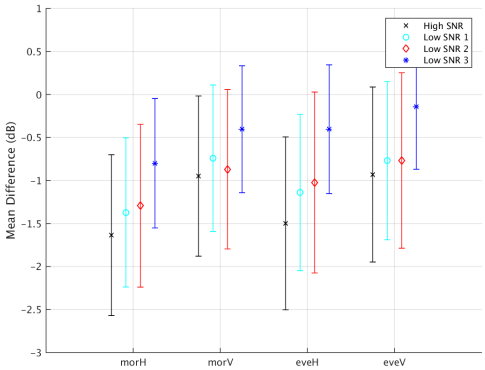

(b) West Sahara

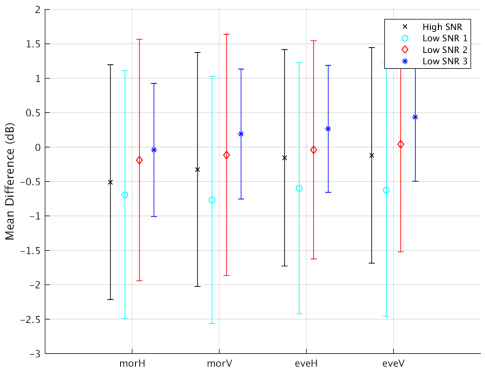

(c) Australian Desert

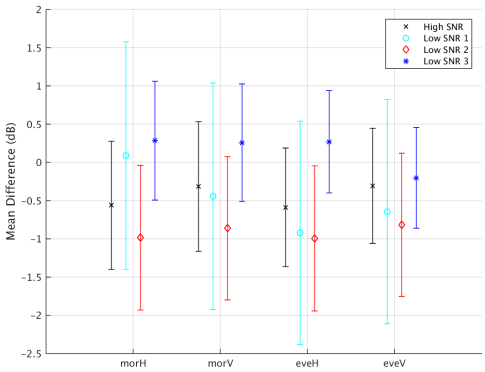

(d) Sahara

Figure 4.9: Mean bias estimates of the bias between RapidScat σ^o and QuikSCAT σ^o by QuikSCAT flavor and RapidScat SNR state.

Study Area	Low SNR 2 Difference			
	morH	eveH	morV	eveV
Amazon	-0.23	-0.33	-0.10	-0.17
Congo	-0.11	-0.22	0.03	-0.05

Table 4.1: Difference between RapidScat Low SNR 2 bias compared to QuikSCAT and High SNR bias.

Chapter 5

RapidScat Low SNR Calibration against RapidScat High SNR

5.1 Introduction

We want to evaluate the consistency of σ^o measurements across all of the RapidScat SNR states and validate the corrections to σ^o applied in RapidScat L1B data by comparing data from from the RapidScat's Low SNR states to data from RapidScat's nominal (High SNR) state. Calibration of the RapidScat Low SNR states against the High SNR state allows for additional data to be used compared to the calibration in Section 4 where only data with QuikSCAT LTOD can be used. A direct comparison between High SNR and Low SNR states also allows for more detailed observations of the small variations between SNR states. We seek to evaluate the consistency of σ^o by directly comparing RapidScat's Low SNR data to the High SNR data.

There are currently two published versions of RapidScat L1B data, v1.1 and v1.2. Version v1.2 includes an updated correction to Low SNR 2 σ^o. All of the calculations and analysis shown in the figures are done using the RapidScat L1B v1.2 dataset. Calculations have also been done using RapidScat L1B v1.1, but only the mean-bias estimates for the Amazon and Congo study areas are reported. Comparisons between the mean-bias estimates calculated using v1.1 and v1.2 data are also considered.

In this chapter, the method for calibrating RapidScat Low SNR state data against the nominal RapidScat state is outlined. Comparisons for Low SNR states 2 and 3 are included (there is no overlap between the Low SNR 1 and High SNR states). Overall trends of the comparisons are discussed to support the linearity of relationship between High and Low SNR σ^o. Detailed results from the individual study areas are included. Mean-bias estimates for each RapidScat Low SNR state are calculated for all study areas and discussed. A comparison of the Low SNR σ^o from the RapidScat L1B v1.1 and v1.2 datasets is made.

5.2 Method

In order to observe the relationship between High SNR and Low SNR data as a function of σ^o, comparisons between High and Low SNR σ^o are made for each the study areas from Table 3.1. Each study area has a different mean σ^o. Using study areas with different mean σ^o is our way of sampling values of σ^o. Corrections by JPL are only based on data from the Amazon rainforest. If the relationship between High and Low SNR states is not linear as a function of σ^o, then corrections based on the Amazon rainforest may not fit for values of σ^o. It is important to establish that calibration of RapidScat's Low SNR states using land targets like the Amazon Rainforest is effective at all ranges of σ^o because the primary function of RapidScat, ocean vector wind (OVW) retrieval, typically is done with low values of σ^o, in the range of -12 dB to -35 dB.

The method used to compare RapidScat High SNR data to Low SNR data is similar to that in Chapter 4. RapidScat σ^o measurements are extracted from the L1B dataset the same way, but is also included here. Comparison selection and mean calibration bias estimation are similar.

5.2.1 Masking

RapidScat data is extracted from L1B data using the spatial mask created using QuikSCAT data for each of the study areas (Figure 3.11). Using the σ^o dB/deg incidence angle from Chapter 3 in Table 3.2, θ is used to adjust each σ^o measurement to QuikSCAT incidence angles. Then σ^o is averaged into ten-day bins. The LTOD for the σ^o estimate is the mean LTOD of the σ^o measurements. The same ten-day bins are used as in Chapter 4 so that the seasonal variation measured in QuikSCAT can be used in the confidence interval calculation. In the following comparison, an 80% confidence interval is used, calculated using $N = 1$ years and $u = 0.9$ in Equation (4.1), which is repeated here for convenience:

$$\sigma^o \pm \left(z_u \frac{s_\square}{\sqrt{M}} + t_u(N) \frac{s_\triangle}{\sqrt{N}} \right), \tag{5.1}$$

where z_u is the standard normal density function, $t_u(n)$ is the student t distribution function, u is the percentile, $s_\square$ is the standard deviation of M measurements made by RapidScat and

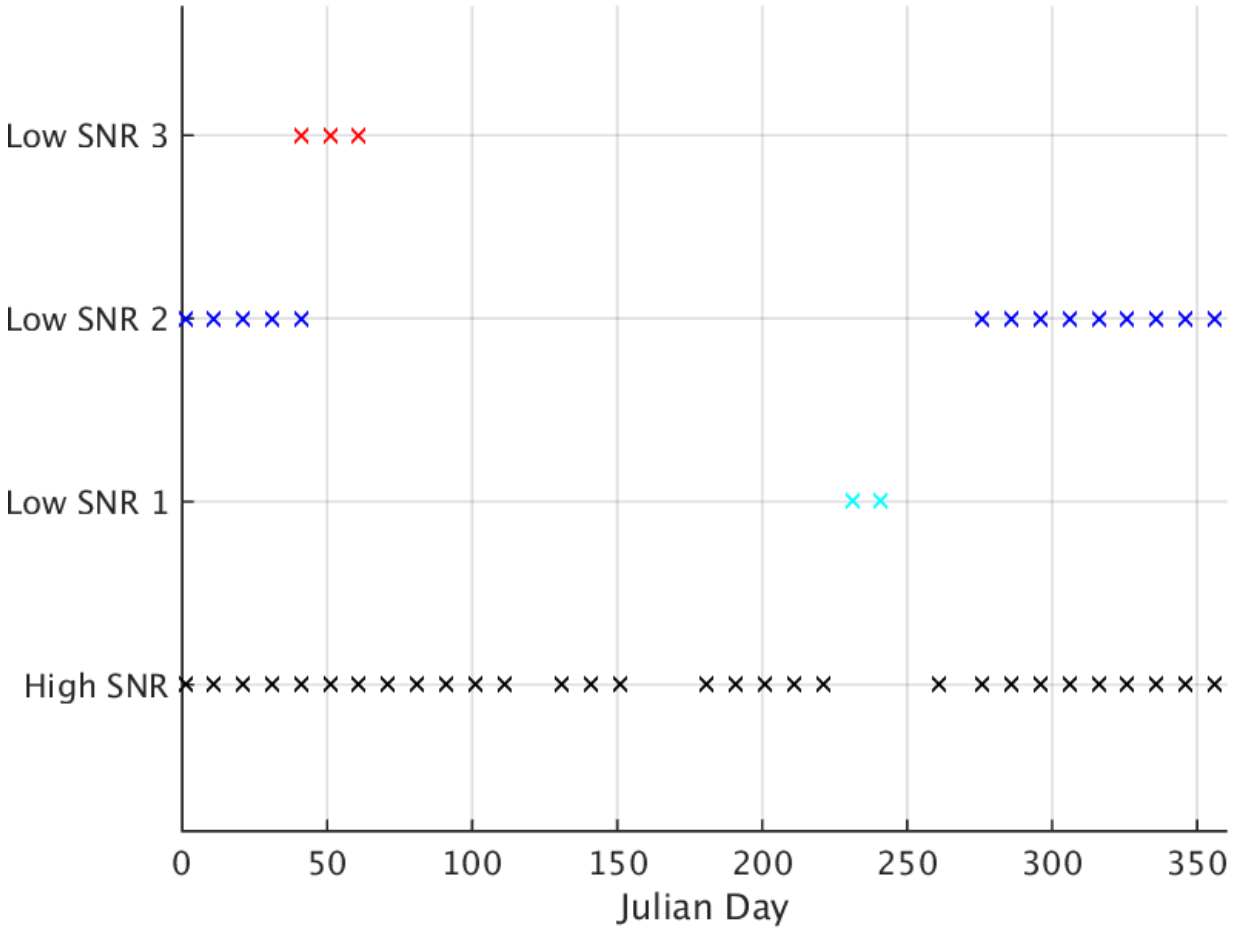

Figure 5.1: SNR states for RapidSCat for each ten-day period of the year.

$s_{\triangle}$ is the seasonal variation as measured by QuikSCAT in Section 4. This process results in with σ^o estimates and confidence intervals for each ten-day bin, SNR state, and study area (mean σ^o value).

5.2.2 Comparison selection

Where measurements exist for both High SNR and a Low SNR state in the same ten-day bin and meet LTOD criteria, a direct comparison can be made. Figure 5.1 shows the overlap of the High SNR state with each of the SNR states for each ten-day bin; however, there may not be qualifying measurements for every ten-day bin with overlap from every study area. Studies of the RapidScat diurnal cycle over land in [13, 14] and Appendix A, for land targets used in this report, show that σ^o is a function of LTOD. In order to limit the

effects of LTOD on the comparison between High SNR and Low SNR σ^o, the LTOD criteria in Table 3.2 is used. Comparisons can be made between between ascending and descending passes of the same polarization as long as the LTOD criteria is met.

5.2.3 Mean calibration bias estimation

Mean calibration bias estimates for each polarization and state combination in each study area are made by calculating the difference of the weighted averages of the High and Low SNR ten-day σ^o estimates. The weights are proportional to the number of measurements for each ten-day estimate. The confidence interval for the mean bias estimates is the weighted average of the confidence intervals for each bias estimate. Let

$$E = z_u \frac{s_\square}{\sqrt{M}} + t_u(N) \frac{s_\triangle}{\sqrt{N}}. \tag{5.2}$$

The confidence interval for the Low SNR σ^o is $\sigma^o \pm E_{Low}$ and for the High SNR σ^o is $\sigma^o \pm E_{High}$. For each bias estimate, the confidence interval is calculated using

$$E_{bias} = \sqrt{E_{Low}^2 + E_{High}^2}. \tag{5.3}$$

The confidence intervals for each mean bias estimate shown in Figure 5.9 are the weighted averages of E_{bias} associated with the bias estimates used to calculate the given mean bias estimate. This results in mean bias estimates with confidence intervals for each polarization, SNR state, and study area.

Confidence intervals for each comparison account for year-to-year seasonal variation for each study area and uncertainty related to the number of measurements used in the ten-day average, e.g., fewer measurements result in a larger confidence interval. The small confidence intervals for the Amazon and Congo rainforests allow for precise evaluation of the linear adjustments to σ^o, while the larger confidence intervals in the lower signal study targets are mostly useful for verifying the gain adjustment, i.e., even with the large confidence intervals, the comparisons from lower signal study areas allow for observations about the relationship between the RapidScat High SNR state and the Low SNR states as a function

of σ^o. Confidence intervals can be used in analysis so as to avoid misclassifying year-to-year seasonal and measurement variation as variation between High SNR and Low SNR data.

5.2.4 Results and Observations

In order to observe the relationship between High SNR and Low SNR data as a function of σ^o, comparisons between High and Low SNR σ^o from all of the study areas are included in Figure 5.2. The comparisons for each calibration target are shown separately for clarity in Figures 5.3 to 5.8. Overall, the trend in Figure 5.2 appears to be linear, even in lower σ^o study areas, so the linear adjustments to σ^o are appropriate. This suggests that the extra noise (specifically due to adjusting the gain during post processing) is zero mean or close to it, and is not affected (biased) by the σ^o of the target. Closer evaluation of the individual study areas suggests that the relationship of High SNR and Low SNR data is a linear function of σ^o.

The Argentina Pampas study area comparisons for the both the Low SNR 2 and 3 states are shown in Figure 5.5. The large year-to-year seasonal variation observed by QuikSCAT is manifest in the large confidence intervals. Most comparisons lie close to the ideal (dotted line), and almost all of the comparisons' confidence intervals include the ideal. The observed mean bias estimates (shown between -10 and -15 dB σ^o in Figure 5.9) of the Low SNR 2 and 3 states lie within the expected year-to-year seasonal variation, supporting the linear model.

Results for the West Sahara study area, which contains many comparisons for both the Low SNR 2 and 3 states, are shown in Figure 5.6. The comparisons appear noisy, in the sense that the spread is large; however the ideal linear line generally lies in the confidence intervals of the comparisons. The mean bias estimates are shown between -15 dB and -20 dB σ^o in Figure 5.9, and do include a mean bias of zero, supporting the linear model..

For the Australian desert study area the comparisons, one Low SNR 3 and several Low SNR 2, (Figure 5.7) are very linear. A linear fit to these points is comparable to the ideal line shown in the figure. The comparisons from this study area support the linear model because the ideal lies well within the confidence intervals of the comparisons.

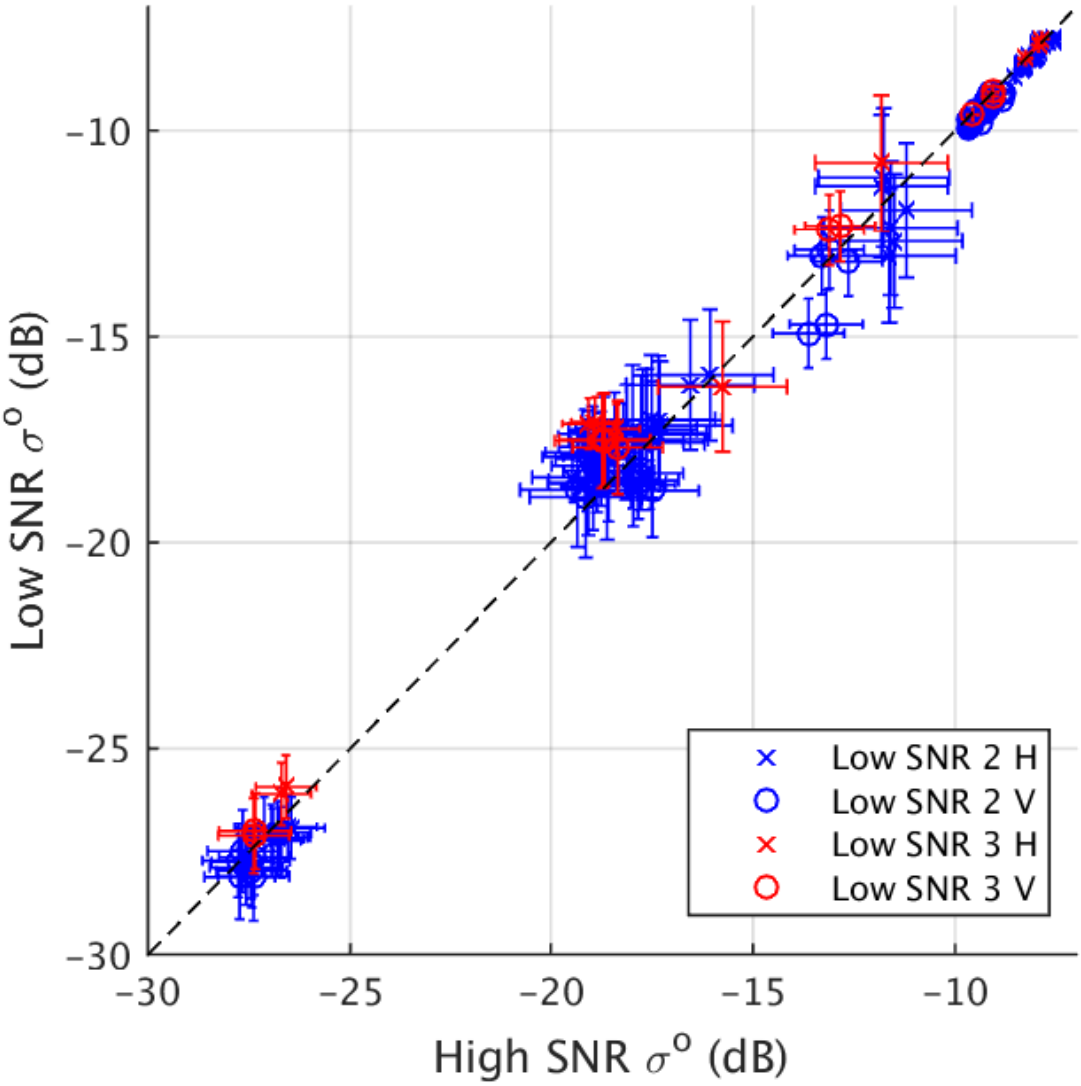

Figure 5.2: Low SNR 1/2/3 σ^o compared to High SNR σ^o for all of the study areas. Although there is some overlap between study areas, the comparisons generally correspond to (from top-right to bottom-left) the Congo Rainforest, Amazon Rainforest, Argentina Pampas, West Sahara, Australian Desert, and Sahara Desert. Comparisons are shown in greater detail by study area in Figures 5.3 to 5.8. This figure suggests that the relationship between RapidScat's High SNR state and each Low SNR state is linear. See text for details about the confidence intervals shown and for further observations.

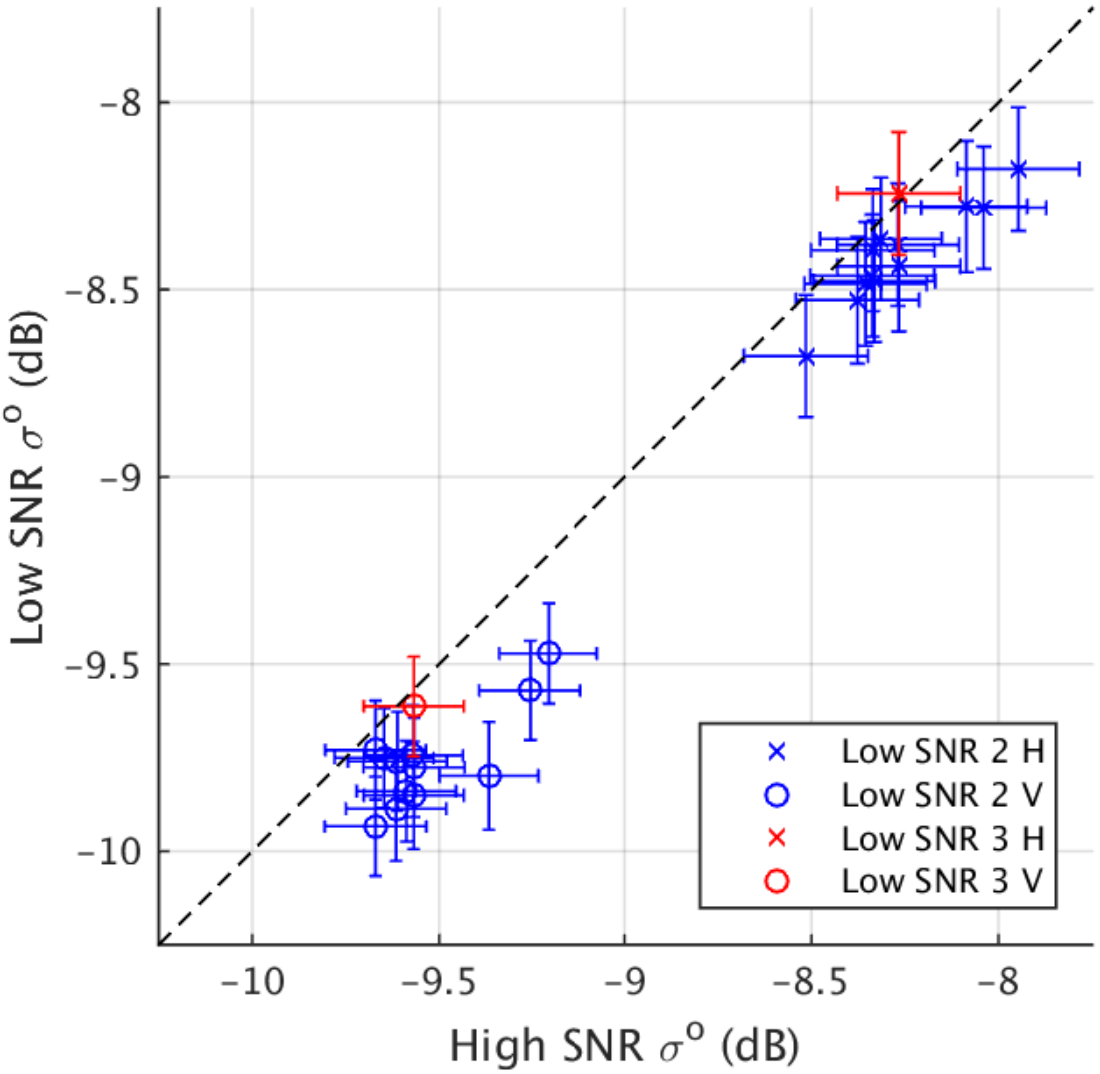

Figure 5.3: From the Amazon Rainforest, Low SNR 1/2/3 σ^o compared to High SNR σ^o. Measurements are within ± 45 minutes or fall within 10-16h LTOD. There is a clear grouping of H-pol (around -8 dB) and V-pol (around -9.5 dB) data.

The comparisons from the Sahara desert study area, Figure 5.8, generally show a linear relationship between RapidScat High SNR σ^o and Low SNR σ^o for both the Low SNR 2 and 3 states. The ideal lies within the confidence intervals for every comparison. Given that this is the lowest signal study area, these results strongly suggest that the data is unbiased by noise. Mean bias estimates from this study area lie between -25 and -30 dB in Figure 5.9.

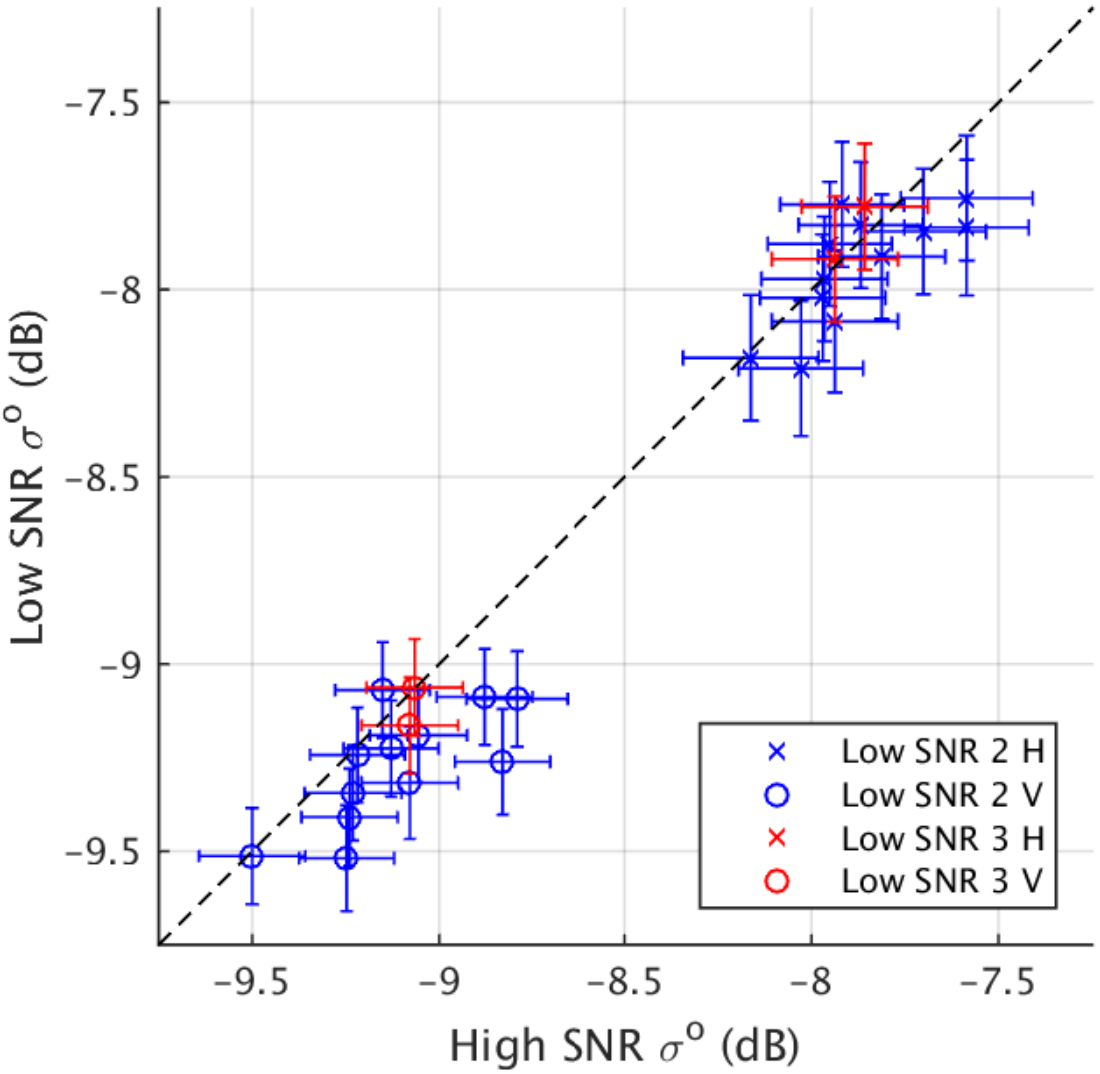

Figure 5.4: From the Congo Rainforest, Low SNR 1/2/3 σ^o compared to High SNR σ^o. Measurements are within ± 45 minutes or fall within 10-16h LTOD. There is a clear grouping of H-pol (around -7.5 dB) and V-pol (around -9 dB) data.

Mean bias estimates in Figure 5.9 average out outliers and clarify the trends in Figure 5.2. Both the Low SNR 2 and Low SNR 3 mean biases measured in the Amazon and Congo study areas generally lie within the confidence intervals of the mean bias estimates from the lower σ^o study areas. This suggests that the relationship between Low SNR and High SNR σ^o is linear. This also suggests that linear gain adjustments based on calibration using Amazon and Congo study areas are appropriate for lower values of σ^o as well.

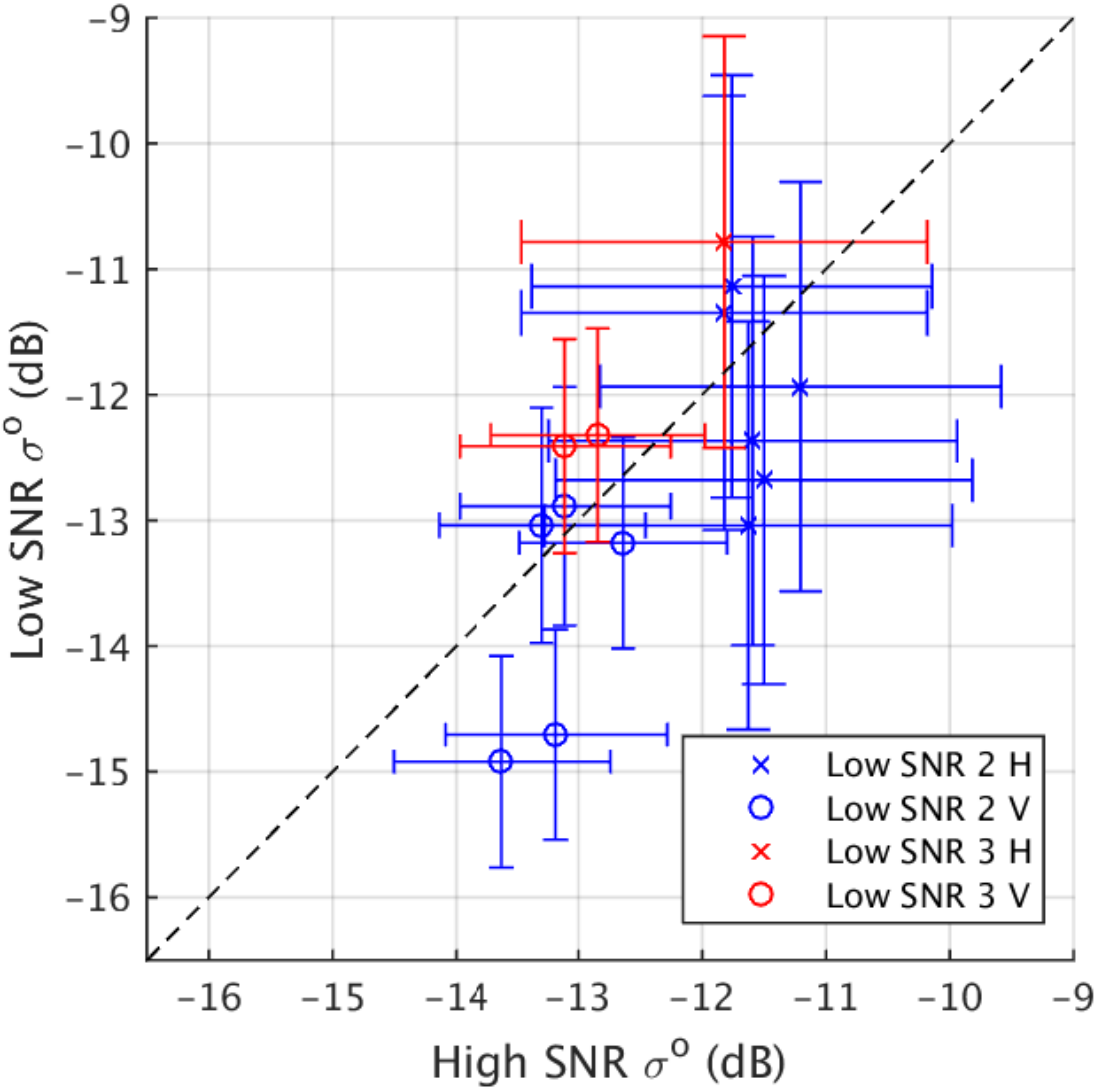

Figure 5.5: From the Argentina Pampas study area, Low SNR 1/2/3 σ^o compared to High SNR σ^o. Measurements are within ± 45 minutes.

The small confidence intervals of the comparisons in the Amazon Rainforest (Figure 5.3) and the Congo Rainforest (Figure 5.4) allow us to make observations about the small variations between the High SNR and the Low SNR data. The Amazon and Congo rainforests have similar mean σ^o, so they do not offer a lot of information about the linearity of the relationship between High and Low SNR data as a function of σ^o. However, use of both study areas creates more comparisons with confidence intervals such that better observations can be made about the bias between RapidScat SNR states. Calibration corrections to Low SNR σ^o such that a mean bias of zero lies in the confidence intervals both of the

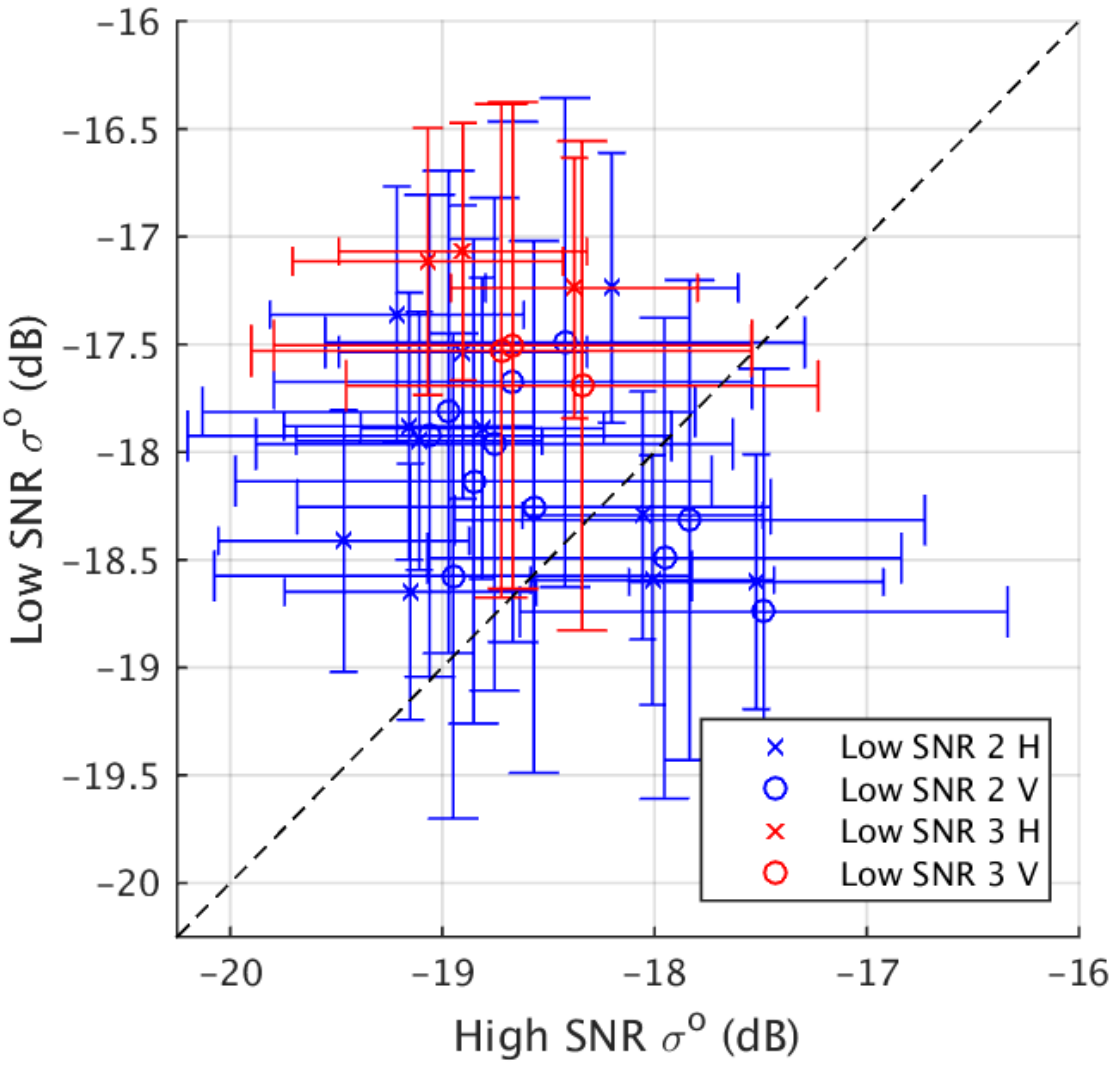

Figure 5.6: From the West Sahara studay area, Low SNR 1/2/3 σ^o compared to High SNR σ^o. Measurements are within ± 45 minutes LTOD or fall within 6-12h LTOD.

Amazon and the Congo rainforests mean bias estimates would more likely to be independent of year-to-year seasonal variations.

The mean bias estimates for RapidScat Low SNR 2 σ^o in L1B v1.1 and v1.2 data sets are shown in Table 5.1 for the Amazon and Congo study areas. Version v1.1 Low SNR 2 σ^o is biased high when compared to High SNR σ^o while version v1.2 Low SNR 2 σ^o is biased low. While the numbers in Table 5.1 might suggest some fine tuning of the calibration could be done, is may not be necessary. RapidScat L1B v1.2 includes calibration corrections based on OVW calibration. That being the case, the v1.2 Low SNR 2 calibration is probably well

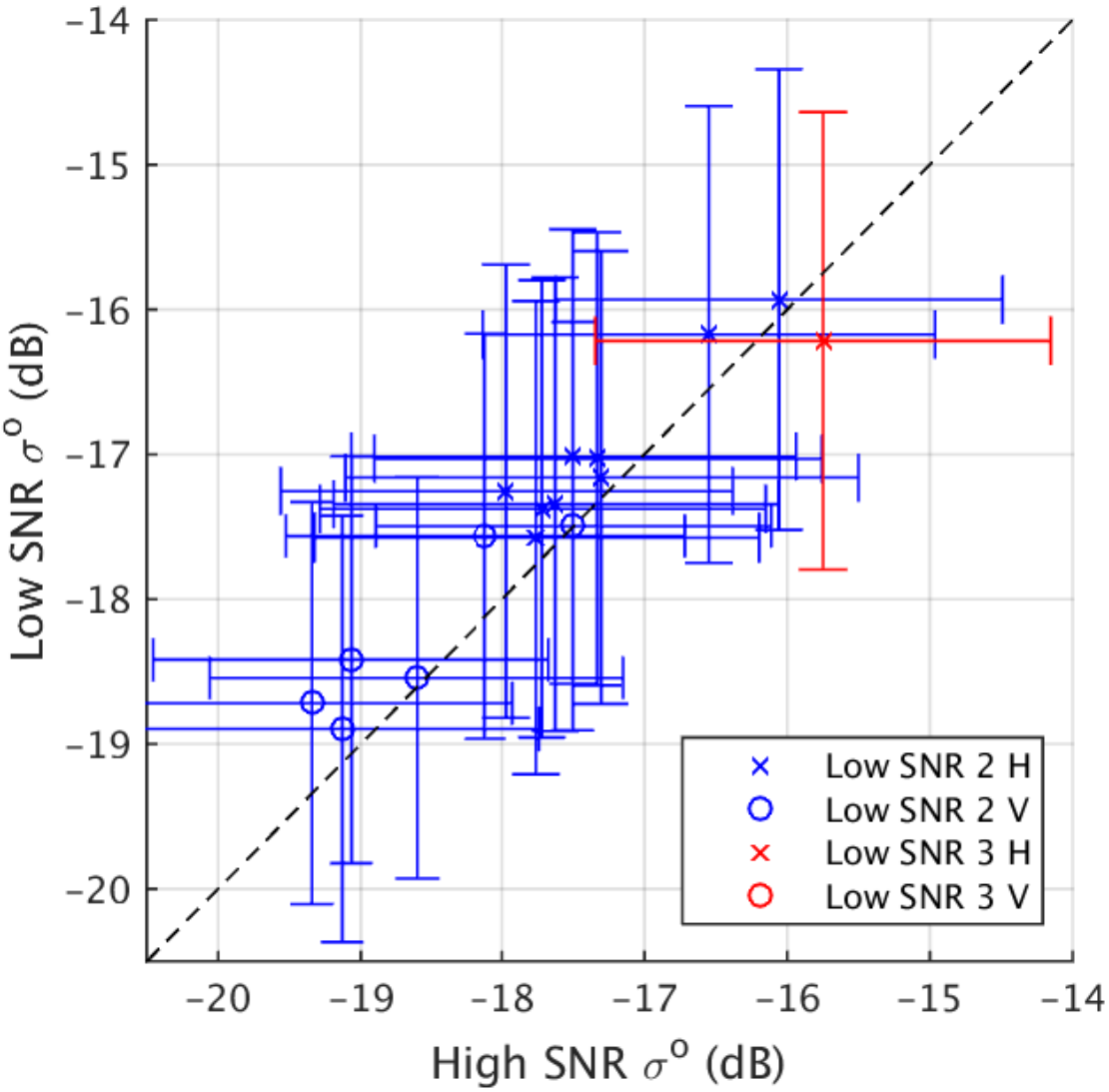

Figure 5.7: From the Australian desert study area, Low SNR 1/2/3 σ^o compared to High SNR σ^o. Measurements are within ± 45 minutes LTOD.

suited for OVW retrieval and the bias to σ^o measurements is not that large (the confidence intervals of the mean bias estimates almost include a mean bias of zero).

The Low SNR 3 comparisons show a small bias in the Amazon and Congo study areas, the corresponding confidence intervals do include a mean bias of zero: suggesting that the bias is within the bounds of year-to-year seasonal variation. The exact measurements for these study areas are reported in Table 5.2.

The question calibration bias may be posed as a detection problem where under $H_0 : \sigma^o$ calibration is unbiased and under $H_1 : \sigma^o$ calibration is biased. Selection of H_0 vs

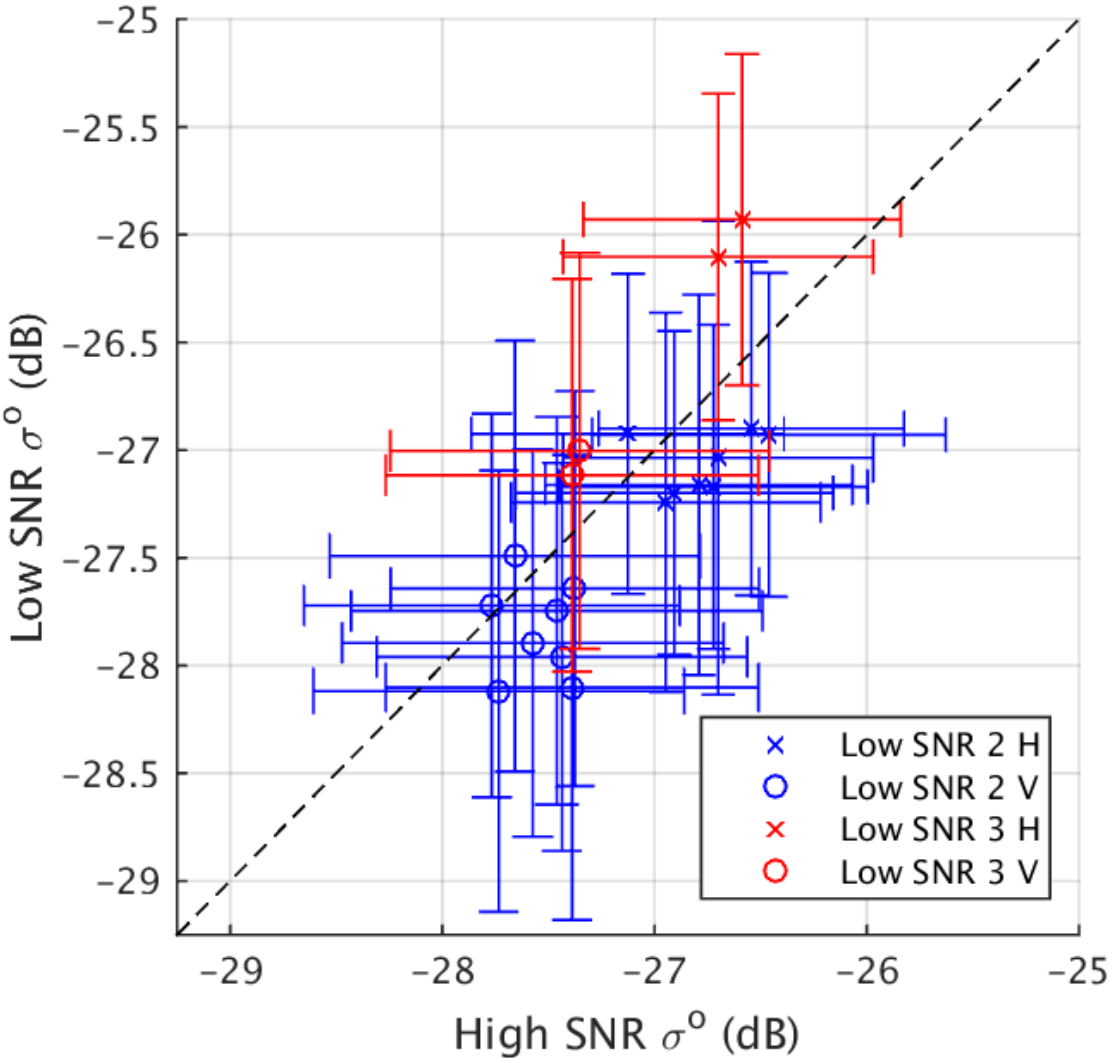

Figure 5.8: From the Sahara Desert study area, Low SNR 1/2/3 σ^o compared to High SNR σ^o. Measurements are within ± 45 minutes LTOD.

H_1 follows the rule,

$$\phi(C_N) = \begin{cases} 1 \sim H_1 & C_N > 0 \\ 0 \sim H_0 & C_N \leq 0, \end{cases} \tag{5.4}$$

where C_N is computed from the mean calibration estimate $M_{mean\ bias} \pm E_{mean\ bias}$,

$$C_N = |M_{mean\ bias}| - |E_{mean\ bias}|. \tag{5.5}$$

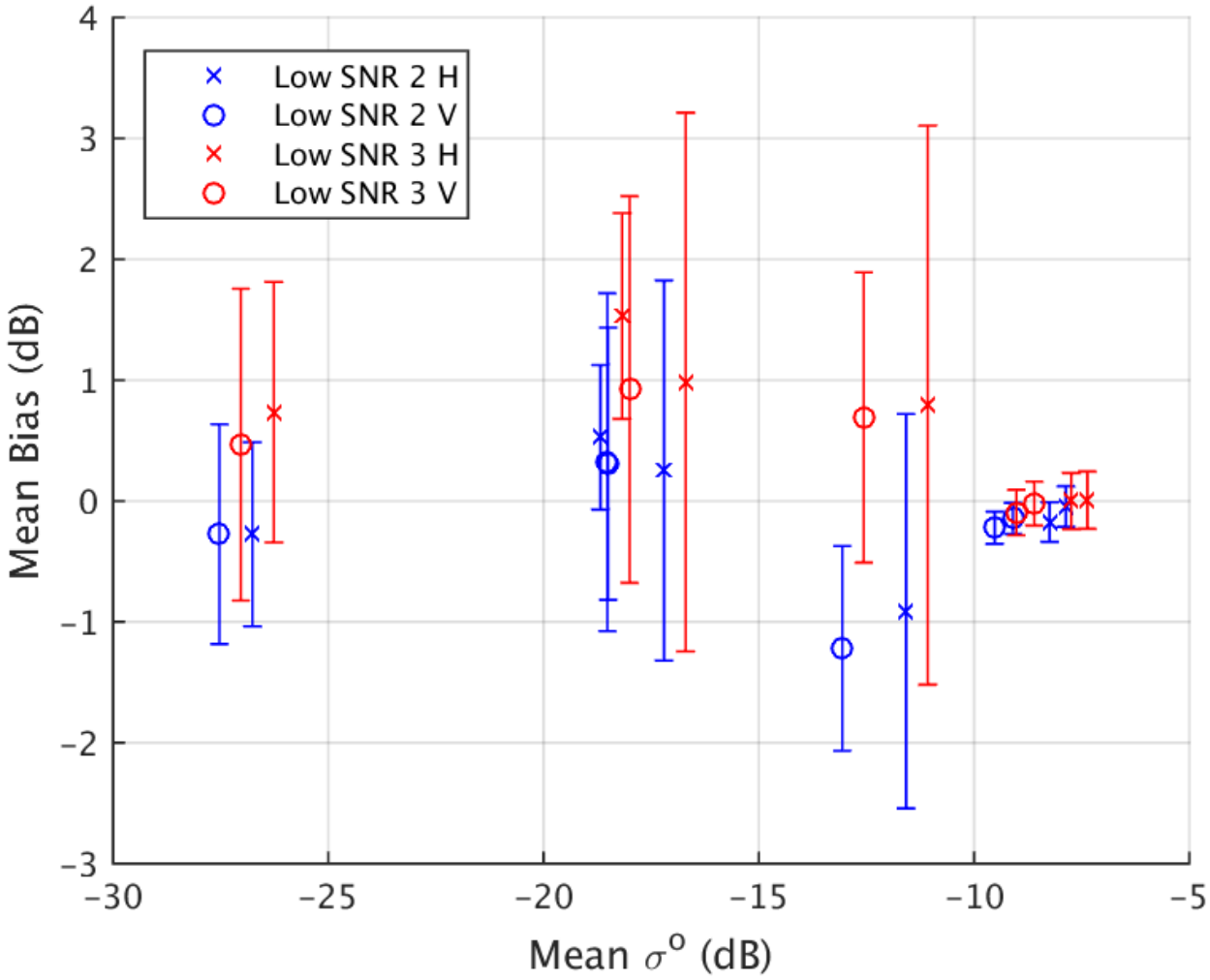

Figure 5.9: Mean bias of Low SNR 1/2/3 σ^o compared to High SNR σ^o for all of the study areas. See text for details.

Using the test statistic ϕ, we can detect if the σ^o calibration is biased or not. Using the values for the Amazon and Congo rainforests in Tables 5.1 we can say with 80% confidence that the Low SNR 2 calibration is biased for V-pol, however for H-pol the bias is only detected in the Amazon study area. The Low SNR 2 calibration bias is also detected in the Argentina study area. Based on Table 5.2 and Figure 5.9, no bias is detected in the Low SNR 3 calibration. [19]

In summary, linear adjustment of σ^o is an appropriate way to compensate for the lower SNR states exhibited in RapidScat data from August 2015 to March 2016. No analysis of the Low SNR 1 σ^o is possible using the method this chapter. Based on the mean bias

Study Area & Polarization	Mean Bias v1.1 (dB)	Mean Bias v1.2 (dB)
Amazon H-Pol	0.29 ± 0.17	-0.16 ± 0. 13
Congo H-Pol	0.42 ± 0.17	-0.08 ± 0.23
Amazon V-Pol	0.24 ± 0.16	-0.28 ± 0.15
Congo V-Pol	0.31 ± 0.13	-0.26 ± 0.17

Table 5.1: Low SNR 2 mean bias (Low SNR 2 σ^o - High SNR σ^o) estimates for the Amazon and Congo study areas.

Study Area & Polarization	Mean Bias v1.2 (dB)
Amazon H-Pol	0.00 ± 0.23
Congo H-Pol	0.01 ± 0.24
Amazon V-Pol	-0.10 ± 0.19
Congo V-Pol	-0.02 ± 0.18

Table 5.2: Low SNR 3 mean bias (Low SNR 3 σ^o - High SNR σ^o) estimates for the Amazon and Congo study areas.

estimates from the study areas, the linear corrections used for Low SNR 2 could be adjusted based on the values in Table 5.1 if consistent σ^o measurements across RapidScat SNR states is desired. The linear corrections for Low SNR 3 appear correct.

Chapter 6

Conclusions

Five land targets are identified and are used to study RapidScat σ^o measurements at different values. Each land target is analyzed for σ^o dependencies with respect to year-to-year seasonal variation, azimuth angle, incidence angle and LTOD. Criteria is developed for how to use these study areas to cross-calibrate RapidScat to QuikSCAT and how to calibrate the Low SNR RapidScat states to the High SNR RapidScat state.

RapidScat instrument drift is observed by cross-calibrating the sensor to QuikSCAT, though it is correlated with the Low SNR RapidScat states. A shift in the calibration is observed when the RapidScat Low SNR 2 state begins. There is a lot of noise observed in the ten-day average mean bias estimates for the RapidScat Low SNR states when compared to the High SNR state. However, the mean bias between RapidScat Low SNR 3 state σ^o and QuikSCAT σ^o is more consistent with the High SNR RapidScat state. Overall, the only instrument drift appears to be related to the Low SNR RapidScat states.

Mean estimates of the bias between RapidScat and QuikSCAT are calculated. RapidScat is biased low compared to QuikSCAT. The RapidScat Low SNR 1 state σ^o appears consistent with the RapidScat High SNR state σ^o. The difference in mean bias estimates is similar to those found when calibrating RapidScat Low SNR state σ^o against the High SNR σ^o. However, these mean estimates have large confidence intervals and are not suitable for precise evaluation of adjustments that should be made to make RapidScat Low SNR state σ^o the same as RapidScat High SNR σ^o.

Mean estimates of the calibration bias between RapidScat Low SNR state σ^o and RapidScat High SNR state σ^o are calculated by directly comparing data from the two states. Observations from the Amazon and Congo study areas suggest that there is a bias in the calibration and that the gain adjustment used could use some fine tuning.

In both the cross-calibration to QuikSCAT and the calibration against the RapidScat High SNR state, the RapidScat Low SNR state is found to be linear. While there is a calibration bias observed in the Amazon and Congo study areas, results from the lower signal study ares suggest that the RapidScat Low SNR state σ^o is unbiased by noise.

6.1 Summary

In summary:

1. The adjustment gain for the RapidScat Low SNR 2 state could use some fine tuning. The RapidScat Low SNR 1 and 3 states are appear consistent with the RapidScat High SNR state.

2. Instrument drift over time is correlated with the Low SNR states.

3. By sampling σ^o using land targets with different radar responses, it is shown that from -7 dB to -27 dB, RapidScat Low SNR state measurements are unbiased by noise.

4. The system is linear and simple gain adjustments are appropriate to make Low SNR state measurements consistent with RapidScat High SNR state measurements.

6.2 Recommendations for future work

Potential future research includes:

1. Future RapidScat SNR states can be calibrated using the method outlined in this work.

2. Land targets developed in this thesis could be used for calibration of other sensors.

Bibliography

[1] F. T. Ulaby and D. G. Long, *Microwave Radar and Radiometric Remote Sensing.* University of Michigan Press, Nov 2014. 4, 5, 6, 7

[2] F. Ulaby and D. Long. (2014, Nov.) Microwave Satellite Sensors. [Online]. Available: http://mrs.eecs.umich.edu/sensors.html 4

[3] (2014, Sept.) RapidScat. [Online]. Available: http://winds.jpl.nasa.gov/missions/RapidScat/ 4

[4] S. Frolking, S. Hagen, T. Milliman, M. Palace, J. Z. Shimbo, and M. Fahnestock, "Detection of large-scale forest canopy change in pan-tropical humid forests 2000-2009 with the SeaWinds Ku-band scatterometer," *IEEE Transactions on Geoscience and Remote Sensing*, vol. 50, no. 7, pp. 2603–2617, July 2012. 5

[5] H. Stephen and D. G. Long, "Study of iceberg B10A using scatterometer data," in *Geoscience and Remote Sensing Symposium, 2000. Proceedings. IGARSS 2000. IEEE 2000 International*, vol. 3, 2000, pp. 1340–1342 vol.3. 5

[6] K. M. Stuart and D. G. Long, "Iceberg size and orientation estimation using SeaWinds," in *Geoscience and Remote Sensing Symposium (IGARSS), 2010 IEEE International*, July 2010, pp. 2394–2397. 5

[7] A. M. Swan and D. G. Long, "Multiyear Arctic sea ice classification using QuikSCAT," *IEEE Transactions on Geoscience and Remote Sensing*, vol. 50, no. 9, pp. 3317–3326, Sept 2012. 5

[8] L. B. Kunz and D. G. Long, "Melt detection in Antarctic ice shelves using scatterometers and microwave radiometers," *IEEE Transactions on Geoscience and Remote Sensing*, vol. 44, no. 9, pp. 2461–2469, Sept 2006. 5

[9] D. G. Long and G. B. Skouson, "Calibration of spaceborne scatterometers using tropical rain forests," *IEEE Transactions on Geoscience and Remote Sensing*, vol. 34, no. 2, pp. 413–424, Mar 1996. 7

[10] H. Stephen and D. G. Long, "Multi-spectral analysis of the Amazon basin using SeaWinds, ERS, Seasat scatterometers, TRMM-PR and SSM/I," in *Geoscience and Remote Sensing Symposium, 2002. IGARSS '02. 2002 IEEE International*, vol. 3, June 2002, pp. 1780–1782 vol.3. 7

[11] N. Patel, L. Hong, W. Jones, and S. Vasudevan, "Evaluation of the Amazon rain forest as a distributed target for satellite microwave radiometer calibration," in *2006 IEEE International Symposium on Geoscience and Remote Sensing*, July 2006, pp. 85–88. 7

[12] S. A. Bhowmick, R. Kumar, and A. S. K. Kumar, "Cross calibration of the OceanSAT-2 scatterometer with QuikSCAT scatterometer using natural terrestrial targets," *IEEE Transactions on Geoscience and Remote Sensing*, vol. 52, no. 6, pp. 3393–3398, June 2014. 7

[13] N. M. Madsen and D. G. Long, "Calibration and validation of the RapidScat scatterometer using tropical rainforests," *Geoscience and Remote Sensing, IEEE Transactions on*, vol. PP, no. 99, pp. 1–9, Dec 2015. 7, 8, 12, 14, 15, 16, 25, 35, 40

[14] A. C. Paget, D. G. Long, and N. M. Madsen, "RapidScat diurnal cycles over land," *Geoscience and Remote Sensing, IEEE Transactions on*, vol. PP, no. 99, pp. 1–9, Jan 2016. 8, 40

[15] BYU MERS (2006), "SeaWinds on QuikScat Enhanced Resolution Image Products (version 2)," [Online] Available: http://www.scp.byu.edu/data/Quikscat/SIRv2/Quikscat_sirV2.html. 9, 11

[16] JPL QuikSCAT Project (2006), "SeaWinds on QuikSCAT Level 1B Time-Ordered Earth-Located Sigma-0 Version 2," PO.DAAC. [Online] Available: http://podaac.jpl.nasa.gov/dataset/QSCAT_LEVEL_1B_V2. 10, 13

[17] RapidScat Project (2015), "RapidScat Level 1B Time-Ordered Geo-Located Sigma-0 Version 1.1," PO.DAAC. [Online] Available: http://podaac.jpl.nasa.gov/dataset/RSCAT_L1B_V1.1. 10, 15

[18] R. G. Kennett and F. K. Li, "Seasat over-land scatterometer data. I. Global overview of the Ku-band backscatterer coefficients," *IEEE Transactions on Geoscience and Remote Sensing*, vol. 27, no. 5, pp. 592–605, Sep 1989. 20

[19] L. L. Scharf and C. C. Demeure, *Statistical signal processing: detection, estimation, and time series analysis*, ser. Addison-Wesley series in electrical and computer engineering. Reading, Mass. Addison-Wesley Pub. Co. cop., 1991. [Online]. Available: http://opac.inria.fr/record=b1088321 50

Appendix A

Additional Calibration Targets

A.1 Congo Rainforest

The Congo Rainforest study area has similar backscatter to the Amazon study area, with a QuikSCAT mean σ^o of -7.2 dB H-pol and -8.5 dB V-pol. QuikSCAT SIR data from the South Africa region is used to identify the homogeneous land target corresponding to the Congo Rainforest shown in Figure A.1, following the method in Chapter 3 (including the subjective removal of spatial outliers). The seasonal variation for the Congo rainforest is found to be similarly homogeneous to the Amazon rainforest (Fig. A.2). The Congo rainforest azimuth variation (Figure A.3) is also similar to the Amazon, and is small enough to be ignored. The first order approximation of the σ^o dB/ deg incidence angle relationship is shown in Figure A.4. Like the Amazon, the Congo rainforest (Fig. A.5) experiences a sharp increase in σ^o around sunrise, but in the afternoon the LTOD curve for σ^o indicates that measurements from 10-16h LTOD are comparable.

Largely, the Congo rainforest study area is very similar to the Amazon in radar response and consistency as measured by the analysis outlined my the method of Chapter 3. Calibration in this study area is expected to be similar to that of the Amazon rainforest.

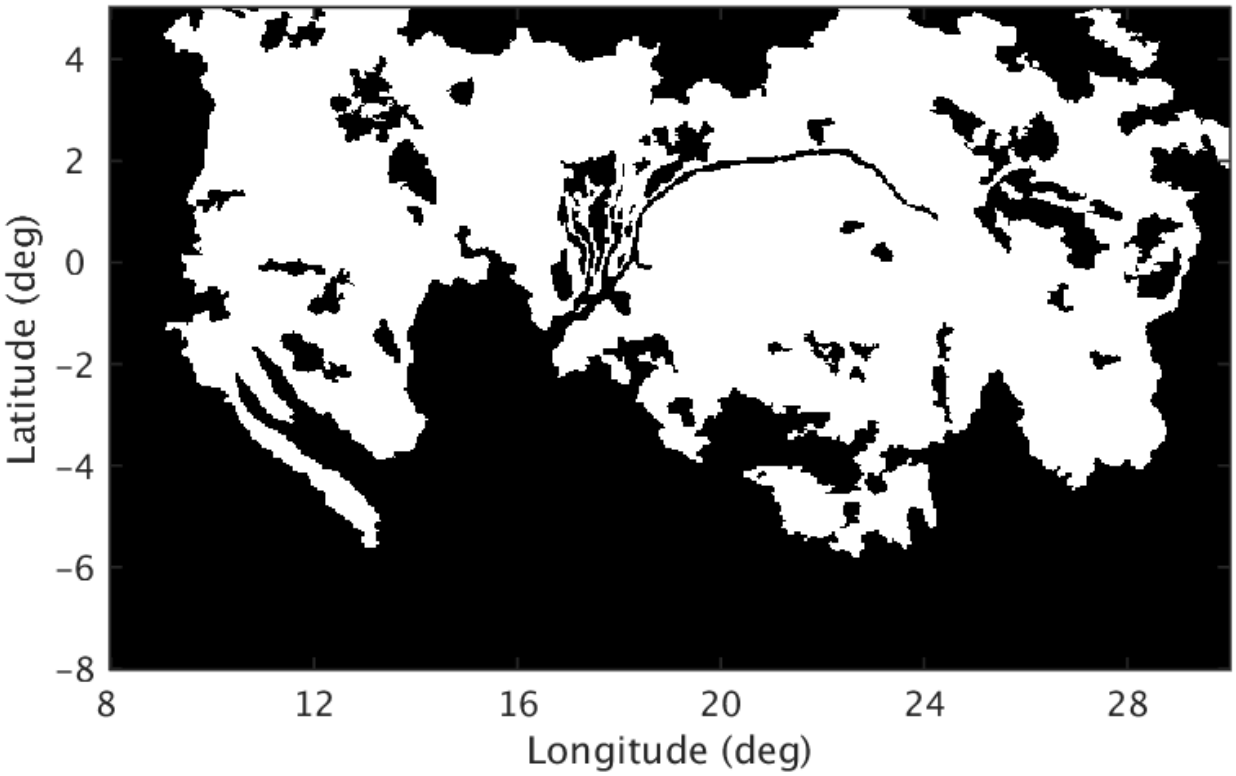

Figure A.1: Latitude/longitude mask representing the Congo rainforest calibration target and contains σ^o values in a 1 dB range.

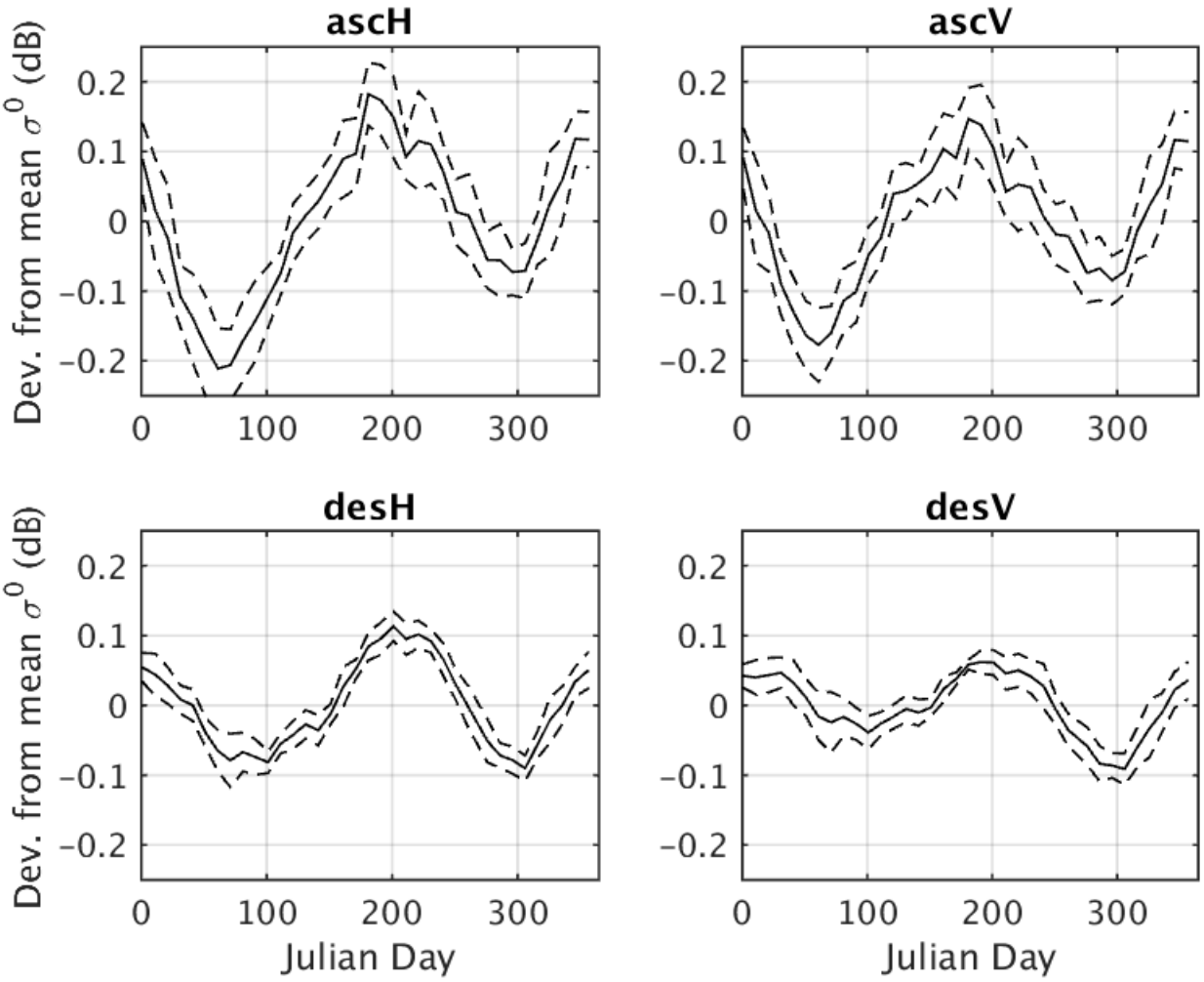

Figure A.2: Seasonal variation of σ^o for the Congo rainforest calibration target shown as the deviation from mean σ^o for each flavor of QuikSCAT (with a confidence interval that is the standard deviation of the deviation from mean σ^o). See text for details of how this plot is generated.

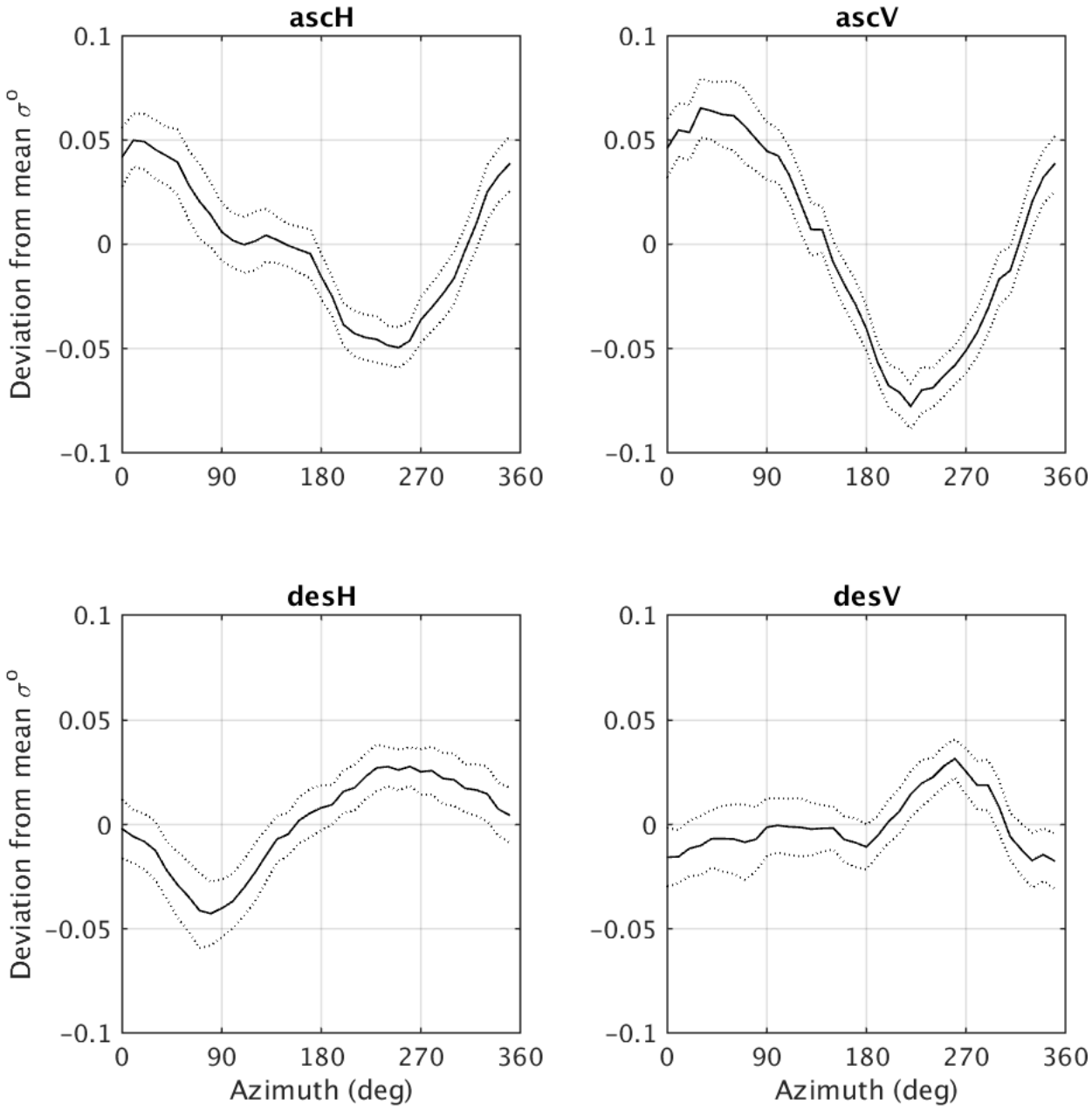

Figure A.3: Azimuth modulation of the Congo rainforest shown with mean σ^o by azimuth angle where the confidence interval is the standard deviation of σ^o.

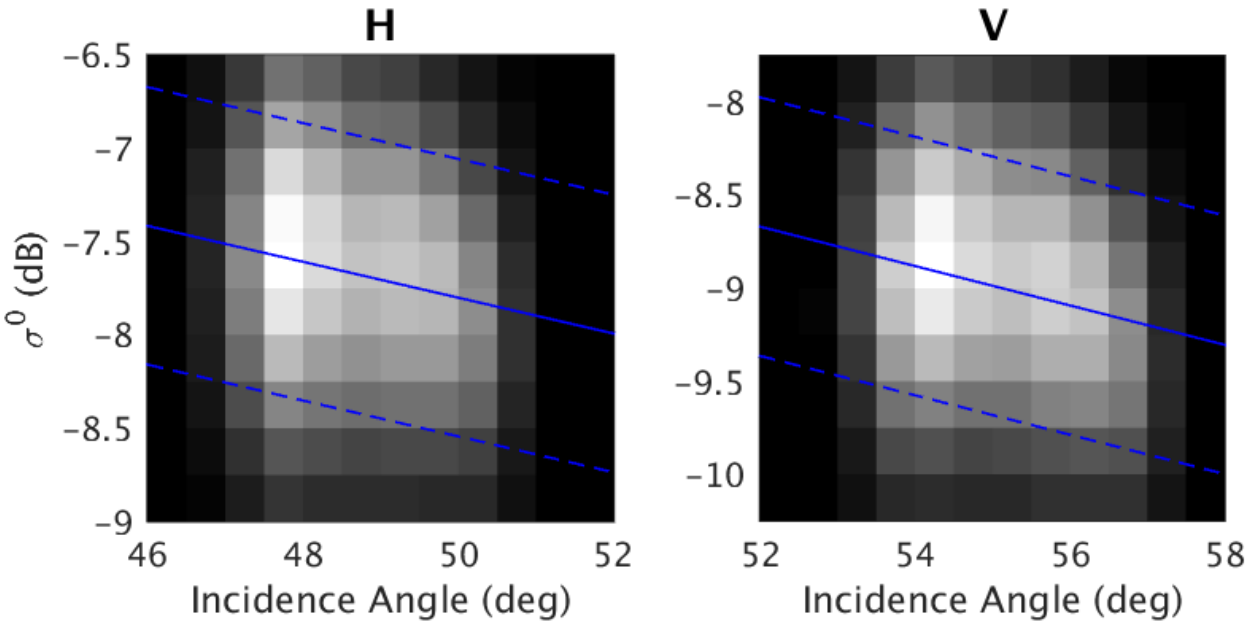

Figure A.4: Two dimensional PDF of the distribution of σ^o measured by RapidScat at each incidence angle (0.25^o bins) for the Congo rainforest study area. The blue line is the first order polynomial fit to the data and the slope of the line represents the σ^o dB/ deg incidence angle relationship. The dashed line is the $\pm$ one standard deviation for the estimate.

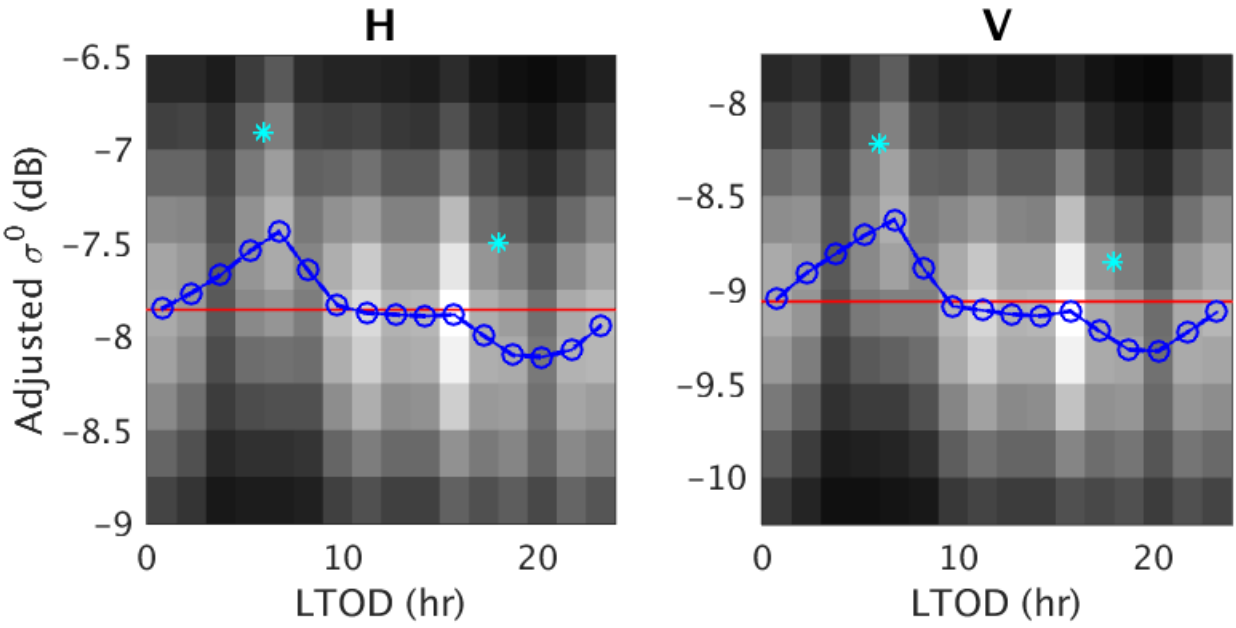

Figure A.5: Two dimensional PDF of RapidScat σ^o from the Congo rainforest calibration target for 90 minute LTOD bins. In blue, the mean σ^o (o) for each LTOD bin is show with a confidence interval that is $\pm$ the standard deviation for that bin. Notice the large increase around sunrise.

A.2 Argentina Pampas

The Argentina Pampas study area has lower backscatter compared to the Amazon study area, with a QuikSCAT mean σ^o of -11.5 dB for H-pol and -13.3 dB for V-pol. QuikSCAT SIR data from the South America region is used to identify the homogeneous land target corresponding to the Argentina Pampas. The method in Chapter 3 is applied to the SIR data within a latitude/longitude box with the same dimensions as Figure A.6. There is a lot more year-to-year seasonal variation of σ^o, but uncertainty because of this is accounted for in the confidence intervals of the calibration estimates. Azimuthal variations (Figure A.8) are larger than seen in the Amazon study area, but on a whole are expected to average out because RapidScat measures σ^o at all azimuth angles and the actual variances are still small. Based on the LTOD curve in Figure A.10, the LTOD criteria for this study area is that σ^o estimates should be within 45 minutes of each other for comparison.

While not as precise as the Amazon or Congo study areas, the Argentina Pampas study area is effectively used sample σ^o at a lower value than is possible with tropical rainforests. Confidence intervals are used to display uncertainty related to the large variances in this calibration target so that variations in the study area are not confused with variations between RapidScat SNR states.

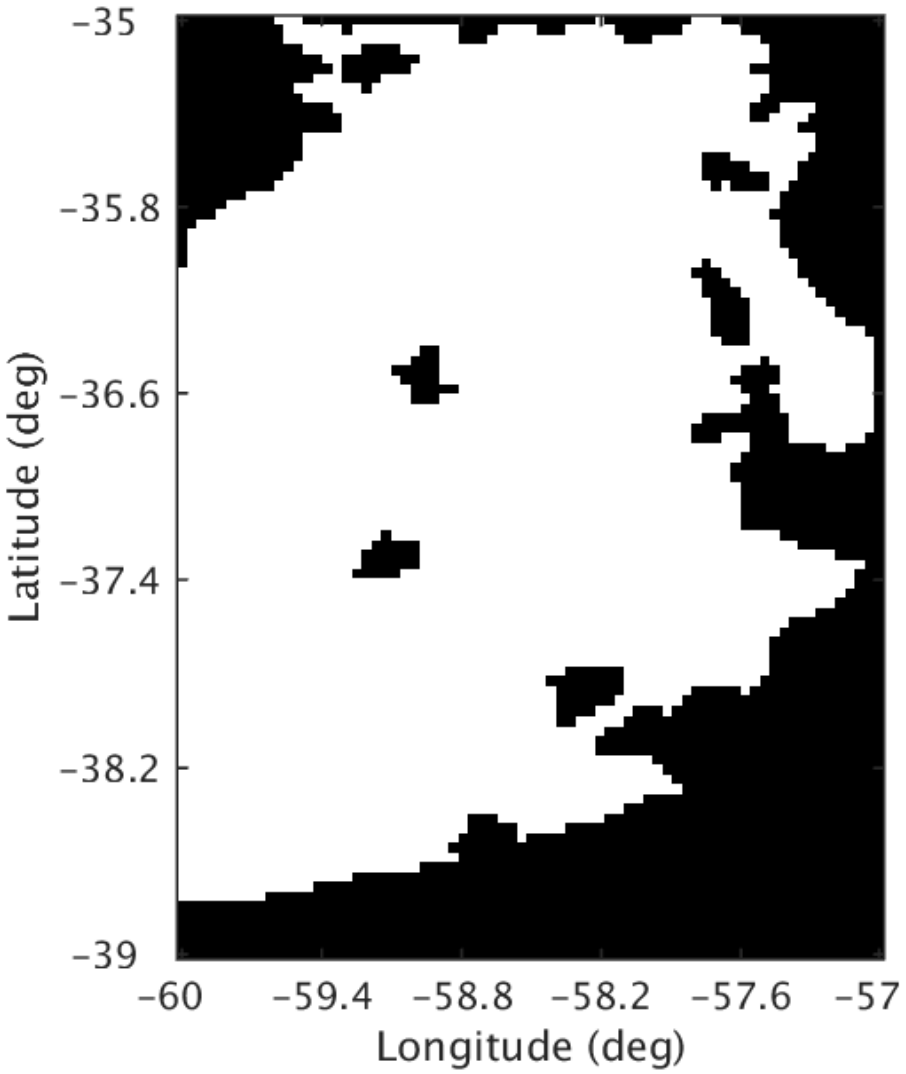

Figure A.6: This latitude/longitude mask represents the Argentina Pampas calibration target and contains σ^o values in a 1 dB range.

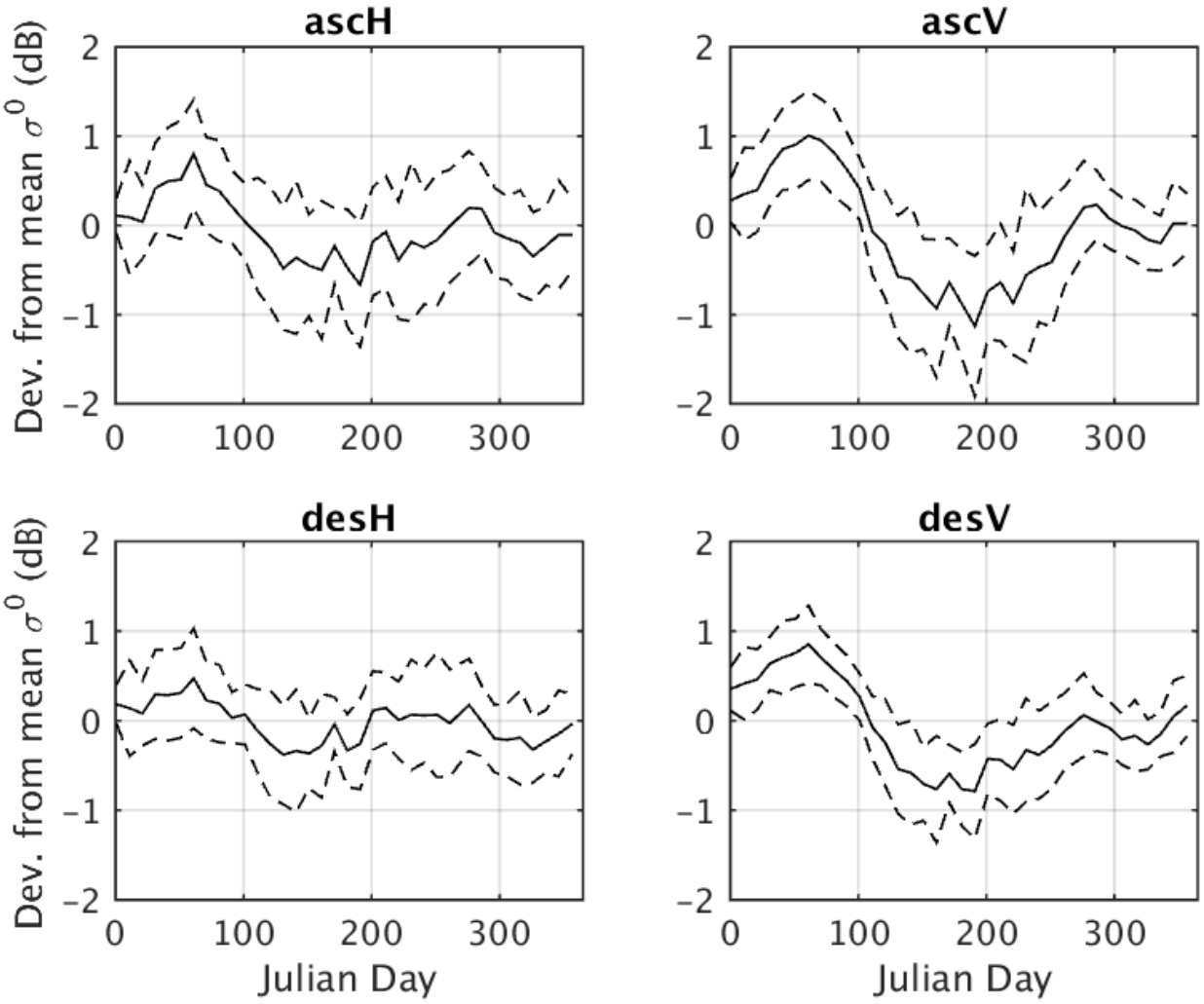

Figure A.7: Seasonal variation of σ^o for the Argentina Pampas calibration target shown as the deviation from mean σ^o for each flavor of QuikSCAT (with a confidence interval that is the standard deviation of the deviation from mean σ^o

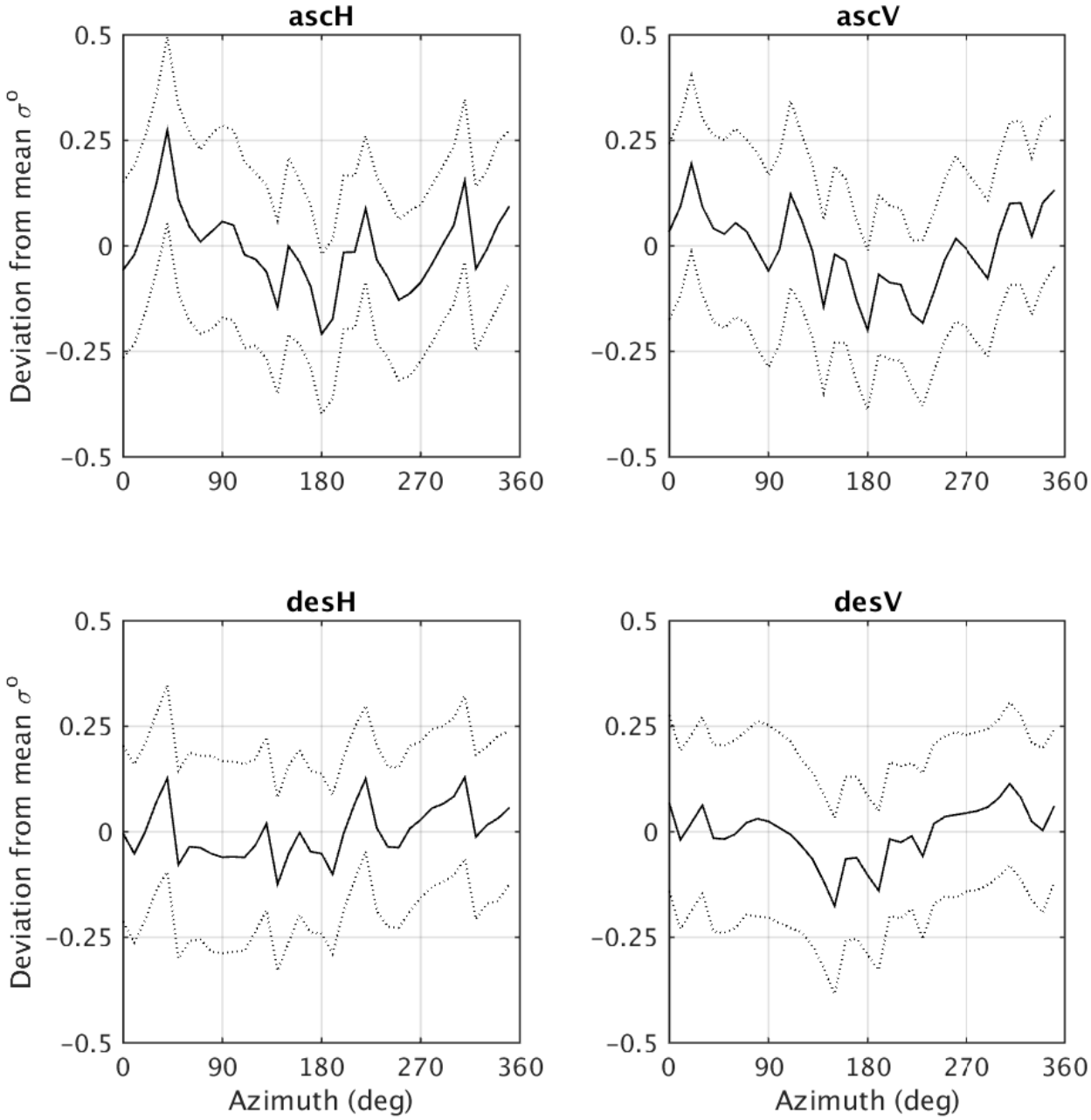

Figure A.8: Azimuth modulation of the Argentina Pampas shown with mean σ^o by azimuth angle where the confidence interval is the standard deviation of σ^o.

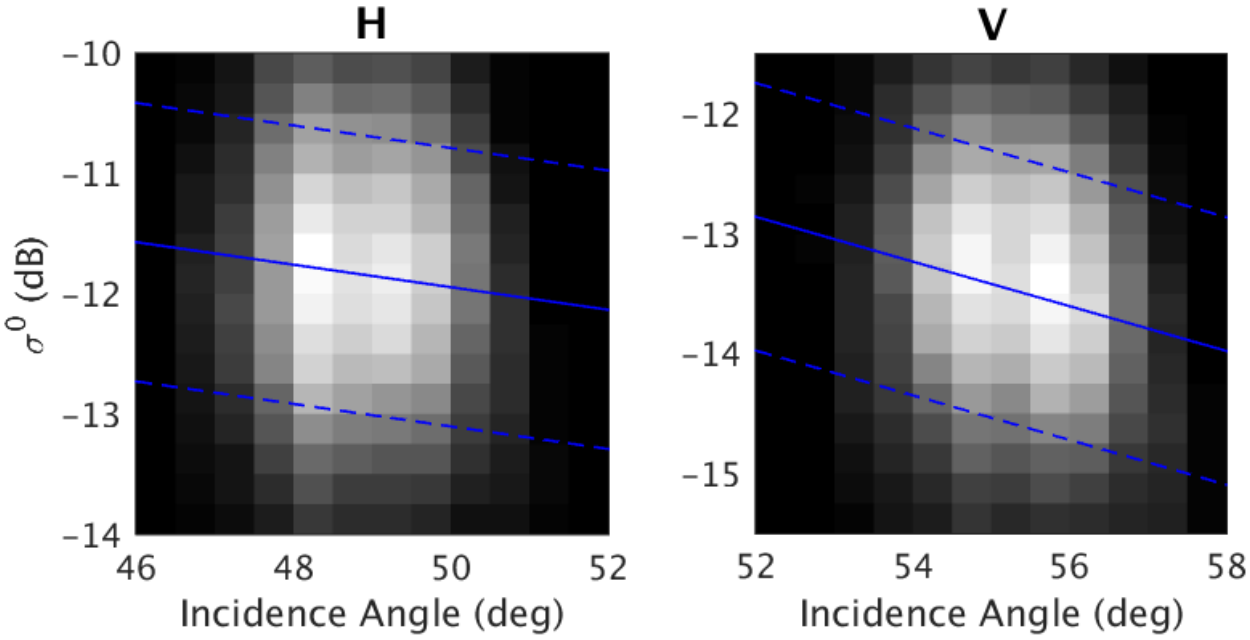

Figure A.9: PDF in two dimensions showing the distribution of σ^o measured by RapidScat at each incidence angle (0.25^o bins) for the Argentina Pampas. The blue line is the first order polynomial fit to the data and the slope of the line represents the σ^o dB/ deg incidence angle relationship. The dashed line is the $\pm$ one standard deviation for the estimate.

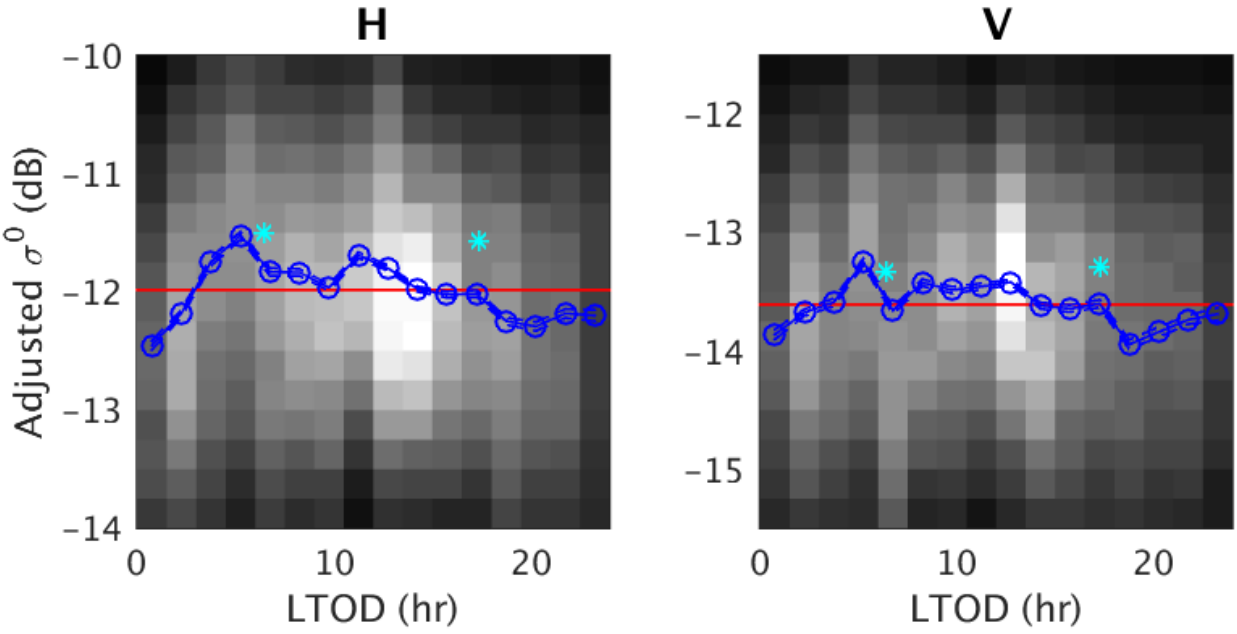

Figure A.10: Two dimensional PDF of RapidScat σ^o from the Argentina Pampas calibration target for 90 minute LTOD bins. In blue, the mean σ^o (o) for each LTOD bin is show with a confidence interval that is $\pm$ the standard deviation for that bin. Notice the large increase around sunrise.

A.3 West Sahara

The West Sahara study area has lower backscatter compared to the Amazon study area, with a QuikSCAT mean σ^o of -17.2 dB for H-pol and -17.3 dB for V-pol. QuikSCAT SIR data from the North Africa region is used to identify a homogeneous area for this land target. The method in Chapter 3 is applied to the SIR data within a latitude/longitude box with the same dimensions as Figure A.11. The latitude/longitude box was chosen to select an area of the Sahara desert that was not an erg sea, which are known to have large azimuthal dependencies. There is a lot more year-to-year seasonal variation of σ^o, but uncertainty because of this is accounted for in the confidence intervals of the calibration estimates. Azimuthal variations (Figure A.13) are larger than seen in the Amazon study area, but on a whole are expected to average out because RapidScat measures σ^o at all azimuth angles and the actual variances are still small. Based on the LTOD curve in Figure A.15, the LTOD criteria for this study area is that σ^o estimates should be within 45 minutes of each other for comparison.

While not as precise as the Amazon or Congo study areas, the West Sahara study area is effectively used sample σ^o at a low value. Confidence intervals are used to display uncertainty related to the large variances in this calibration target so that variations in the study area are not confused with variations between RapidScat SNR states.

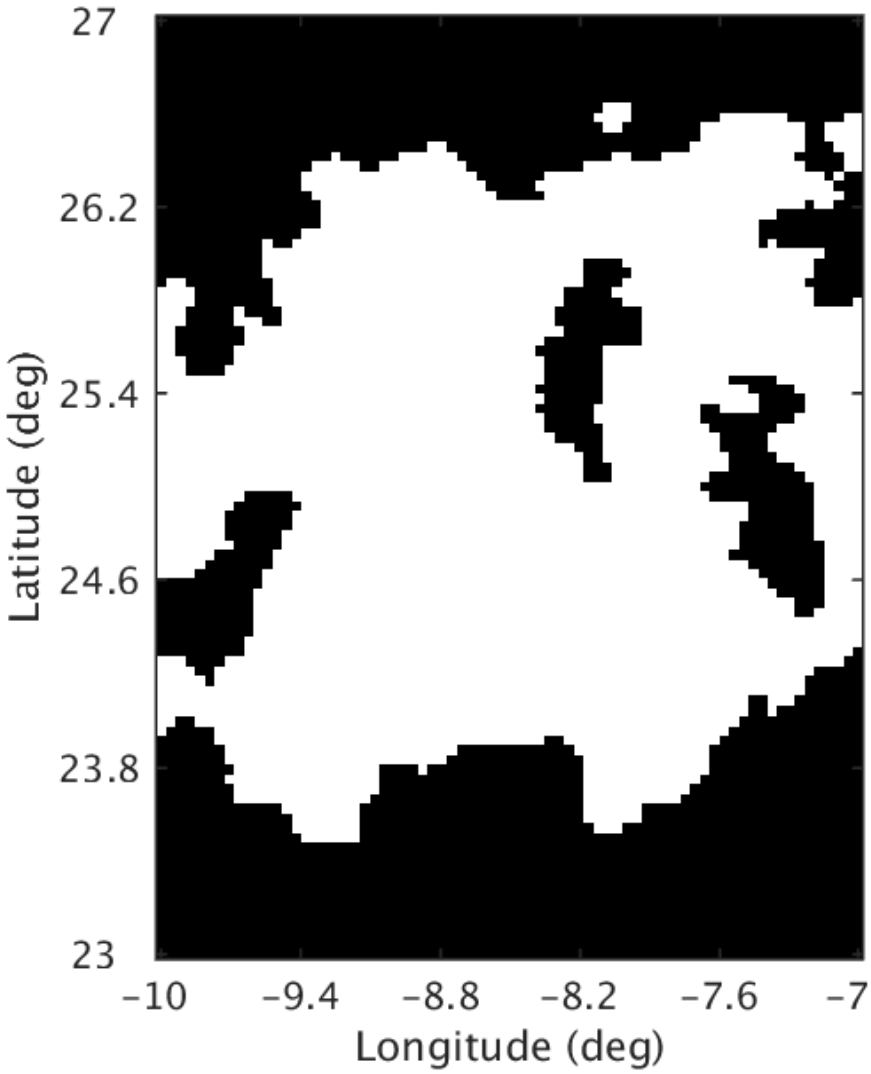

Figure A.11: This latitude/longitude mask represents the West Sahara calibration target and contains σ^o values in a 2 dB range.

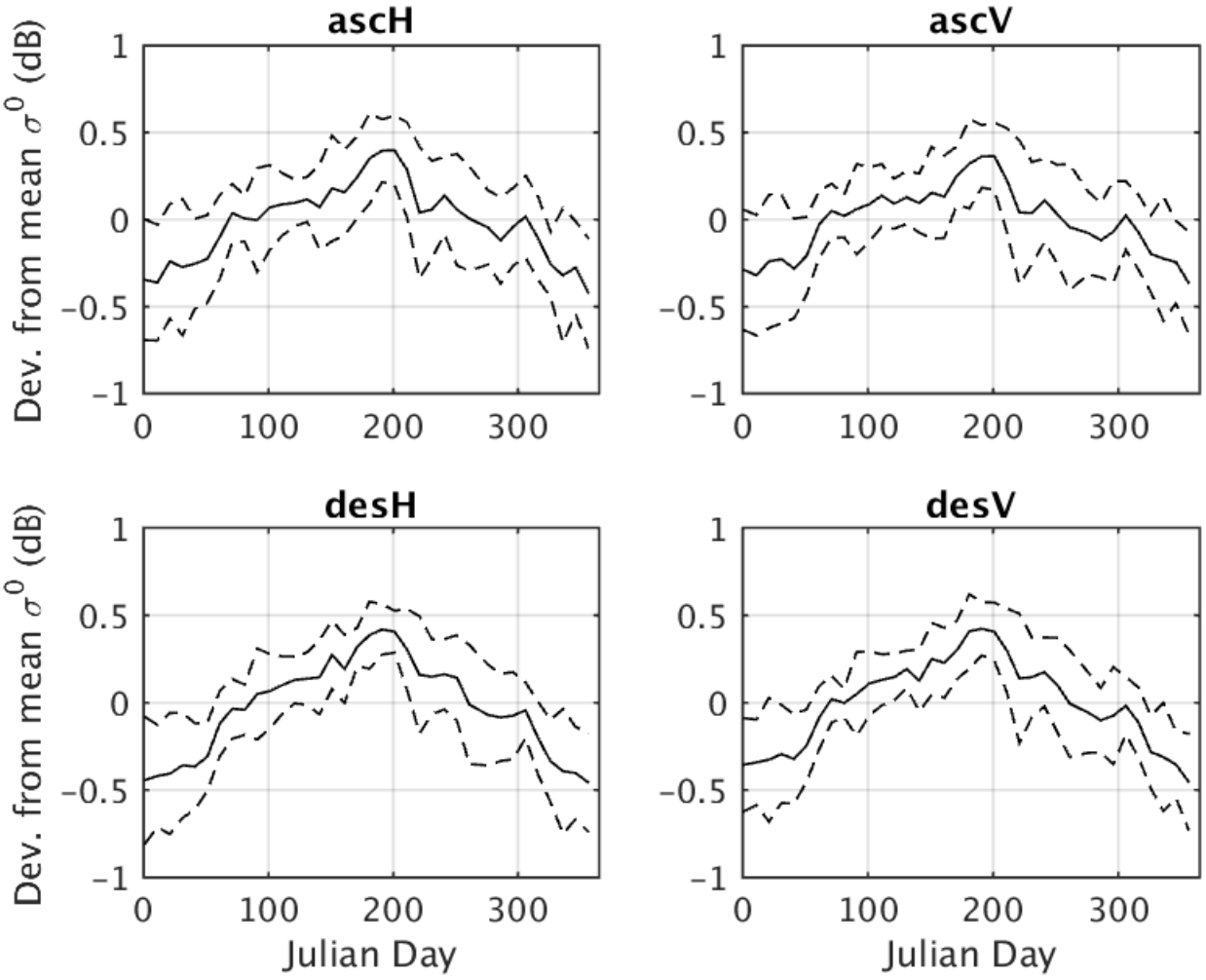

Figure A.12: Seasonal variation of σ^o for the West Sahara calibration target shown as the deviation from mean σ^o for each flavor of QuikSCAT (with a confidence interval that is the standard deviation of the deviation from mean σ^o

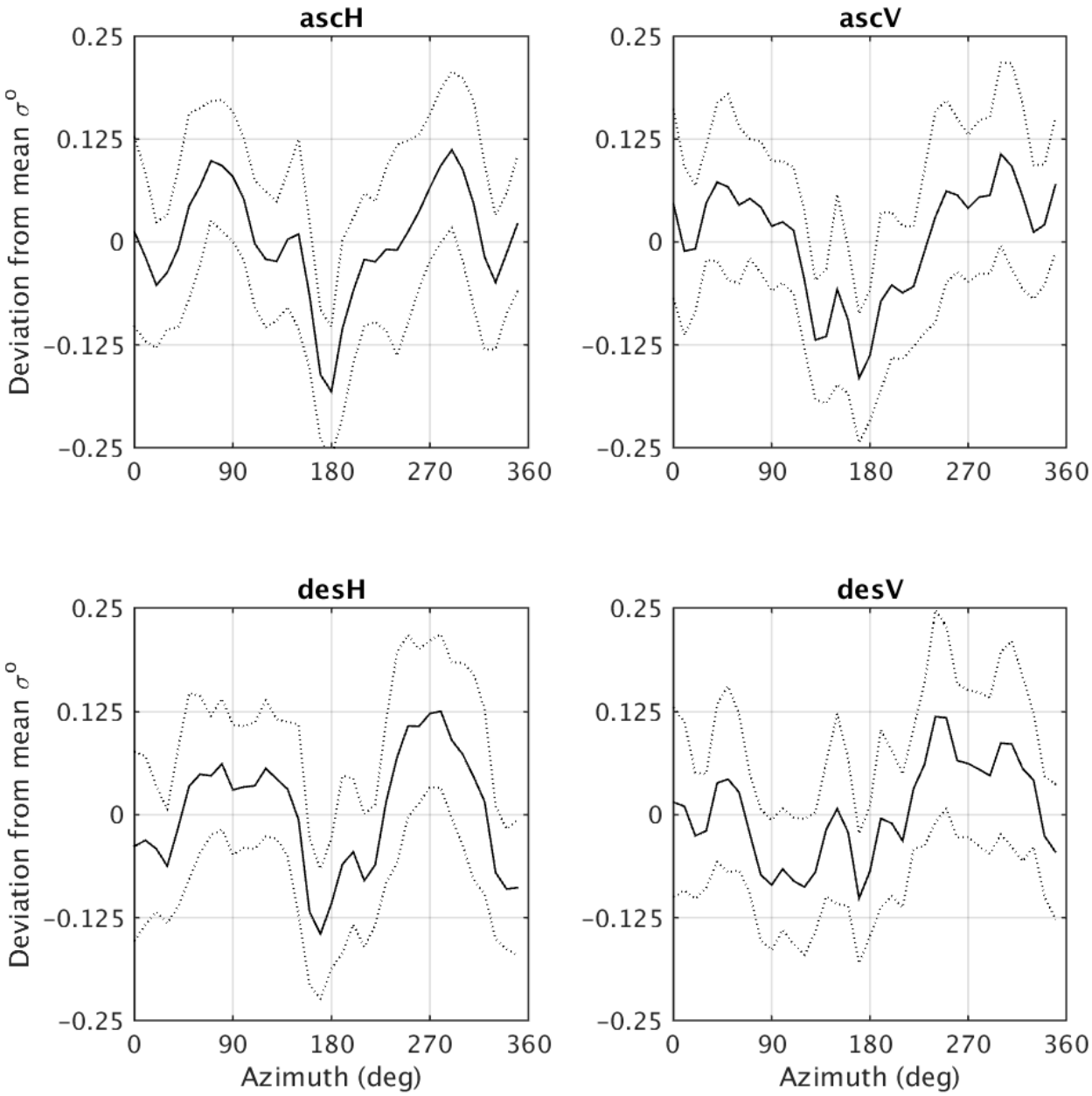

Figure A.13: Azimuth modulation of the West Sahara shown with mean σ^o by azimuth angle where the confidence interval is the standard deviation of σ^o.

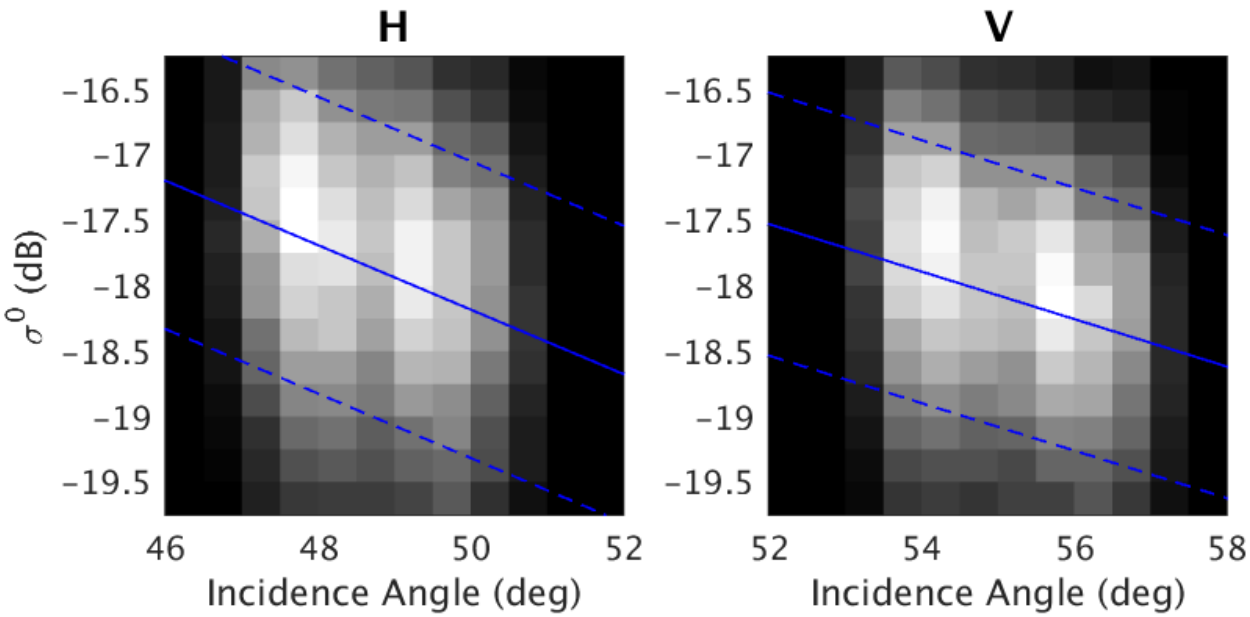

Figure A.14: PDF in two dimensions showing the distribution of σ^o measured by RapidScat at each incidence angle (0.25^o bins) for the West Sahara calibration target. The blue line is the first order polynomial fit to the data and the slope of that line represents the σ^o dB/deg relationship. The dashed blue line is the $\pm$ one standard deviation for the estimate.

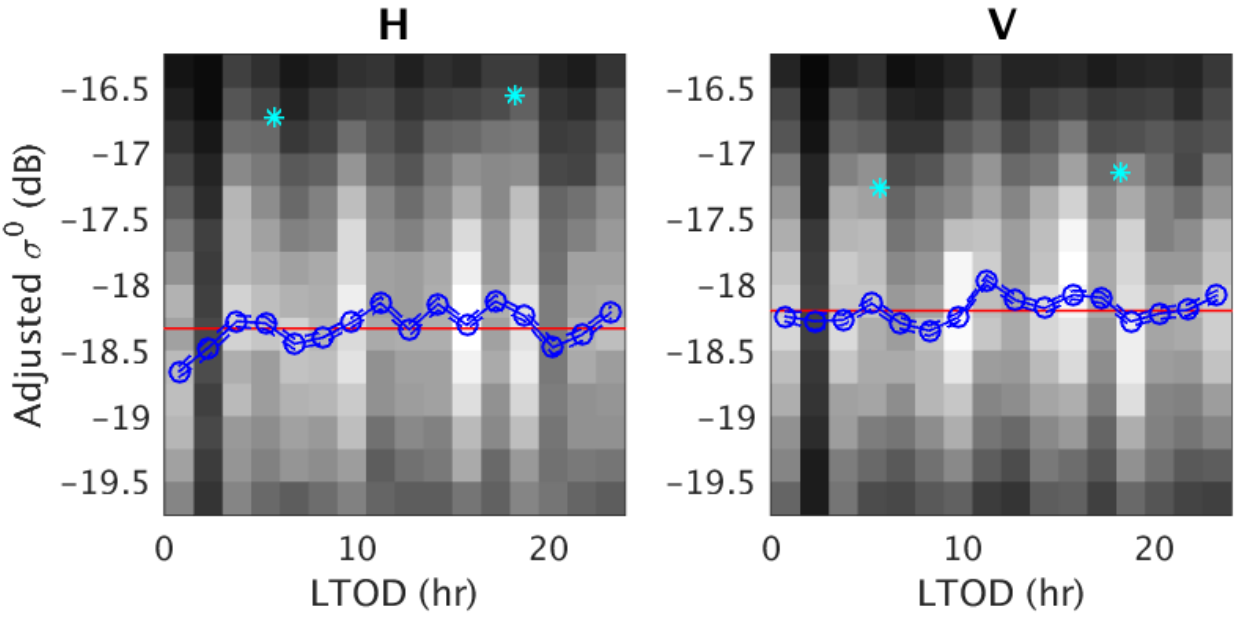

Figure A.15: Two dimensional PDF of RapidScat σ^o from the West Sahara calibration target for 90 minute LTOD bins. In blue, the mean σ^o (o) for each LTOD bin is show with a confidence interval that is $\pm$ the standard deviation for that bin.

A.4 Australian Desert

The Australian Desert study area has lower backscatter compared to the Amazon study area, with a QuikSCAT mean σ^o of -16.9 dB for H-pol and -18 dB for V-pol. QuikSCAT SIR data from the Austrailia region is used to identify a homogeneous area for this land target. The method in Chapter 3 is applied to the SIR data, except that a mean σ^o was subjectively chosen to center the mask on in Figure A.16. There is a lot more year-to-year seasonal variation of σ^o, but uncertainty because of this is accounted for in the confidence intervals of the calibration estimates. Azimuthal variations (Figure A.18) are larger than seen in the Amazon study area, but smaller than in the Argentina Pampas study area. Overall, the azimuth variation is expected to average out because RapidScat measures σ^o at all azimuth angles and the actual variances are still small. Based on the LTOD curve in Figure A.20, the LTOD criteria for this study area is that σ^o estimates should be within 45 minutes of each other for comparison.

While not as precise as the Amazon or Congo study areas, the Australia study area is effectively used sample σ^o at a low value. Confidence intervals are used to display uncertainty related to the large variances in this calibration target so that variations in the study area are not confused with variations between RapidScat SNR states.

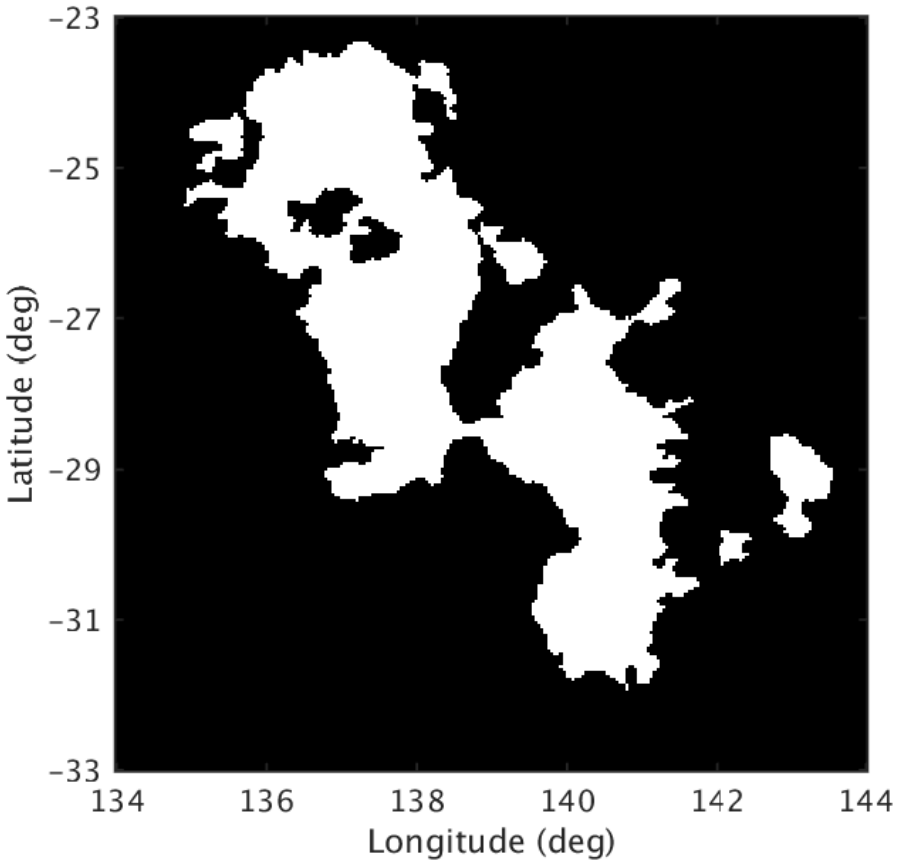

Figure A.16: This latitude/longitude mask represents the Australian desert calibration target and contains σ^o values in a 2 dB range.

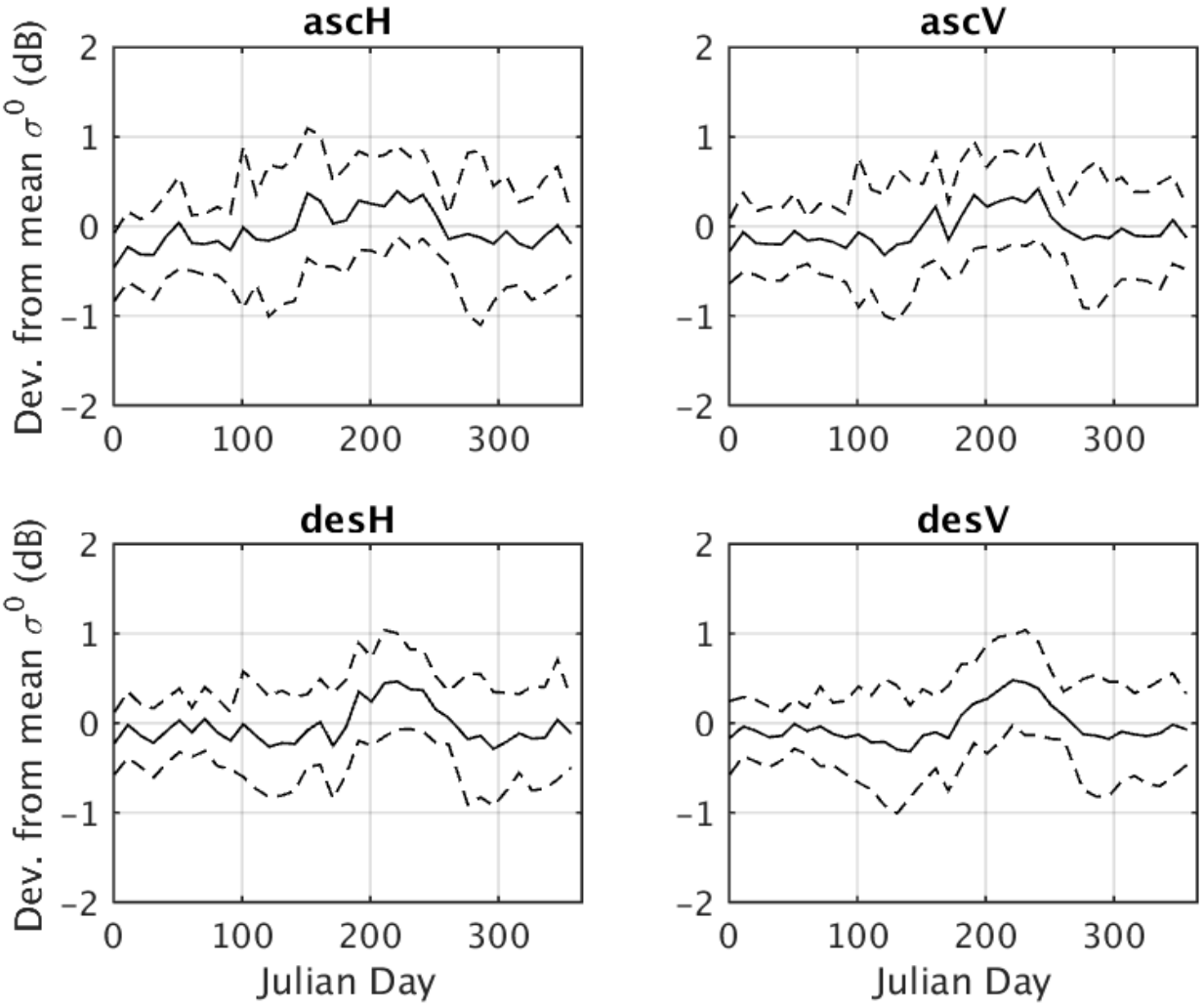

Figure A.17: Seasonal variation of σ^o for the Australian desert calibration target shown as the deviation from mean σ^o for each flavor of QuikSCAT (with a confidence interval that is the standard deviation of the deviation from mean σ^o

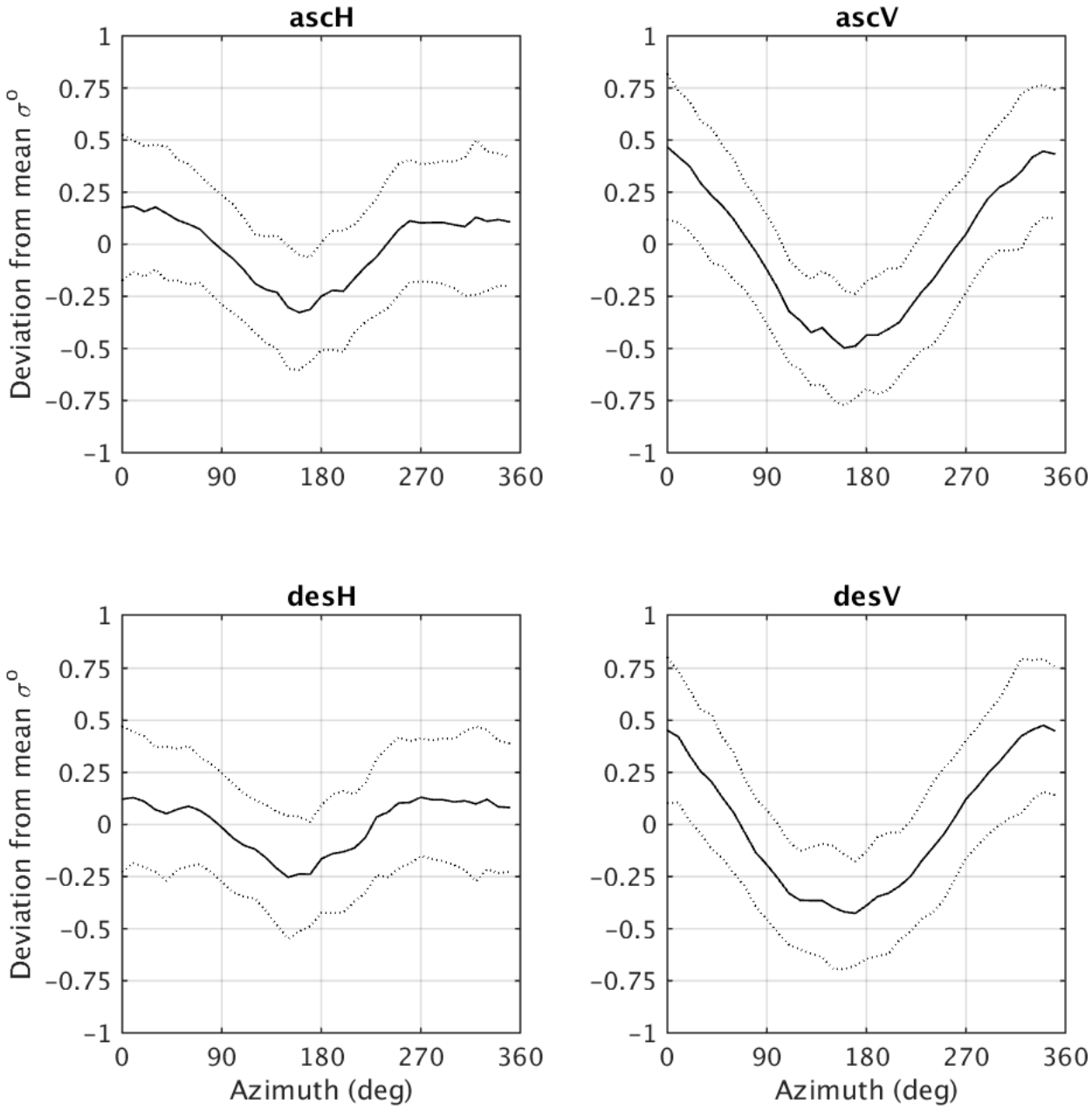

Figure A.18: Azimuth modulation of the Australian desert shown with mean σ^o by azimuth angle where the confidence interval is the standard deviation of σ^o.

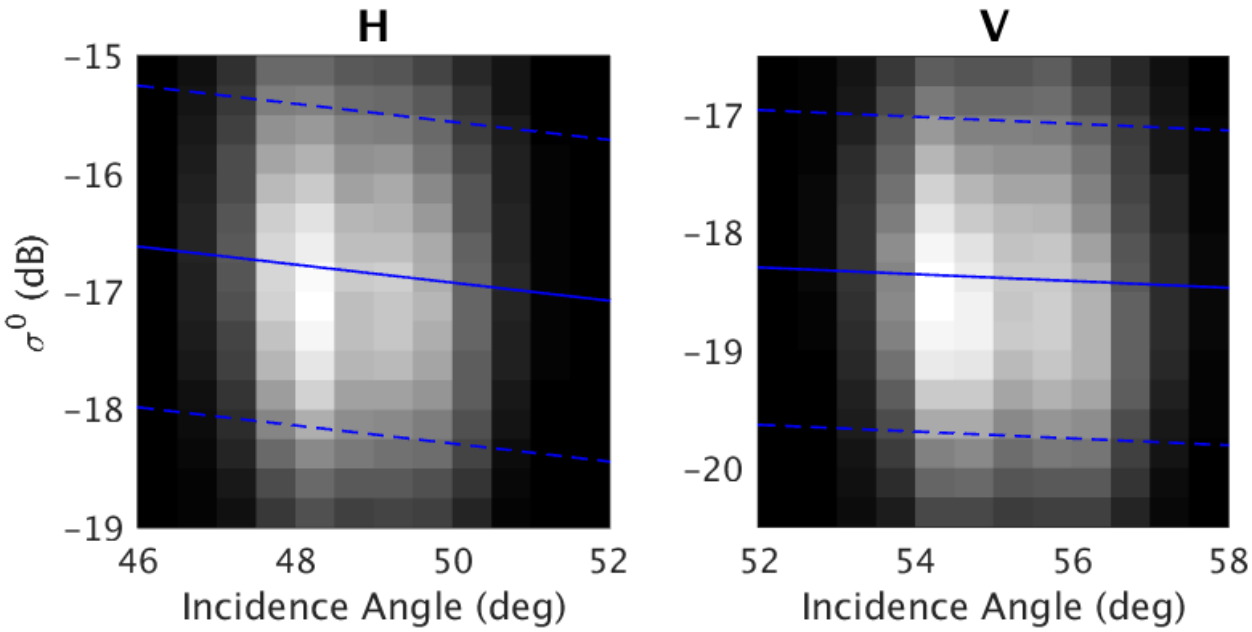

Figure A.19: PDF in two dimensions showing the distribution of σ^o measured by RapidScat at each incidence angle (0.25^o bins) for the Austrialian Desert calibration target. The blue line is the first order polynomial fit to the data and the slope of that line represents the σ^o dB/deg relationship. The dashed blue line is the $\pm$ one standard deviation for the estimate.

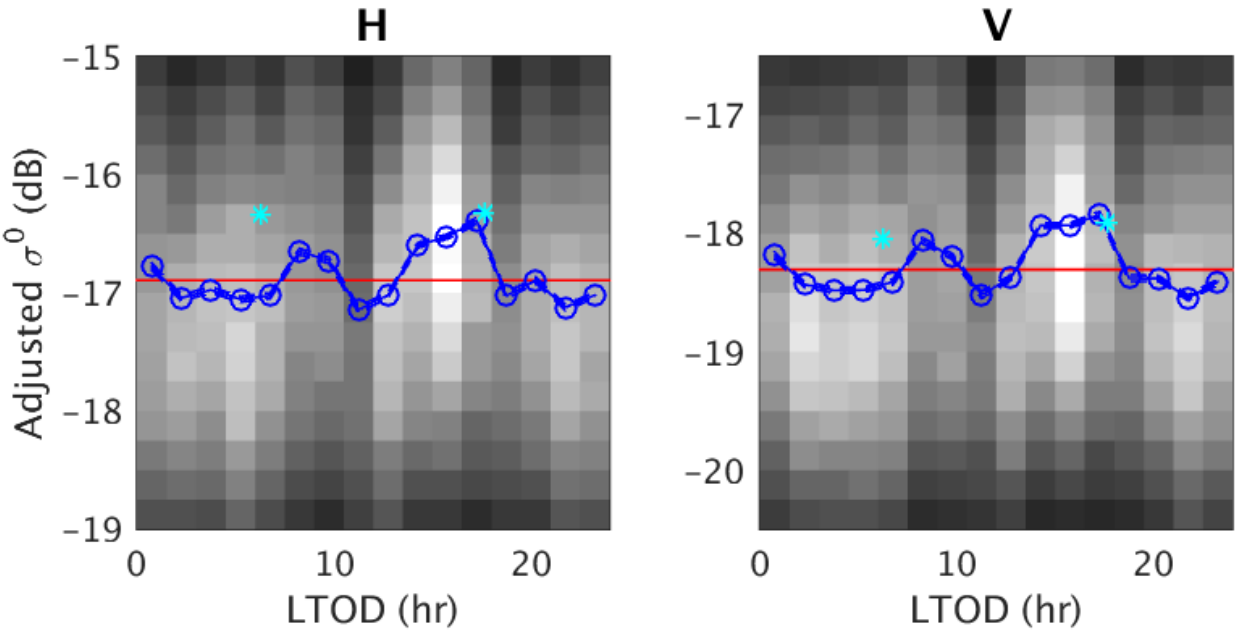

Figure A.20: Two dimensional PDF of RapidScat σ^o from the Austrialian Desert calibration target for 90 minute LTOD bins. In blue, the mean σ^o (o) for each LTOD bin is show with a confidence interval that is $\pm$ the standard deviation for that bin.

A.5 Sahara Desert

The Sahara Desert study area has the lowest backscatter compared to the other study areas, with a QuikSCAT mean σ^o of -26 dB for H-pol and -27 dB for V-pol. QuikSCAT SIR data from the North Africa region is used to identify a homogeneous area for this land target. The method in Chapter 3 is applied to the SIR data, except that a mean σ^o was subjectively chosen to center the mask on in Figure A.21. There is a lot more year-to-year seasonal variation of σ^o, but uncertainty because of this is accounted for in the confidence intervals of the calibration estimates. Azimuthal variations (Figure A.23) are very large due to the presence of erg seas in the study area. However, the azimuth variation is expected to average out when there are many measurements because RapidScat measures σ^o at all azimuth angles. Based on the LTOD curve in Figure A.25, the LTOD criteria for this study area is that σ^o estimates should be within 45 minutes of each other or between 6h and 12h LTOD for comparison.

While not as precise as the Amazon or Congo study areas, the Sahara Desert study area is effectively used sample σ^o at a very low value. Confidence intervals are used to display uncertainty related to the large variances in this calibration target so that variations in the study area are not confused with variations between RapidScat SNR states.

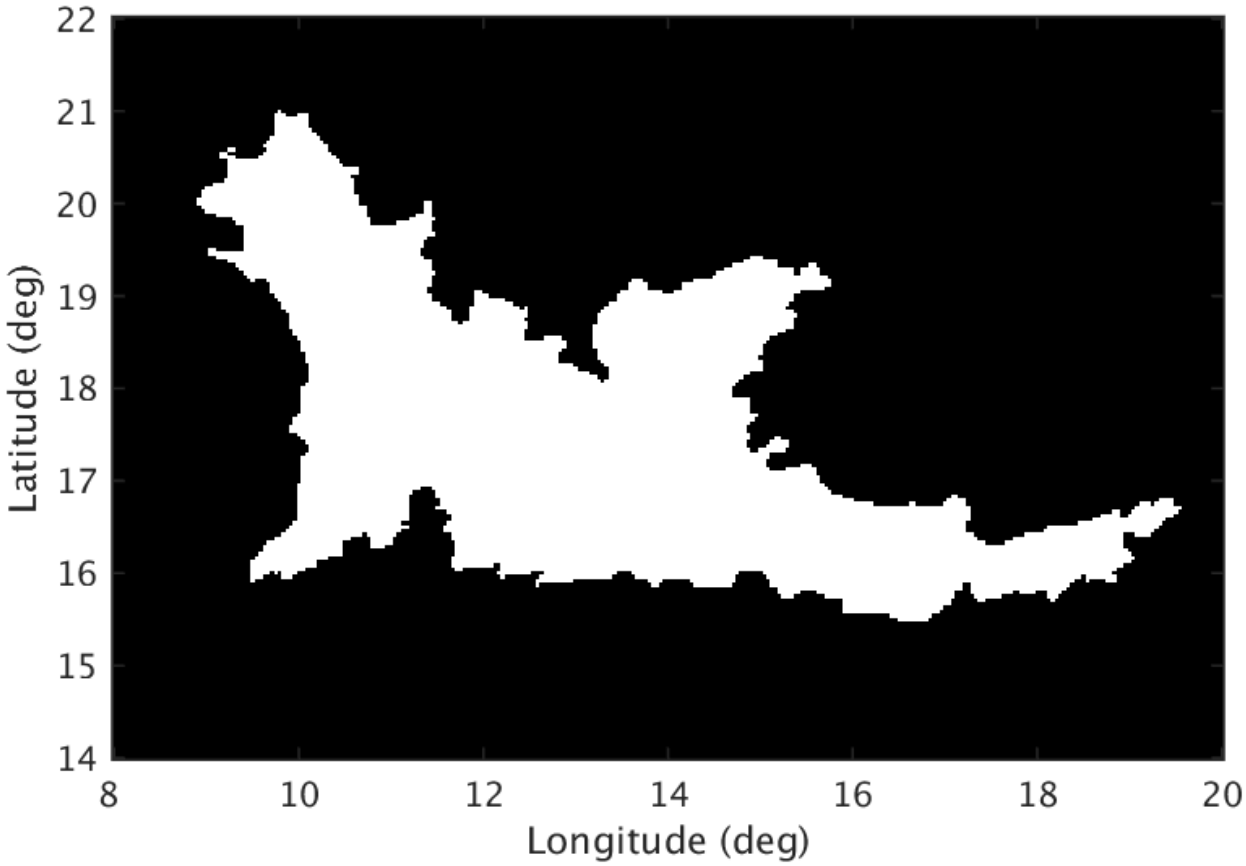

Figure A.21: This latitude/longitude mask represents the Sahara desert calibration target and contains σ^o values in a 5 dB range.

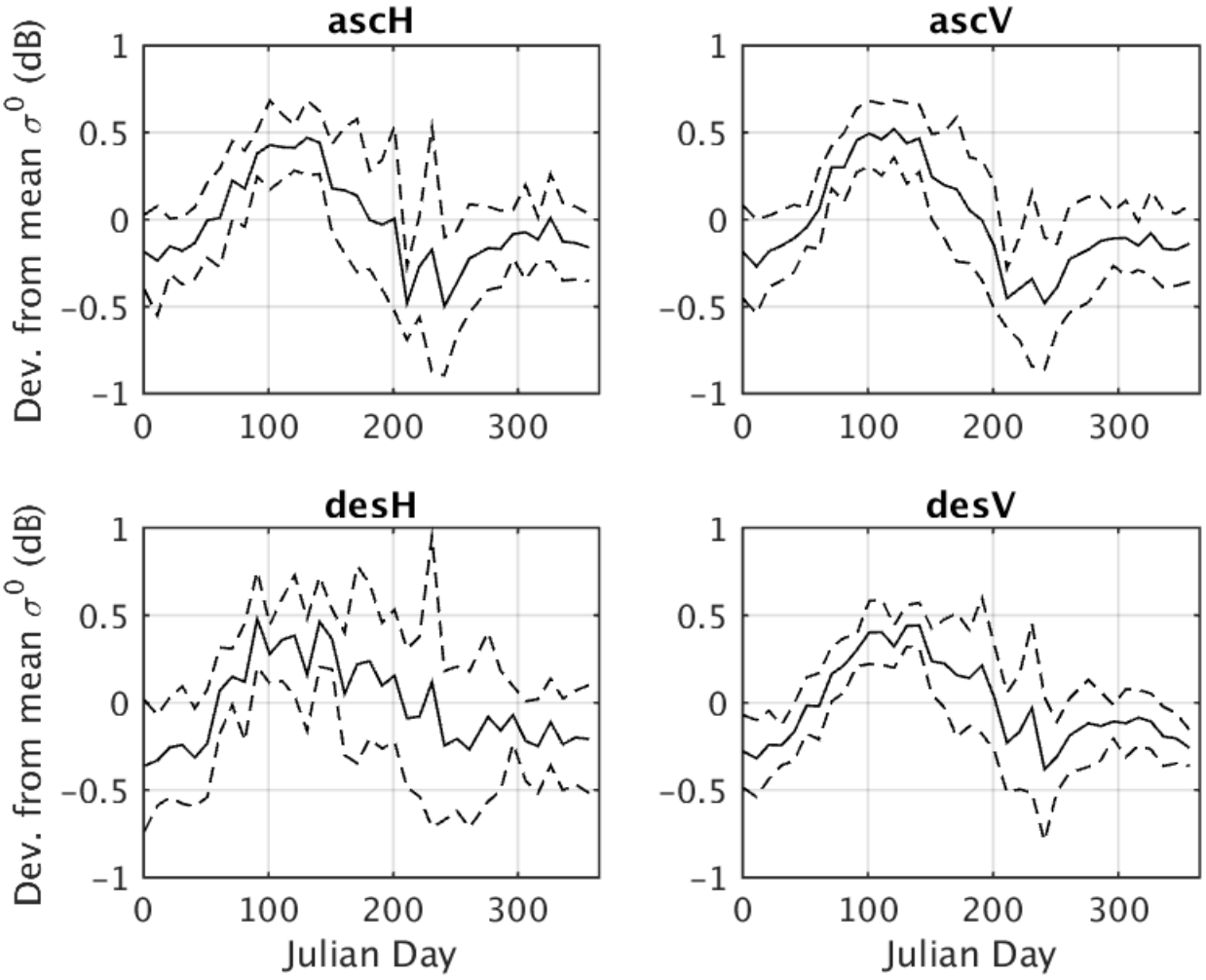

Figure A.22: Seasonal variation of σ^o for the Sahara desert calibration target shown as the deviation from mean σ^o for each flavor of QuikSCAT (with a confidence interval that is the standard deviation of the deviation from mean σ^o

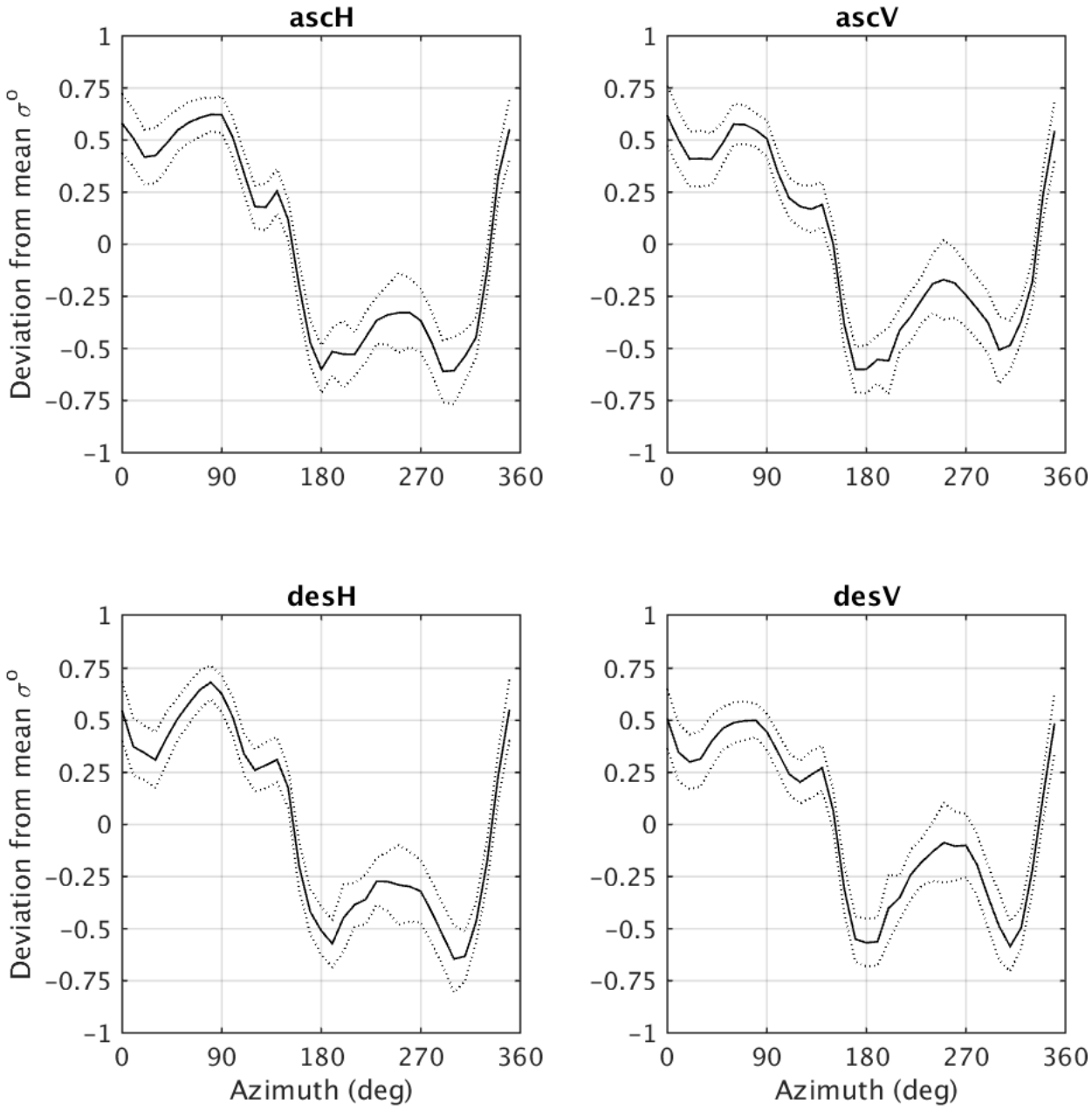

Figure A.23: Azimuth modulation of the Sahara desert shown with mean σ^o by azimuth angle where the confidence interval is the standard deviation of σ^o.

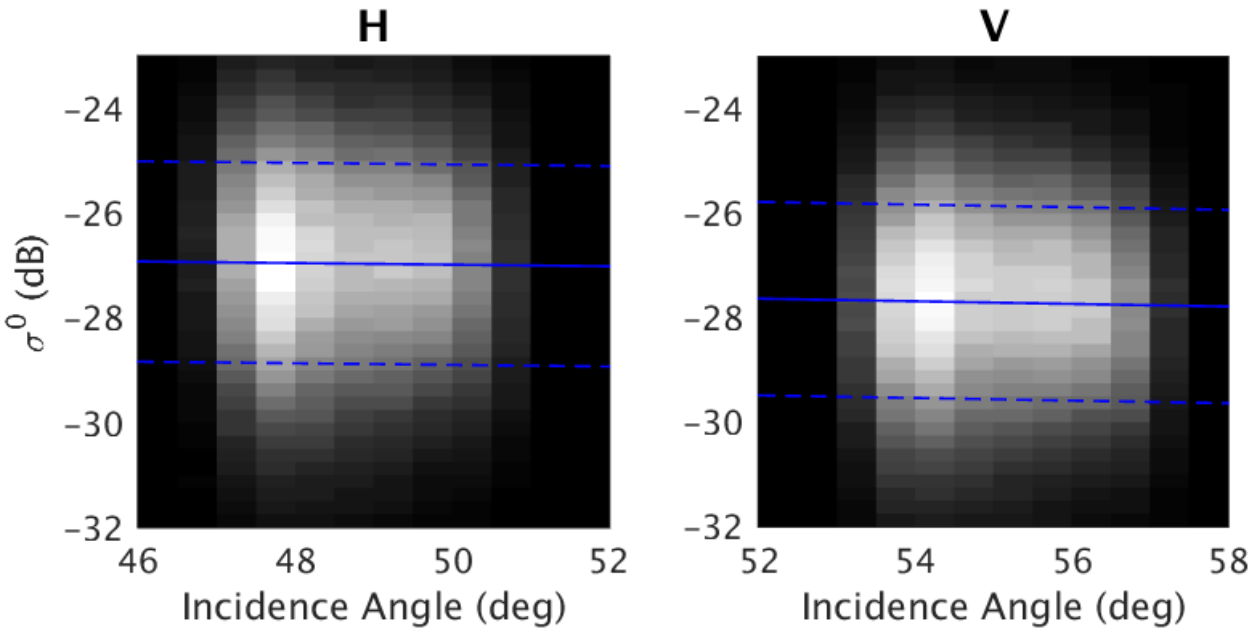

Figure A.24: PDF in two dimensions showing the distribution of σ^o measured by RapidScat at each incidence angle (0.25^o bins) for the Sahara desert. The blue line is the first order polynomial fit to the data and the slope of the line represents the σ^o dB/ deg incidence angle relationship. The dashed line is the $\pm$ one standard deviation for the estimate.

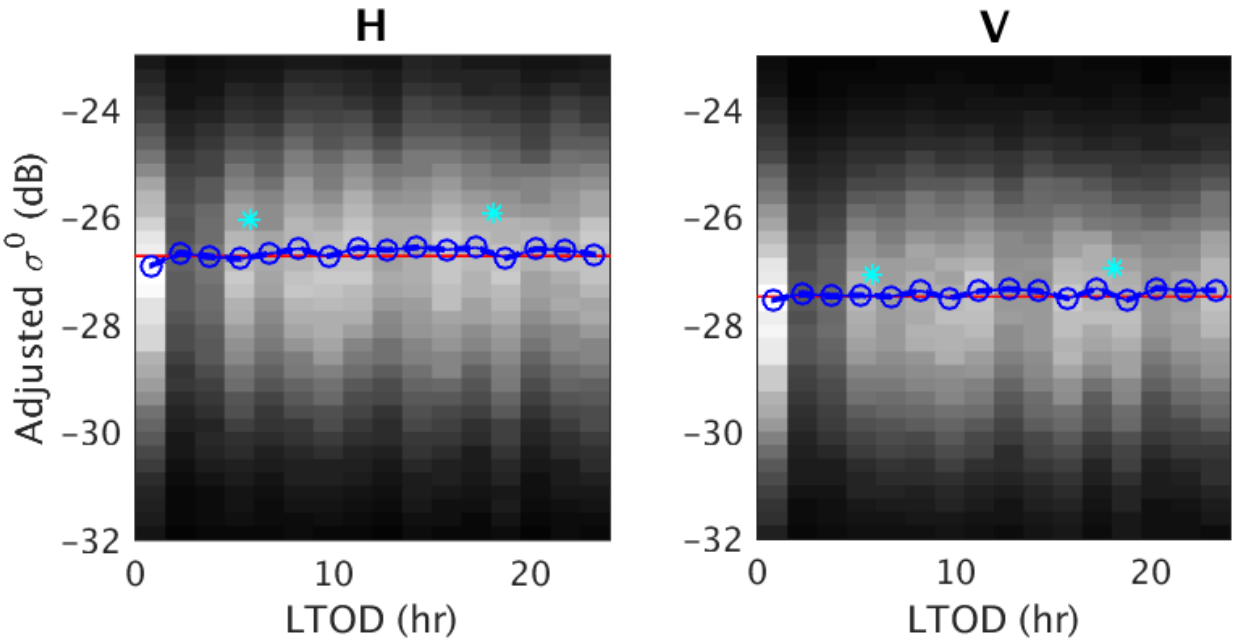

Figure A.25: Two dimensional PDF of RapidScat σ^o from the Sahara desert calibration target for 90 minute LTOD bins. In blue, the mean σ^o (o) for each LTOD bin is show with a confidence interval that is $\pm$ the standard deviation for that bin. Notice the large increase around sunrise.